PHRC Research Series Report No. 110

The Pennsylvania Housing Research Center

Determination of Seismic Performance Factors for Structural Insulated Panel Shear Walls Based on Fema P695 Methodology

219 Sackett Building
University Park, PA 16802
Telephone: (814) 865-2341
Facsimile: (814) 863-7304
E-mail: phrc@psu.edu
URL: www.engr.psu.edu/phrc

May 2011

Disclaimer:

The Pennsylvania Housing Research Center (PHRC) exists to be of service to the housing community, especially in Pennsylvania. The PHRC conducts technical projects—research, development, demonstration, and technology transfer—under the sponsorship and with the support of numerous agencies, associations, companies and individuals. Neither the PHRC, nor any of its sponsors, makes any warranty, expressed or implied, as to the accuracy or validity of the information contained in this report. Similarly, neither the PHRC, nor its sponsors, assumes any liability for the use of the information and procedures provided in this report. Opinions, when expressed, are those of the authors and do not necessarily reflect the views of either the PHRC or anyone of its sponsors. It would be appreciated, however, if any errors, of fact or interpretation or otherwise, could be promptly brought to our attention. If additional information is required, please contact:

Mike Turns
Associate Director
PHRC

Andrew Scanlon
Director of Research
PHRC

PHRC Research Series Report No. 110

The Pennsylvania Housing Research Center

Determination of Seismic Performance Factors for Structural Insulated Panel Shear Walls Based on Fema P695 Methodology

by

Luke T. Donovan
Ali M. Memari

219 Sackett Building
University Park, PA 16802
Telephone: (814) 865-2341
Facsimile: (814) 863-7304
E-mail: phrc@psu.ed
URL: www.engr.psu.edu/phrc

May 2011

DETERMINATION OF SEISMIC PERFORMANCE FACTORS FOR STRUCTURAL INSULATED PANEL SHEAR WALLS BASED ON FEMA P695 METHODOLOGY

by

Luke T. Donovan

Former Graduate Student, Department of Architectural Engineering
The Pennsylvania State University, 104 Engineering Unit A, University Park, PA 16802

and

Ali M. Memari

Professor, Department of Architectural Engineering
The Pennsylvania State University, 104 Engineering Unit A, University Park, PA 16802

May 2011

ABSTRACT

The Applied Technology Council recently developed a new approach for derivation of seismic performance factors (SPFs) needed to design seismic-force-resisting systems. The ATC-63 Project report, published as FEMA P695, is an iterative procedure intended to utilize collapse evaluation to determine acceptable SPFs to provide an equivalent level of safety against collapse for buildings having different seismic-force-resisting systems. Structural response prediction is assessed through the combination of traditional code concepts, non-linear dynamic analyses, and risk-based assessment techniques.

This report presents the results of a pilot project for the quantification of SPFs for Structural Insulated Panels (SIPs) as the seismic force resisting system for residential and light commercial building based on the methodology presented in FEMA P695. The panelized SIP system consists of a rigid foam insulation core sandwiched between two structural wood-based skins, which provides high whole-wall thermal resistance, limited construction waste, and reduced on-site construction time. Multiple panels are linked with traditional dimensional lumber or other spline types and fasteners. Section R614 of the 2007 International Residential Code Supplement added design provisions for SIP construction in Seismic Zones A, B, and C. Modeling and evaluation with the SAPWood computer Program of four building models for SDC D has proven optimistic for SIPs meeting full FEMA P695 acceptance criteria.

ACKNOWLEDGEMENT

This research presented in this report was partially made possible through the support provided by the United States Air Force to Captain Luke T. Donovan (first author) to complete his Master of Science degree in Architectural Engineering. The authors would like to acknowledge the contribution of Dr. Shiling Pei for offering invaluable comments and suggestions in using the software SAPWood. The authors also acknowledge the helpful comments and suggestions by Professor Bo Kasal as the former Hankin Chair of Residential Construction (Penn State, Civil and Environmental Engineering Department, Pennsylvania Housing Research Center) and Professor Andres Lepage (Department of Architectural Engineering). The views and opinions expressed in this report are those of the authors and do not reflect the official policy or position of the United States Air Force, Department of Defense, or the U.S. Government. The authors' view and opinions in this report do not necessarily represent those of Penn State University or PHRC.

DISCLAIMER

The material presented in this report is for general public information on the subject. The material in this report including any test data presented and analytical results shall not be relied upon under any circumstances for any specific application or actual projects involving the SIP systems without consultation by a licensed design professional experienced in the field of light-frame design. Anyone using the material in this report assumes all liability resulting from such use, and the authors, Penn State University, or PHRC are not in any way liable for such use.

TABLE OF CONTENTS

LIST OF FIGURES

LIST OF TABLES

Chapter 1: Introduction

1.1 Background

Structural insulated panels (SIPs) are factory manufactured composite wall panels composed of a rigid foam insulation core sandwiched between two structural skins. SIPs are primarily used for residential and light commercial building construction and have been in use since the mid 1950s. SIP wall systems provide high whole-wall thermal resistance, limited construction waste, an airtight building envelope, and can be used for floors, walls, and roofs. Section R614 of the 2007 International Residential Code (IRC) Supplement added design provisions for SIP construction in Seismic Zones A, B, and C. The prescriptive provisions allow SIPs to be used without added engineering analysis, but limit their scope to oriented strand board (OSB) faced and Expanded Polystyrene (EPS) cored panels.

Currently SIPs are not mentioned in the International Building Code (IBC) or ASCE 7-05, *Minimum Design Loads for Buildings and Other Structures*, and acceptance into these standards is a substantial issue for the SIP industry (FAS, 2009). The International Code Council (ICC) develops and updates the IRC and IBC, which are the primary building code documents adopted by municipalities to govern construction. The prescriptive ICC Codes specify a set of rules to achieve a desired effect. The primary mode of SIP evaluation has been through comparative performance evaluation of SIPs and traditional wood-frame walls with structural sheathing. The ICC Evaluation Service (ICC-ES) drafted two acceptance criteria standards specific to SIPs but neither AC236 nor AC130 (ICC, 2009) have been implemented. Alternatively, products can be evaluated through Guide 65 Product Certification Agencies (PCAs) which permit analysis under general

loading and support conditions. A key parameter in defining the appropriate testing method is the ability to systematically evaluate the performance attributes of SIPs when subjected to seismic loading (FAS, 2009).

Extensive research has been conducted on the performance evaluation of wood-frame shear walls subjected to seismic loading, but a limited number of studies have been conducted on SIPs. The majority of SIP testing conducted to date is proprietary to individual manufacturers (Terentiuk, 2009). The complexity of wood-based structural components has also limited the availability of realistic wood-frame computer modeling programs and the ability to accurately predict the response of wood-frame shear walls subjected to seismic ground motions.

Prescriptive code provisions follow a complex seismic analysis procedure in accordance with ASCE 7-05 to ensure the building can distribute the applied forces safely. Each building is assigned Seismic Performance Factors (SPFs) representative of the specific materials and detailing used for the structural system. These performance factors are developed from the evaluation of the system under seismic loading. The development of seismic provisions has evolved over many decades in different countries. Various numerical values of SPFs have been developed and used in other countries. The variability demonstrates the need for a standardized, systematic, and rational procedure for determining these values.

In response to this need, the Federal Emergency Management Agency (FEMA) awarded the Applied Technology Council (ATC) a contract in 2004 with a variety of seismic and multi-hazard related tasks. The objective of one task was “to develop a procedure to

establish consistent and rational building system performance and response parameters (R, C_d, Ω_O) for the linear design methods traditionally used in current building codes." Implementation of the procedure is intended to provide an equivalent level of safety against collapse for buildings having different seismic force-resisting systems (ASCE, 2008a). In fulfillment of this task, the ATC-63 Project was completed and later published as FEMA P695 in June 2009 (FEMA, 2009).

1.2 Objective

The objective of this research is to develop a pilot project for the quantification of SPFs for wood-skinned structural insulated panels based on the methodology presented in FEMA P695. The scope of this pilot study is limited to studying one panel, spline, and fastener type selected based the results of the study presented by Terentiuk (2009) and summarized by Terentiuk and Memari (2011). Specifically, the pilot study presented here considers SIPs with OSB splines and 8d nail fasteners. Analytical studies in this pilot project are limited to residential dwellings and light commercial facilities comparable to the wood-frame structures in FEMA P695. This research primarily follows guidelines of the FEMA P695 methodology and applicable building codes to quantify the SPFs of R, C_d, and Ω_o for the selected type of SIP shear wall.

1.3 Research Approach

The ability to provide a reliable response prediction is dependent on the compilation of detailed system information. A well-defined seismic resistant concept including the configuration, energy dissipation mechanisms, and application range for the system must be developed. The system information is used to develop the selected system prototype buildings, referred to as "archetypes", and nonlinear analysis models for such archetypes.

Each archetype model is meant to simulate specific mode(s) of deterioration and is evaluated through nonlinear static and dynamic analysis using component test data obtained experimentally through cyclic loading. SIP experimental data used was obtained by tested 8ft x 8ft SIP shear wall piers in accordance with the CUREE loading protocol (CUREE, 2002). The testing, reported by Terentiuk (2009), is used in this study to conduct finite element analyses of four archetype models with the SAPWood computer program (Pei and van de Lindt, 2007). Evaluation of the nonlinear structural analyses against an appropriate level of safety against collapse will be used to determine suggested values for the SPFs for SIPs.

1.4 Report Organization

The research presented in this report is based on the following outline:

Chapter 2 – Literature review of past wood-frame and SIP shear wall studies.

Chapter 3 – FEMA P695 methodology review.

Chapter 4 – Description of the analytical testing program and procedures.

Chapter 5 – Finite element modeling of shear walls and structures for nonlinear analysis.

Chapter 6 – FEMA P695 based evaluation and analysis of SPFs.

Chapter 7 – Summary of work, conclusions, and recommendations for future studies.

Chapter 2: Literature Review

2.1 Introduction

Understanding the seismic performance of a structural system is one of the most important aspects to gaining recognition in building codes. The primary means of acquiring seismic performance data for wood-based systems is through monotonic and cyclic racking of wall components in combination with computer analysis. The following sections summarize reports and articles pertaining to the performance of wood-frame and SIP shear walls, and methods of deriving the seismic force coefficients used for design and analysis. A limited number of resources are available for SIP design methods, but useful insight is gained through comparative analysis between wood-frame and SIPs.

Response modification factors have been developed based on the knowledge that structural systems are able to develop lateral strength (capacity) greater than their nominal design strength and have ductile behavior characteristics (able to withstand inelastic deformation without collapse). The three primary coefficients used in seismic load calculations for buildings that will be discussed throughout this report consist of the response modification factor (R), deflection amplification factor(C_d), and system overstrength factor(Ω_O).

The horizontal force factor (K), the predecessor of the response modification factor (R), was presented as part of the base shear equation in the 1959 Structural Engineers Association of California Recommended Lateral Force Requirements (also known as the SEAOC Blue Book) (ATC 19, 1995). This was the first time a minimum design base

shear explicitly considered the type of structural system used. The 1978 ATC-3-06 report was the initial document to propose the response modification factors. The R factor is defined as "the ratio of the force level that would be developed in the system for design earthquake ground motions (if the system remained entirely linearly elastic) to the base shear prescribed for design" (FEMA, 2009). The factors for various systems used in the ATC-3-06 report were selected on the basis of "(a) general observed performance of like buildings in past earthquakes, (b) estimates of general system toughness, and (c) estimates of the amount of damping present during inelastic response" (ATC 19, 1995). This method of determining the factors was based on a limited number of existing lateral-force resisting systems. The complexity and quantity of systems has dramatically increased since the initial introduction and their ability to meet seismic demands are, "both untested and unknown" (ASCE, 2008a). The development of seismic provisions has evolved over decades and is by no means restricted to building design in the United States. The various numerical values of response modification factors have been developed and used in different countries. International variability and domestic uncertainty demonstrates the need for a standardized, systematic, and rational procedure for determining R factors. To meet this need, the primary goal of the ATC-63 Project was to establish a methodology for quantitatively determining the R factor and the directly related design parameters that affect building seismic response and performance for use in seismic design.

2.2 Manufacturers

The limited scope of SIPs in the International Residential (IRC) Code has compelled some SIP manufacturers to consider ICC-ES reports as one way to demonstrate their

product meets the intent of the code. Each manufacturer has a minor variation in panel framing, fastener schedule, or spline design. Table 1, Terentiuk (2009), summarizes the variation in capacity and description of SIPs produced by four manufactures.

Table 1: SIP Shear Wall Capacity

Manufacturer	**Description of SIP**	**Allowable Load (lb/ft)**	**Ultimate Load (lb/ft)**	**Ultimate Load for 8ft Long Wall (lb)**
Insulspan	5.5in. x 3 in. OSB spline, 8d nails at 6 in. o.c., 6 in. thick SIP	349	1,047	8,376
	(2) 2x6 spline, 8d nails at 6 in. o.c., 6 in. thick SIP	502	1,506	12,048
	(1) 2x6 spline, 8d nails at 4 in. o.c., 6 in. thick SIP	803	2,409	19,272
	(2) 2x6 spline, 8d nails at 2 in. o.c., 6 in. thick SIP	881	2,643	21,144
Precision Panel Building Products	3 in.x7/16 in. surface spline, 8d nails at 6 in. o.c., 4.5 in. thick SIP	170	510	4,080
	3 in.x7/16 in. surface spline, 8d nails at 6 in. o.c., 6.5 in.-12.5 in. thick SIP	155	465	3,720
Intermountain Building Panels	1.25 in. long steel drill screws at 3 in. o.c., 6.5 in. thick SIP	415	1,245	9,960
	1.25 in. long steel drill screws at 6 in. o.c., 6.5 in. thick SIP	360	1,080	8,640
R-Control Building Panels	4.5 in.-6.5 in. thick SIP (spline and hardware not specified)	335	1,005	8,040

SIPs act similar to a slender column when subjected to lateral out-of-plane loading. The sheathing resists tension and compression while the inner core provides continuous bracing. There are a limited number of design methods available for SIPs, but the

systems are highly comparable to wood-frame shear walls, which have been studied extensively.

2.3 Experimental Research

In 1997 Jamison tested 4 - 8ft x 8ft SIP configurations under monotonic and cyclic loading. This is the first notable published study on in-plane shear loading of SIPs. Each of the four wall configurations tested had varied anchorage, connection types, and used construction adhesive and drywall screws between panel and framing members. Jamison's (1997) monotonic tests included four static one-dimensional ramp tests, and eight static load-controlled tests performed as specified by ASTM E564. Cyclic testing was conducted on 11 wall samples and followed the Sequential Phased Displacement (SDP) testing procedure developed by Porter (1987). After defining testing frequencies and removal of the stabilization cycles, to produce more realistic nail fatigue results, this procedure was adopted by the Structural Engineers Association of Southern California (SEAOSC) as a standard test method for fully-reversed cyclic loading and is known as the "SEAOSC Method."

Jamison (1997) concluded: 1) SIP shear wall performance is governed by the connection at the bottom plate; 2) the SIP to bottom plate connection is the primary failure mode unless tie-down anchors were used, which in-turn increases stiffness, capacity and wall energy dissipation; and 3) monotonic and cyclic testing produced comparable levels of capacity. In comparison with wood-framed walls, anchors must be provided for SIP walls to reach equivalent levels of capacity. The study also mentioned the need for future research to address the effects of varied fastener types and configurations, contribution of

adhesives to stiffness, and the stiffness, ductility, energy dissipation, and damping characteristics important to seismic design.

Mosalam et al. (2008) tested cementitious SIPs (CSIPs) and OSB faced SIPs under prism shear, monotonic and cyclic loading. OSB SIP testing included three 2ftx2ft panels tested in accordance with ASTM E519, three 4ftx8ft panels tested under the CUREE monotonic and cyclic protocol (Krawinklet et al., 2000), and two 4ftx8ft panels tested pseudo-dynamically. The preliminary conclusion of the small scale seismic evaluation assesses SIPs to have reasonable energy dissipation and adequate strength capacity to meet the demands of the design basis earthquake with 10% probability of exceedance in 50 years.

Terentiuk (2009) tested 21 - 8ft x 8ft SIP shear walls under monotonic (ASTM 564-06) and cyclic (CUREE protocol and ASTM 2126-08) loading. Gatto and Uang's (2003) study of numerous cyclic loading protocols concluded that the deformation controlled CUREE protocol, which was developed specifically for wood-frame shear wall testing, reflected wood-frame shear walls failure modes most consistently. The deflection-controlled protocol consists of symmetric initiation, primary, and trailing cycles. The initiation cycles determine the small amplitude force-deformation response and act as a check for facility equipment and measuring devices. The primary cycles increase in amplitude and are followed by the trailing cycles, which have amplitude equal to 75% of its preceding primary cycle (CUREE, 2002). The protocol is provided in Table 2 and demonstrated graphically in Figure 1.

Table 2: CUREE Loading Sequence for Wood-frame Structures

Cycle Number	% δ
1 to 6	5.0
7	7.5
8 to 13	5.6
14	10.0
15 to 20	7.5
21	20.0
22 to 24	15.0
25	30.0
26 to 28	22.5
29	40.0
30 to 31	30.0
32	70.0
33 to 34	52.5
35	100.0
36 to 37	75.0
38	150.0
39 to 40	112.5

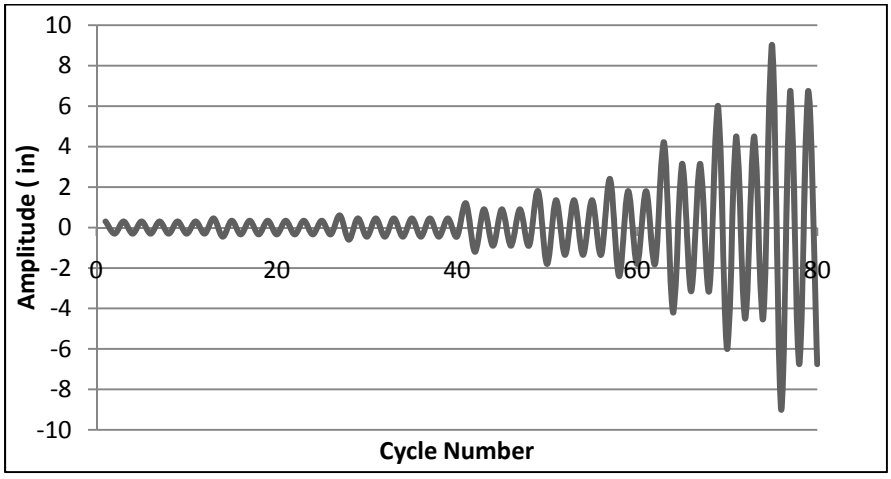

Figure 1: CUREE Loading Protocol (After: CUREE, 2002)

The sequencing cycles are based on the ultimate displacement (δ_u) as determined in the monotonic testing.

$$\delta = 0.6\,\delta_u \qquad (1)$$

The 40% reduction in deflection (0.6 factor in the equation) accounts for the cumulative damage incurred during the cyclic loading (Krawinkler et al., 2001).

4ft x 8ft SIP panels from the Timberline Panel Company, LLC out of Cambridge, New York with three hardware variations and two spline designs were evaluated (Terentiuk, 2009). Each panel was 4.5 in. thick and composed of a 3.5 in. thick expanded polystyrene (EPS) core and 7/16 in. oriented strand board (OSB) facings. 8ft x 8ft wall sections consisting of two connected panels were used for each test. Each SIP was manufactured to accept: a nominal 2 x 4 on the 4ft long top and bottom; various spline types on one of the 8ft sides; and double nominal 2 x 4 on the other 8ft side. Results from the Terentiuk (2009) study found that the OSB spline type and nail combination proved the most effective for load capacity, ductility, resistance under fatigue loading and seismic compatibility. Therefore, the data from that configuration was selected for the SIP archetype models for this study. The OSB spline wall configuration is shown in Figures 2 and 3.

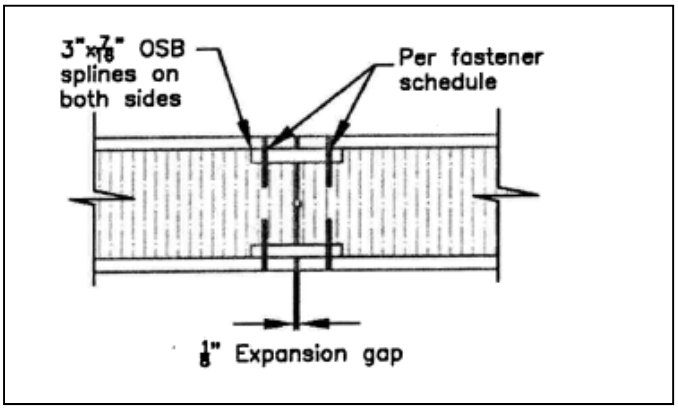

Figure 2: Surface Spline Configuration

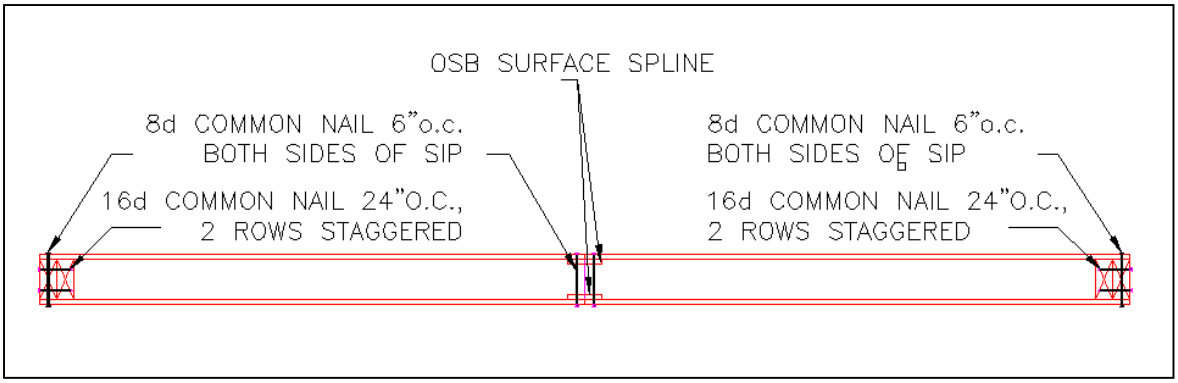

Figure 3: SIP Wall Plan Section

The selection of SIP walls that utilized hold-downs to resist overturning without using sealants was intended to provide results that are applicable to the widest possible range of the SIP industry. Toothman (2003), Lebeda et al. (2005), and Johnston et al. (2006) studied the effects of hold-downs anchors on wood-frame shear walls. Each concluded that hold-down had a significant effect on the strength and failure mode of the walls, but had minimal effects on stiffness and energy dissipation. PHD6-SDS3-WEST hold-downs produced by the Simpson Strong Tie Company were used by Terentiuk (2009) and are consistent with field conditions. Each hold-down was connected to the vertical end stud with 18 WS3 wood screws and into the sill plate and base support with 7/8 in. diameter bolts in accordance with ASTM E 2126-09 (2009). Johnston et al. (2006) concluded an increase in vertical load will in turn increase the lateral stiffness and energy dissipation capacity of the wall, and ASTM E 2126-09 (2009) states substantial vertical load (a maximum of 350 lb) may not be added to the wall. A continuous MC8x20 weighing approximately 200 lb was connected to the top plate as a safety restraint and to distribute the actuator load horizontally across the wall section. The sheathing was placed in accordance with Section 5.1.2.8 ICC-ES AC130 (2009), "when the primary shear-

resisting element of the prefabricated wood shear panels is wood-based structural-use sheathing, the sheathing shall not bear on the top or bottom fixtures of the test frame."

The Terentiuk (2009) testing program concluded: 1) fasteners were the primary mode of failure in every test; 2) common nails outperformed staples and screws; 3) varied spline types did not have significant effects on performance; 4) monotonic testing produced non-conservative results compared to cyclic loading; and 5) specimens can be repaired after loading and will reflect minimal losses in strength. Experimental facility strength and drift capacity limitations did hinder the complete assessment of numerous panels, but the testing provided definitive information regarding the performance of SIPs with various fasteners and spline configurations. The data obtained from the instrumentation was used to develop the monotonic backbone and hysteretic response curves for the wall sections, used for the equivalent single degree of freedom (SDOF) analytical models, and compared to analysis against the Nail-Parameter computer models in Chapter 5.

Blackwood (2009) developed a database of wood-frame shear wall models. Models were initially developed and calibrated by fitting 5 sets of experimental data to a 10-paramater hysteretic model. Additional variations were developed through the use of the systematic scaling and the SAPWood Nail Pattern analysis tool. The resultant hysteretic models compare well to full scale shear wall experimental data. These parameters, as developed by Blackwood (2009), were used to develop the wood-frame archetype models in this study, and are provided in Appendix Table A.7.

2.4 Analytical Studies

Although wood-frame residential buildings are the most common structures in North America, few analysis tools to evaluate their performance under lateral loads are available and those available are primarily used in research projects. Several studies to model wood-frame shear walls have been completed, but each is limited by the characteristics of wood, which is inhomogeneous and anisotropic, and its sheathing-to-framing connection response, which is nonlinear and exhibits strength and stiffness degradation under cyclic loading. These characteristics in combination with a significant degree of system redundancy create a complex modeling process. Therefore, reduction techniques have been used to produce computationally usable wood frame shear wall and building models. Table 3, summarized from Ayoub (2006), provides an extensive review of the progressive work with wood-frame numerical models.

Table 3: Analytical Studies of Wood-frame Shear Walls Using Numerical Methods of Analysis

Researcher(s)	Year	Analytical Study
Chehab	1982	• Created a linear elastic model of a two-story building
Itani and Cheung Falk and Itani	1984 1989	• Developed model with elastic plane stress and beam elements, and nonlinear joint elements
Gupta and Kua	1987 1985	• Model composed of seven "super-elements" and nine global DOF
Stewart Filiatrault Kasal and Leichti	1987 1990 1992	• Developed SDOF models with pinching and strength and stiffness degradation
Kasal et al.	1997	• Molded a one-story structure with the ANSYS computer program
Dolan Dolan and Foshchi White and Dolan	1989 1991 1995	• Developed a model with four sub-elements o elastic beam elements for studs o elastic orthotropic element for plywood shear wall o nonlinear spring for nails o bilinear compression spring for gap between walls
Davenne et al.	1998	• Developed a 3D model with nail strength degradation
Foshci	1995 2000	• Developed the computer program DAP-2D (diaphragm analysis program) • Added nail pinching effects
He et al.	2001	• Developed the computer program LightFrame 3D o thin plate elements for plywood, beam elements for studs, nonlinear spring elements o demonstrates nail shear and pullout characteristics
Folz and Filiatrault	2001	• Developed the computer programs CASHEW and SAWS
Ayoub	2006	• Developed SDOF pinched hysteretic model which represented four types of degradation o strength o unloading stiffness o accelerated stiffness o cap deterioration
Pei and van de Lindt	2007	• Developed SAPWood computer program capable of time domain analysis for structural and loss analysis

The work conducted by Folz and Filiatrault (2001) addressed the need for a comprehensive understanding of the response of wood-frame shear walls subjected to seismic ground motions. They developed a numerical model with the ability to

accurately capture the interaction between framing members and connectors during cyclic loading of wood-frame shear walls . While previous studies focused on the influence of panel size, fastener type, contribution from gypsum wall board, and effects of hold-downs to the degrading response of wood-frame shear walls under cyclic loading, Folz and Filiatrault aimed to provide a better representation of the interaction and load sharing between components.

Dolan and Madsen (1992) concluded that the response of a dowel-type connector in a wood shear wall is "highly nonlinear under monotonic loading and exhibits a pinched hysteretic behavior with strength and cyclic degradation." The degrading pinched hysteretic plot of cyclically loaded sheathing-to-framing connectors is analogous to the strength and stiffness degradation characteristics in the hysteretic response of a shear wall. Therefore, a greater correlation to a wood-frame structure's hysteretic response to seismic loading is provided through cyclic loading than monotonic loading, and a "specific hysteretic model based on a minimum number of path-following rules" would eliminate the need for full-scale shear wall test. The data needed for numerical analysis would be reduced to the shear modulus for the sheathing panels and cyclic test data from the sheathing-to-framing connectors. The model proposed by Folz and Filiatrault (2001) is composed of equivalent SDOF zero-height shear wall spring elements that connect infinitely in-plane stiff diaphragms and is characterized by 10 parameters that "assume that a shear wall is composed of pin-connected rigid framing members, elastic shear deformable-sheathing members, and nonlinear sheathing-to-framing connectors." The data was incorporated into the CASHEW (Cyclic Analysis of SHEar Wall) computer program, and the resulting calibrated spring elements reflect the strength and stiffness

degrading hysteretic characteristics of wood-frame shear walls. As addressed in Folz and Filiatrault (2001), the resulting SDOF system was then used to predict the load-displacement response of a shear wall subjected to ground motions. The equivalent shear spring element accurately represents the pinched, strength, and stiffness degrading hysteretic response demonstrated in experimental results, and accurately predicts the stiffness and strength degradation represented in the load-displacement diagram of the experimental model.

In 2004, Folz and Filiatrault expanded upon their research in order to "present a simple and versatile numerical model that predicts the dynamic characteristics, quasistatic pushover, and seismic response of wood-frame buildings." In Part II of a set of companion papers, Folz and Filiatrault (2004b) addressed the implementation and verification of the SAWS (Seismic Analysis of Wood-frame Structures) model to simulate the dynamic behavior of a building. The model results were compared to the Phase 9 and 10 results of a two-story wood-frame house tested on a shake table for the CUREE-Caltech Wood-frame Project. The results from Phases 9, bare wood-frame structure, and Phase 10, exterior and interior wall finishes added to the structure, produce good pushover capacities and seismic response and moderate relative displacement predictions. Prediction limitations were contributed to the simplification of the model, specifically with the assumed rigid behavior of the diaphragms. In conclusion, the results were deemed acceptable because they met the primary objectives of producing an implementable simplified wood-frame model.

The SAPWood (Seismic Analysis Package for Wood-frame Structures) computer program (Pei and van de Lindt, 2007) is based on the SAWS and CASHEW computer

program concepts. The program was created as part of the NEESWood Project and is capable of performing nonlinear seismic analysis and loss analysis for wood-frame structures. Linear spring, bilinear spring, 10-parameter hysteretic, and 16-paramater hysteretic models can be analyzed through nonlinear time domain excitation and Incremental Dynamic Analysis (IDA). The program also enables the user to conduct the analysis of structures beginning at the fastener level. The fastener hysteretic parameters are used in conjunction with the displacement-controlled loading protocols to model the lateral load-resistance behavior of wood-frame shear walls. A review of the SAPWood computer program including analysis options, model parameters, and loading protocols are discussed in-depth in Chapter 4.

Chapter 3: FEMA P695 Methodology

3.1 Methodology Introduction

The methodology for quantification of building SPFs is based on the collapse safety of archetype buildings. Each archetype model is subjected to nonlinear time-history analysis for a set of scaled ground motions until median collapse is reached. Evaluation of the collapse safety of the models is, "expressed as a minimum margin between median value of collapse capacity and intensity of the MCE (maximum considered earthquake) for which the models are designed" (ASCE, 2008b). The key elements of the methodology are shown in Figure 4 and are discussed in Chapter 3 and demonstrated through testing, calculations, and conclusions in Chapters 4 through 7. Key phrases, words, and process descriptors used in this report mimic those of the methodology for clarity and comparability.

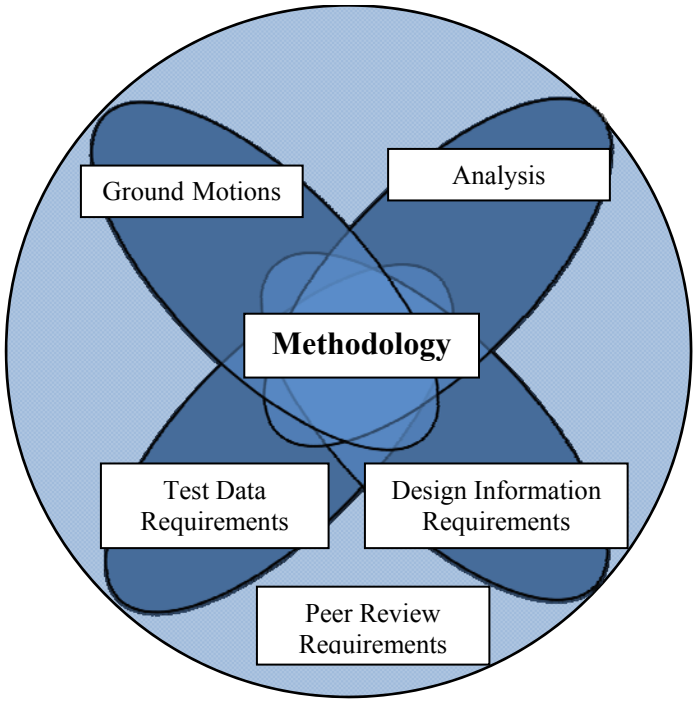

Figure 4: Methodology Key Elements (After: FEMA, 2009)

The FEMA P695 methodology is a combination of code concepts and nonlinear dynamic analysis and collapse predictions. It requires representative models of the system and valid MCE ground motions. Model development requires definitive design requirements and comprehensive test data of the system components and/or assemblies. Conversely, the ground motions and analysis methods are generalized for the majority of systems, and are clearly defined in the methodology. The NEHRP Provisions (FEMA, 2004) and ASCE 7-05 (ASCE, 2005) provide the primary guiding seismic design criteria for the methodology. The primary life safety objective of the NEHRP Provisions is to "provide the minimum criteria considered prudent for protection of life-safety in structures subject to earthquakes….. if a structure experiences a level of ground motion 1.5 times the design level, the structure should have a low likelihood of collapse" (FEMA, 2004b). To meet the primary life-safety objective, the methodology considers an acceptably low probability of collapse of the seismic force resisting system for MCE ground motions (ASCE, 2008a). The iterative methodology process is depicted in Figure 5.

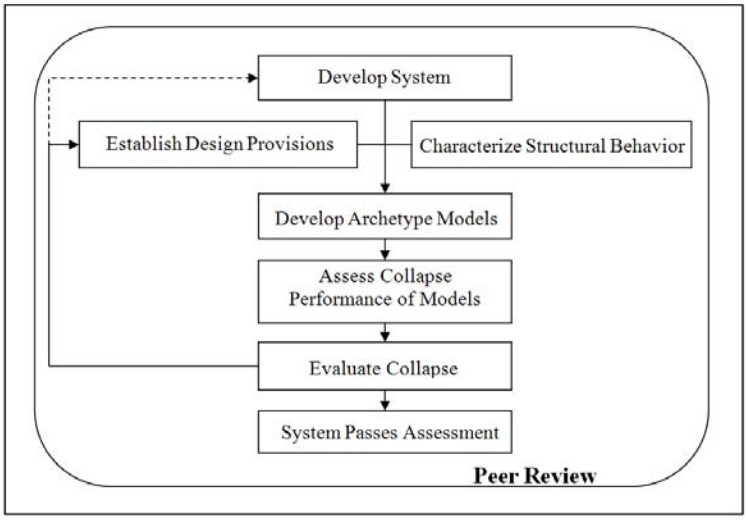

Figure 5: Methodology System Performance Assessment Flowchart (After: ASCE, 2008b)

A summary of the iterative process is outlined as follows:

- Archetype seismic force-resisting systems are designed to cover the expected range of building sizes, seismic design categories, and gravity loads.
- Experimental data and other supporting data is compiled and evaluated for the characterization of monotonic and cyclic behavior of the system.
- Analytical models of the building archetypes are developed to reflect the system data.
- Each archetype building model is subjected to nonlinear static pushover analysis to determine the overstrength factor and characterize the system ductility.
- Each building model is subjected to nonlinear dynamic analysis using 22 pairs of predetermined ground motion records. The ground motions are

incrementally scaled until half of the ground motions have caused collapse of the archetype.

- The collapse margin ratio (CMR) is determined as the ratio of the median collapse intensity to the maximum considered earthquake (MCE) intensity, and is then adjusted for analysis procedures and to account for the unique spectral shape effects of rare ground motions.
- The Adjusted CMR (ACMR) is evaluated with the total system collapse uncertainty (β_{TOT}) against methodology defined acceptance criteria.
- When minimum criteria are met, then the initial SPFs assumed for the system are deemed appropriate. Adjustments to the system scope, testing, design, and/or analysis and another evaluation of the iterative methodology must be completed if the minimum criteria are not met.
- The entire process must be evaluated by a peer review panel consisting of members qualified to critically evaluate the development of the proposed system.

3.2 System Information

The ability to provide a reliable structural response prediction is gained through the compilation of detailed system information. This information is specifically used to develop structural system "archetypes" and nonlinear analysis models. An archetype is defined as a "prototypical representation of a seismic-force-resisting system", and is "intended to reflect the range of design parameters and system attributes that are judged to be reasonable representations of the feasible design space and have a measurable impact on system response" (FEMA, 2009). This concept includes the material types,

configuration, dissipation mechanisms, and intended application range. The amount of information gathered is varied based on the establishment of the system. A system with less uncertainty needs a smaller amount of margin to resist collapse while still meeting the same levels of safety. However, a newer concept system, such as SIPs, requires more definitive design requirements and more comprehensive test data to meet the same margin of safety as that of an established system.

Each system is assigned four numerical values based on the following: 1) the confidence in basis of design requirements related to the actual level of behavior to intended results (β_{DR}); 2) the effectiveness of the testing program to quantify properties, behaviors, and failure modes of the system (β_{TD}); 3) the accuracy and robustness of models to represent collapse characteristics (β_{MDL}); and 4) total system collapse uncertainty based on record-to-record variability (β_{RTR}), which is assigned a set value of 0.4 for the methodology. Numerical values assigned to each quality ratings are tabulated in Appendix Table A.2 through A.4.. A single quality rating (β_{TOT}) is calculated as the square root of the sum of the squares of the individual quality ratings and defined the level of uncertainty in the system. Increased uncertainty in turn increases the probability of collapse and will consequently flatten the collapse fragility curve resulting from incremental dynamic analysis. A summary of the variables considered for quality ratings are provided in Table 4 and a summary of the values assigned for quality rating is summarized in Table 5.

Table 4: Quality Ratings Variables

Characteristics	**(Un)certainty**
Unanticipated failure modes	Confidence in Basis of Design Requirements
Design and quality assurance issues	
Material, component, connection, assembly, and system behavior	Confidence in Experimental Test Results

Testing program and data	
Representation of design parameters	Accuracy and Robustness of Models
Representation of failure modes	

Table 5: System Quality Ratings (After: FEMA, 2009)

Completeness, Robustness, and Representation of Characteristics	**Confidence and Accuracy**		
	High	**Medium**	**Low**
High	(A) Superior β = 0.10	(B) Good β = 0.20	(C) Fair β = 0.35
Medium	(B) Good β = 0.20	(C) Fair β = 0.35	(D) Poor β = 0.50
Low	(C) Fair β = 0.35	(D) Poor β = 0.50	--

Design requirements must be based on current and applicable codes and material standards and must conform to strength limit states. The design criteria of the system must also address: the overstrength if the system has small inelastic deformation capacity; the material properties and strength and stiffness requirements of each component and connection; a formulation of the fundamental period (T). The quality rating considers the completeness and robustness of failure modes, design, and quality assurance issues. It also considers the confidence in the basis for the design requirements. ASCE 7-05 (ASCE, 2006) and ANSI/AF&PA (ANSI/AF&PA, 2005) are used as the primary sources for design requirements for this project.

The methodology requires system information acquired in analytical modeling to be balanced with that of experimental investigation. Experimental data can come from differing, but reliable, programs to supplement the design information. A comprehensive experimental testing program must consider a wide range of variables, and its' quality

rating not only considers the quality of testing but also how well it represents the key system parameters and system behavior. The confidence in test results is related to reliability and repeatability of test results within the testing program and to other relevant testing programs. The procedures for the SIP laboratory tests and testing results used for analytical study are presented in Chapters 5. Selection of the design requirements and experimental test program quality ratings are addressed in Chapter 6.

3.3 Archetype Development

Archetype models, as addressed above, are a prototypical representation of a seismic-force-resisting system as characterized by its system information. Simply stated, they are meant to demonstrate how the system, in its varied forms and applications, will behave. The FEMA P695 methodology specifies terminology to delineate archetype levels and this report maintains term standardization for consistency. This section describes the properties and criteria used to define these models. The models will then be used for collapse simulation.

- *archetype design space* - the overall range of permissible configurations
- *index archetype configurations* – a set of building configurations
- *performance groups* – groups sharing common features or behavior characteristics
- *index archetype designs* – specified structural designs based on design criteria
- *index archetype models* – nonlinear analysis models analyzed to assess collapse performance

An index archetype configuration is suggested to have 20 to 30 structural configurations, but must be broad enough to cover the complete range of possible design requirements for the system. For feasibility, the configuration quantity can be reduced if specific non-design controlling characteristic trends form. The quantity may also be reduced if system design and detail requirements rule out specific failure modes. The formation of the information necessary for each configuration is summarized in Table 6 and provided in detail in Chapter 6. Configurations should only consider the system that does resist seismic forces. The mass and P-Delta effects of the remaining portion of the structural system should be considered in the archetype designs.

Table 6: Index Archetype Variables

Configuration Design Variables	**Seismic Behavioral Effects**
Occupancy and Use	Strength
Elevation and Plan Configuration	Stiffness
Building Height	Inelastic-deformation Capacity
Structural Component Type	Seismic Design Category
Seismic Design Category	Inelastic-system Mobilization
Gravity Load	

Configurations are divided into performance groups which reflect the major divisions in system configuration, loading, and period. Performance group design variations include SDC, gravity load, and building height variations. The groups are then subdivided into index archetype designs containing multiple building models. Index archetype designs should be developed using one of the following three ASCE 7-05 (2005) seismic design methods: Section 12.8, Equivalent Lateral Force (ELF); Section 12.9, Response Spectrum Analysis (RSA); or Chapter 16, Response History Analysis (RHA).

Index archetypes must be designed for the minimum and maximum SDC corresponding to the highest SDC unless unusual circumstances otherwise govern. Simply stated, if SDC D is the highest SDC the system will be used in, then analysis must be completed for SDC D_{min} and SDC D_{max}. Similar consideration must be given to gravity loads when they are of significant influence to the collapse mechanism of the seismic-force-resisting system. Analysis with minimum and maximum values of the gravity loads must be considered in the design variations. Building height also contributes heavily to the fundamental period of the structure and will influence the number of index archetype designs, where 3 is the typical number in each performance group. Table 7 summarizes the considerations for developing index archetype models.

Table 7: General Considerations for Developing Index Archetype Models (FEMA, 2009)

Model Attributes	Considerations
Mathematical Idealization	• Continuum versus phenomenological elements
Plan and Elevation Configurations	• Number of moment frame bays, regularity. • Planar versus 3-D wall representations, opening, coupling beams, regularity. • Variations to reflect diaphragm effects on stiffness and 3-D force distributions
2-D versus 3-D Component Behavior	• Prevalence of 2-D versus 3-D systems in design practice • Impact on structural response, including provisions for 3-D (out-of-place) failures in 2-D models
2-D versus 3-D System Behavior	• Characteristics of index archetype configurations such as diaphragm flexibility • Impact on structural response that is specific to certain structural systems

Each model within an index traditionally represents the system response through equivalent nonlinear springs, while nonlinear continuum finite elements models represent the model more directly. Wood-frame shear wall systems primarily can be two-

dimensional models, but are not excluded from three-dimensional modeling to demonstrate effects such as out-of plane instabilities. The structural components are idealized as combinations of beam elements, plate, and shell elements. Wall system models must reflect nonlinear stress and strain within the wall; particular attention must be given to punched shear walls (e.g., a shear wall with a window opening).

Models should simulate the modes of deterioration, and is simulated through the use of reversed cyclic loading. The load versus displacement response resulting from the application of the reversed cyclic loading represents the response properties of the components/system. The comparison of monotonic curve and cyclic loading backbone curve, which confines the hysteresis loops, illustrates the reduction in plastic deformation capacity. The displacement relative to 80% of the maximum strength measured in the cyclic loading can be used as a "conservative estimate of the ultimate deformation capacity of a component" (FEMA, 2009). The parameters of the component backbone curve are presented in the Chapter 4.

Alternate modes of collapse, defined as non-simulated collapse (NSC), can occur prior to the point typically considered. A NSC typically is associated with component failure, and its timing presumes it will lead to the collapse of the system. In wood-frame shear walls a possible NSC is failure of tie-downs. The variability's in collapse are factored into the system performance evaluation. Index archetype models are assigned a quality rating (β_{MDL}) based on:

- How well index archetype models represent the range of structural collapse characteristics and associated design parameters of the archetype design space
- How well the analysis models capture structural collapse behavior through both direct simulation and non-simulated limit state checks (FEMA, 2009)

The rating scale previously summarized in Section 3.2 represents the ability for the index archetype models to correlate the range of design parameters to structural collapse.

3.4 Seismic Design Provisions

The following information and equations summarize the seismic design requirements within ASCE 7-05 (2005) used to establish index archetype designs. The methodology only applies to Seismic Design Category (SDC) B, C, and D and Occupancy Category I and II. The following definitions from ASCE 7-05 (2005) and FEMA (2009) help to clarify the provisions defining the Maximum Considered Earthquake (MCE).

- S_s = mapped MCE, 5-percent damped, spectral response acceleration parameter at short periods as defined in Section 11.4.1 of ASCE 7-05.
- S_1 = mapped MCE, 5-percent damped, spectral response acceleration parameter at a period of 1 second as defined in Section 11.4.1 of ASCE 7-05.
- F_a = short-period site coefficient (at 0.2-second period) as given in Section 11.4.3 of ASCE 7-05.
- F_v = long-period site coefficient (at 1.0-second period) as given in Section 11.4.3 of ASCE 7-05.

MCE is defined in terms of these four variables, and the Design Earthquake (DE) is two-thirds that of the MCE demand. "For SDC B, C, and D, maximum and minimum ground motions are based on the respective upper-bound and lower-bound values of MCE and DE spectral acceleration, as given in Table 11.6-1 of ASCE 7-05 (2006), for short-period response, and Table 11.6-2, for 1-second response." The methodology requires "archetype systems to be designed for DE criteria, and then evaluated for collapse with respect to MCE demand." The methodology uses Site Class D (stiff soil) for all archetype designs. It also defines S_s =1.1g and S_1 = 0.6g as the maximum values of spectral acceleration in SDC D. By defining these bound, simplified tables, provided in the Appendix from FEMA P695, can be used for parameter selection in the methodology. The base shear (V) equation, containing the Seismic Response Coefficient (C_s) and the effective seismic weight (W), is the basis of defining the forces for the ELF procedure.

$$V = C_S W \tag{2}$$

The transition period (T_S) is defined as the "boundary between the region of constant acceleration and the region of constant-velocity of the design response spectrum" (FEMA, 2009).

$$T_S = \frac{S_{D1}}{S_{DS}} = \frac{S_{M1}}{S_{MS}} \tag{3}$$

Where $T \leq T_s$ the seismic coefficient is defined as:

$$C_S = \frac{S_{DS}}{R} \tag{4}$$

And when $T > T_s$ it is defined by:

$$C_S = \frac{S_{DS}}{T\,R} \geq 0.44\,S_{DS} \qquad (5)$$

R is the trial value being used for the seismic-force-resisting system. The equations have an implied Importance Factor of I = 1.0, and are constrained by ASCE 7-05 (ASCE, 2006) Equations 12.8-5 and 11.7-1, which limits C_s to 0.01 and F_x to $0.01w_x$, respectively. Also, Equation 12.8-6 does not apply considering S_1 <0.60 (g). T_L, from Section 11.4.5, does not come into consideration due to a maximum value of T=4 seconds for the methodology.

The fundamental period of the building (T) is defined in Section 12.8.2.1 of ASCE 7-05 (2006).

$$T = C_S\,T_a = C_u\,C_t\,H_n^x \geq 0.25\ seconds \qquad (6)$$

Coefficient values (C_u), (C_t), and (x) can be found in Tables 12.8-1 and 12.8-2 of ASCE 7-05, respectively. The building height is defined by the term (h_n). The method for defining the approximate fundamental period, T_a, must be defined in the system design requirements.

Seismic load effects combinations are to be defined in accordance with Section 12.4 of ASCE 7-05 and the methodology. Snow load and foundation loads are not considered for evaluation of the seismic-force resisting system. A sequential definition of the coefficients is as follows; structural self-weight and superimposed dead loads (D), live load with reduction factors (L), horizontal seismic-force effect from base shear (Q_E), and overstrength factor (Ω_O). If minimum wind values control over seismic loading, then

values should be based from the guidance in Chapter 6 of ASCE 7-05. The load combinations for strength design provided from ASCE 7-05 (2006) Section 12.4.3.2 are:

$$(1.2 + 0.2S_{DS})D + Q_E + L \quad (7)$$

$$(0.9 - 0.2S_{DS})D + Q_E \quad (8)$$

or when overstrength factor is required:

$$(1.2 + 0.2S_{DS})D + \Omega_O Q_E + L \quad (9)$$

$$(0.9 - 0.2S_{DS})D + \Omega_O Q_E \quad (10)$$

The trial values of the seismic performance factors (R), (C_d), and (Ω_O) are required to determine index archetype designs. Guidance on the selection of trial values will be discussed in the performance evaluation section of the methodology review.

3.5 Nonlinear Analysis

This section describes the static and dynamic nonlinear analysis procedures to be conducted on the archetype models developed. Model analyses are conducted to acquire statistical data on system overstrength (Ω), period-based ductility (μ_T), median collapse capacities ($\hat{S}_{CT}$), and collapse margin ratios (CMRs).

The gravity loads used for nonlinear analysis are not equal to those used for gravity load design. The load factors are based on median values. The loads may be reduced for influence area, but may not be reduced for other factors.

$$1.05D + 0.25L \quad (11)$$

D is the nominal structure and superimposed dead load and L is the nominal live load.

The software used for nonlinear analysis must have the capacity to perform static pushover and dynamic response history while accounting for strength and stiffness degradations.

Nonlinear static (pushover) analysis is used to develop the monotonic backbone curve and the hysteretic response of each model. The models must be able to reflect the strength and stiffness degradation effects of the system. As observed by Ibarra et al. (2005) the post-capping degradation portion of the monotonic backbone curve is essential to simulating collapse due to the combined effects of inelastic softening and P-Δ effects.

Pushover analysis is conducted to calculate the archetype overstrength (Ω) and period-based ductility (μ_T) factors. The idealized nonlinear static pushover curve (FEMA, 2009) in Figure 7 shows the design base shear (V), maximum base shear capacity (V_{max}), ultimate displacement, (δ_u), and effective roof drift displacement ($\delta_{y,eff}$). The lateral load is applied until the system reaches a loss of 20% of the base shear capacity, $0.8V_{max}$.

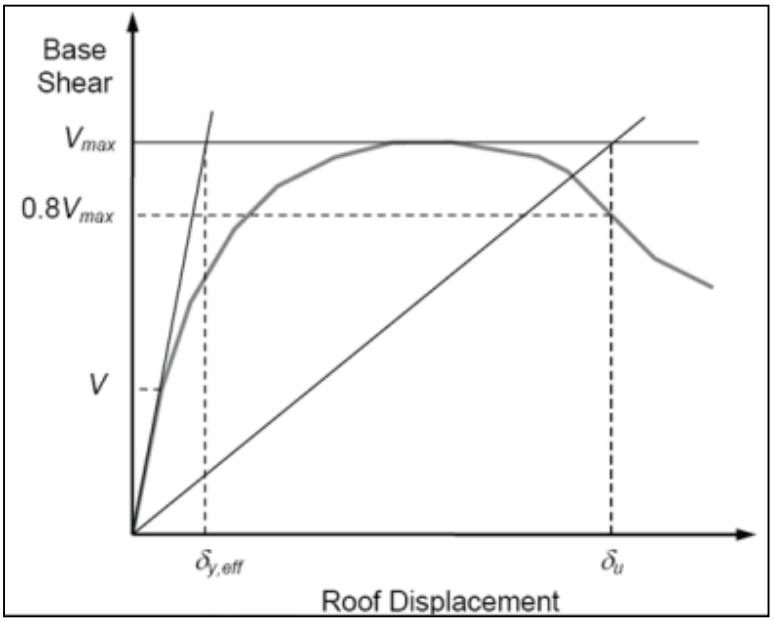

Figure 6: Nonlinear Static Pushover Curve (Source: FEMA, 2009)

Pushover analysis shall be performed in accordance with Section 3.3.3 of ASCE 7-05 (2006). The lateral force at each story is proportional to the mode shape of the model:

$$F_x \propto m_x \, \phi_{1,x} \tag{12}$$

The archetype overstrength factor is defined as:

$$\Omega = \frac{V_{max}}{V} \tag{13}$$

The archetype overstrength factor (Ω) is the calculated overstrength of the pushover analysis of one specific model. The overstrength factor (Ω_O) is defined as the most appropriate value selected Ω to use in design of the entire system.

The period-based ductility is defined as:

$$\mu_T = \frac{\delta_u}{\delta_{y,eff}} \tag{14}$$

The effective yield roof drift displacement is defined as:

$$\delta_{y,eff} = C_O \frac{V_{max}}{W} \left[\frac{g}{4\pi^2}\right] (\max(T, T_1))^2 \tag{15}$$

where g is the constant gravity, T is the code-based fundamental period of the model, and T_1 is the fundamental period of the model based on eigenvalue analysis . The coefficient C_O is based on Equation C3-4 of ASCE 41-06 (ASCE, 2006b) and is defined as:

$$C_O = \phi_{1,r} \frac{\sum_1^N m_x \phi_{1,x}}{\sum_1^N m_x \phi_{1,x}^2} \tag{16}$$

where r and x represent a floor level and the roof level, respectively, and N is the total number of levels.

The global SPF's (R, C_d, Ω_O) used for collapse probability assessment are defined by dimensionless ratios, but are depicted below as incremental differences between parameters with dimensions. In Figure 7, the SPFs are defined "in terms of global inelastic response (idealized pushover curve) of the seismic force-resisting system" (FEMA, 2004b).

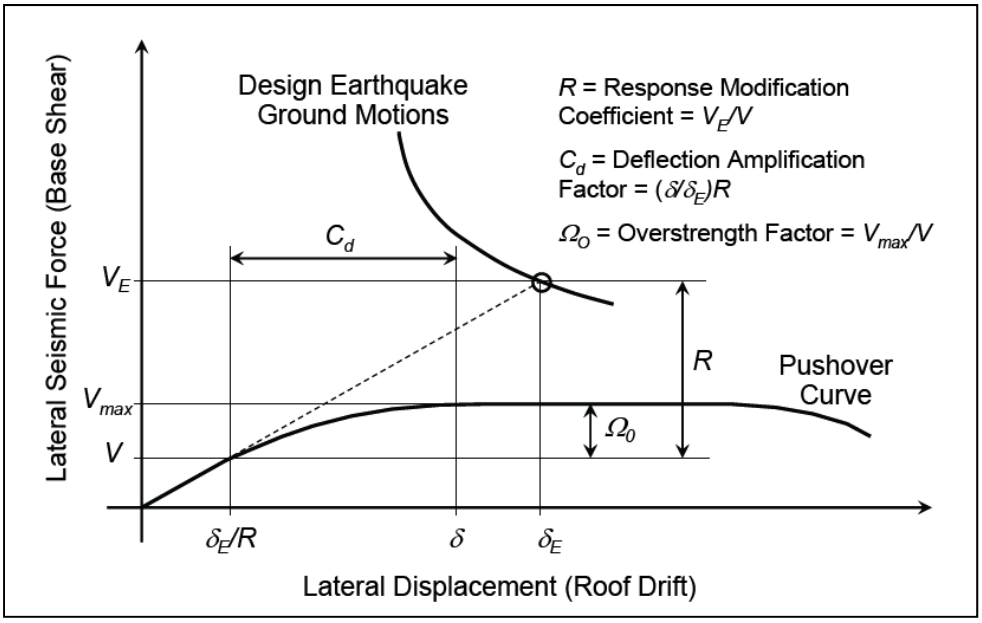

Figure 7: Code Illustration of Seismic Performance Factors (Source: FEMA, 2004b)

Equations for SPFs are in accordance with the Commentary of the NEHRP Provisions (FEMA, 2004b). The response modification factor (R) is the ratio of the force level developed in the system for design earthquake ground motions (V_E) (if the system

remained linear elastic for the earthquake motions) to the seismic base shear required for design (V):

$$R = \frac{V_E}{V} \tag{17}$$

The overstrength factor (Ω_O) is defined as the ratio of the actual fully yielded system strength (V_{max}) to the design base shear:

$$\Omega_O = \frac{V_{max}}{V} \tag{18}$$

The deflection amplification factor (C_d) is defined by the roof drift of the system corresponding to the base shear (δ_E/R) (if the system remained linear elastic for the level of force) and the assumed roof drift of the yielded system:

$$C_d = \frac{\delta}{\delta_E}\, R \tag{19}$$

The conversion to spectral coordinates is based on the base shear (V) equation (Equation 12.8-1, ASCE, 2006), and the assumption that all the effective seismic weight of the structure (W) participates in the fundamental mode at period (T) (FEMA, 2004b). The

SPF's are defined in terms of spectral coordinates in Figure 8.

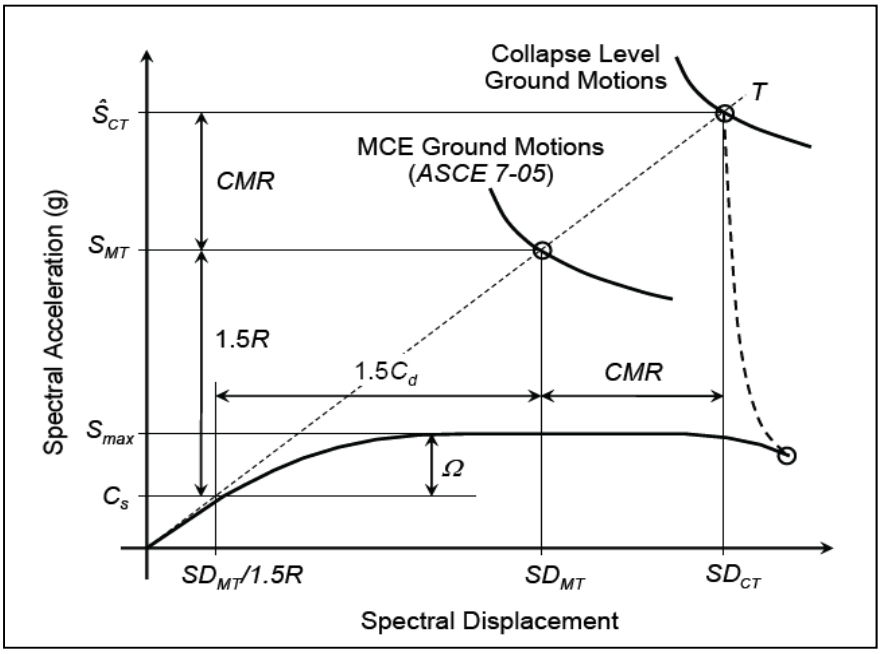

Figure 8: Methodology Illustration of Seismic Performance Factors (Source: FEMA, 2004b)

The terms MCE spectral acceleration at period T (δ_{MT}) and the fully-yielded strength normalized by W (S_{max}) are represented in Figure 8. The base shear (V) equation remains unchanged, and is define by W and the seismic response coefficient (C_s):

$$V = C_S W \tag{20}$$

Equations for SPFs in terms of spectral coordinates are in accordance with the methodology (FEMA, 2009). 1.5 times R is shown in the figure and defined as:

$$1.5\ R = \frac{S_{MT}}{C_s} \tag{21}$$

The archetype overstrength parameter (Ω) is defined as the ratio of (δ_{max}) to W:

$$\Omega = \frac{S_{max}}{C_s} \quad (22)$$

Ω is based on pushover analysis and the most appropriate value for the design of the system is used for the system overstrength factor (Ω_O), and should be conservatively increased to be larger than the average value of the calculated archetype overstrength (Ω) from any performance group. The system overstrength must not exceed 1.5 times the response modification factor (R), must be defined in an increment of 0.5, and has a practical maximum limit of 3.0.

The deflection amplification factor (C_d) is based on the acceptable response modification factor (R) and the damping factor (β_I). C_d is based on the "Newmark rule", "which assumes that inelastic displacement is approximately equal to elastic displacement (at the roof)." An assumed value of 5% damping may be used to effectively define C_d as (FEMA, 2009):

$$C_d = R \quad (23)$$

The calculated seismic performance factors are used for collapse assessment evaluation.

3.6 Collapse Assessment

Each model is subjected to the predefined ground motions that are "systematically scaled to increasing intensities until median collapse is established….Collapse performance is evaluated relative to ground motion intensity associated with the MCE." The methodology defines the collapse level ground motions as, "the intensity that would result in median collapse of the seismic-force-resisting system" (FEMA, 2009). Response History analysis is used to calculate the median collapse capacities ($\hat{S}_{CT}$) and

the CMR. The ground motion sets are scaled based on the fundamental vibration period of the model being evaluated. The level at which one-half of the structures at this level of ground motions collapse, defined as median collapse, is used to determine the CMR.

Ground motion sets are provided for nonlinear dynamic analysis collapse assessment. The sets of ground motion used in the methodology are meant to be "generally applied to any geological site" (FEMA, 2009). Two sets of ground motions, "Near-Field" and "Far-Field", are supplied in the methodology to provide an unbiased group that "represents strong ground motion shaking with earthquake magnitudes of 6.5 to 7.9" (ASCE, 2008b). Far-Field record sets are provided for archetypes indexes in SDC B, C, or D and include 22 component pairs of horizontal ground motions from sites located greater than or equal to 10km from fault rupture. They are meant to be used to evaluate all SDC's, seismic regions, and soil classification, but may not be used for buildings with a fundamental period of vibration greater than 4 seconds. Near-Field sets are used to evaluate potential differences in the CMR for SDC E structure and contain 22 component pairs of horizontal ground motions recorded at sites less than 10km from fault rupture. Record sets are from all large-magnitude, strong-motion events in the Pacific Earthquake Engineering Research Center (PEER) Next Generation Attenuation (NGA) database (PEER, 2006a). A maximum of two strongest records from an individual earthquake is included in the record sets.

The records are scaled in a two-step process: normalizing and scaling. The normalization portion of the process was completed during the development of the record sets. Scaling is analogous to Section 16.1.3.2 of ASCE 7-05 (2006). The normalized ground motions are collectively scaled to a specific ground motion intensity such that "the median

spectral acceleration of the record set matches the spectral acceleration at the fundamental period (T) of the index archetype that is being analyzed" (FEMA, 2009).

Each model is subjected to the ground motions through Incremental Dynamic Analysis (IDA). IDA is a technique to systematically process the effects of increasing earthquake ground motion intensity on structural response up to collapse (Vamvatsikos and Cornell, 2002). The results of each analysis are plotted as a single point on a record spectral intensity to peak inter-story drift graph. Curves on the graph represent the response of one structure subjected to increasing ground motion intensity until collapse is reached. Curves are "cut short" if a vertical collapse mode is detected prior the simulated sidesway collapse mode is reached. Hundreds of points (multiple analyses of varying intensity times 22 pairs of earthquake ground motions) are plotted on the horizontal axis (maximum recorded story drift) and vertical axis (spectral ground motion intensity) graph. Each point is for one ground motion record, scaled to one intensity level, for one archetype model.

The collapse margin ratio is defined in terms of the ratio of median 5% damped spectral acceleration at the collapse level ground motions ($\hat{S}_{CT}$) (or corresponding displacement, SD_{CT}) to the 5% damped spectral acceleration of the MCE ground motions (S_{MT}) (or displacement, SD_{MT}) (FEMA, 2009). The CMR is calculated as:

$$CMR = \frac{\hat{S}_{CT}}{S_{MT}} = \frac{SD_{CT}}{SD_{MT}} \quad (24)$$

For short-period archetypes ($T \leq T_S$), the MCE ground motion intensity, S_{MT}, is defined as:

$$S_{MT} = S_{MS} \quad (25)$$

For long-period archetypes ($T>T_S$) it is defined as:

$$S_{MT} = \frac{S_{M1}}{T} \quad (26)$$

Table 8 summarizes the methodology tabulated values of the 5% damped spectral acceleration of the MCE ground motions.

Table 8: Summary of Maximum Considered Earthquake Spectral Accelerations and Transition Periods Used for Collapse Evaluation of Seismic Design Category D, C, and B Structure Archetypes, Respectively (Source: FEMA, 2009)

Seismic Design Category		**Maximum Considered Earthquake**		**Transition Period**
Maximum	**Minimum**	**S_{MS} (g)**	**S_{M1} (g)**	**T_S (sec.)**
D		1.5	0.9	0.6
C	D	0.75	0.30	0.4
B	C	0.50	0.20	0.4
	B	0.25	0.10	0.4

An illustration of an IDA plot with corresponding S_{MT}, $\hat{S}_{CT}$, and CMR is shown in Figure 9.

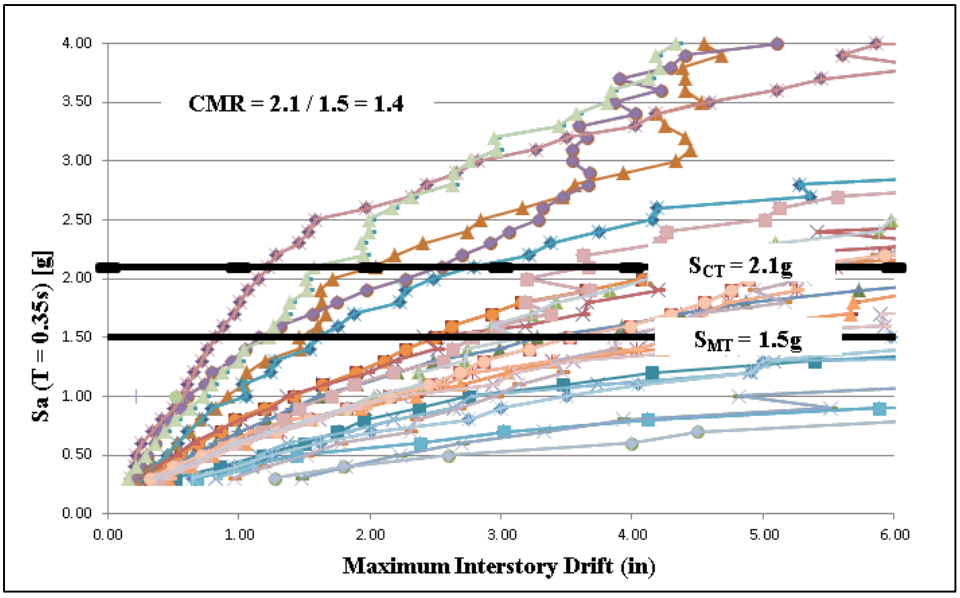

Figure 9: IDA Plot of Ground Motion Intensity Versus Building Drift

The collapse of the seismic-force resisting system is based on system characteristic uncertainty and ground motion variability. These characteristics, from the IDA collapse statistics, are represented in a collapse fragility curve. The lognormal curve is dependent on median collapse intensity, $\hat{S}_{CT}$ and the dispersion or standard deviation of the natural logarithm,$(\sigma(\ln(Sa)))$.

The fragility curves are modified to account for modal uncertainty (β_{TOT}) and spectral shape factor (SSF), and describe the probability of collapse as a function of ground motion intensity. The SSF is dependent on fundamental period, period-based ductility, and the applicable SDC.

$$ACMR = SSF \; x \; CMR \qquad (27)$$

The resulting adjusted collapse margin ratio (ACMR) is related to the probability of collapse at the MCE ground motion intensity. The calculated ACMR is compared to the

acceptable ACMRs, which are provided in Chapter 6. Different amount of collapse uncertainty between systems (with the same R factor and C_S values) will result in different CMR values and collapse fragility curves. Figure 10 (FEMA, 2004a) depicts how a system with greater uncertainty, System No.1, will have a "flatter" collapse fragility curve than a similar system with less uncertainty, System No. 2. In order to achieve the same design R value, System No.1 would have a larger CMR than System No. 2.

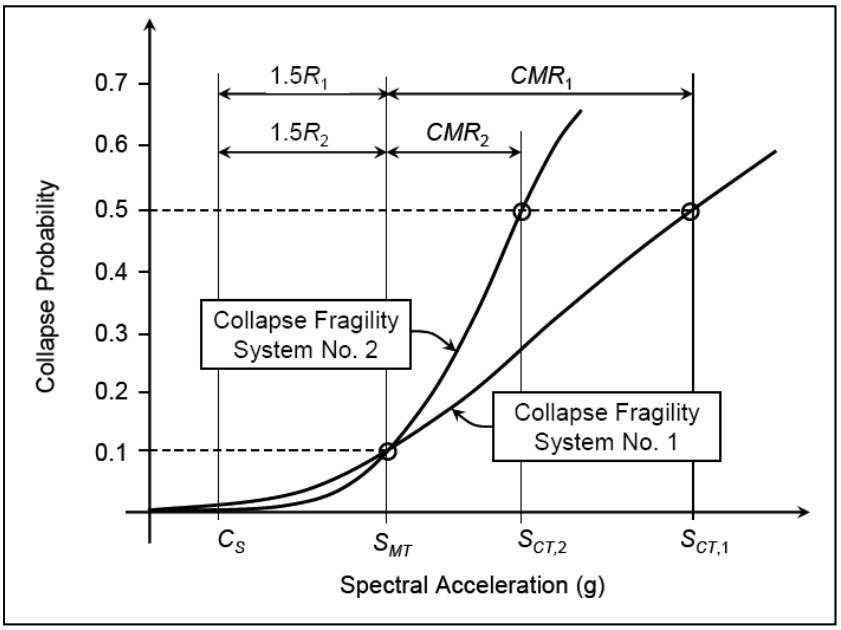

Figure 10: Fragility Curves and CMR Comparing Same Design Level Systems (Source: FEMA, 2004a)

Acceptable values of the CMR are defined in terms of uncertainty and probability of collapse for MCE ground motions. The evaluation of both terms is addressed in subsequent section.

3.7 Performance Evaluation

This section of the methodology evaluates the performance of the systems and the trial value of the response modification factor. Calculation of the system overstrength factor and amplification factor are also addressed. The methodology clearly outlines the step-by-step performance evaluation process:

- Obtain calculated values of overstrength (Ω), period-based ductility (μ_T), and collapse margin ratio (CMR) for each archetype from the nonlinear analysis results.
- Calculate the adjusted collapse margin ratio (ACMR) for each archetype using the spectral shape factor (SSF) which depends on the fundamental period (T) and period-based ductility (μ_T).
- Calculate total system collapse uncertainty (β_{TOT}) based on the quality ratings of design requirements and test data and the quality rating of index archetype models.
- Evaluate the adjusted collapse margin ratio (ACMR) for each archetype and average values of ACMR for each archetype performance group relative to acceptable values.
- Evaluate the system overstrength factor (Ω_O).
- Evaluate the displacement amplification factor (C_d).

If evaluation of the ACMR is found unacceptable then the system definitions should be adjusted and the procedure should be repeated. The methodology procedure is intended to have no more than one iteration to reach a point where AMCR evaluation finds acceptable seismic performance factors.

3.7.1 Performance Group Evaluation Criteria

The response modification factor (R) and system overstrength factor (Ω_O) are evaluated for each performance group. The trial value of the R factor must be acceptable for all groups. Ω_O is based on the largest average value of overstrength (Ω) from all performance groups. The same performance group does not have to govern R and Ω_O.

3.7.2 Acceptable Probability of Collapse

The methodology strives to not exceed a probability of collapse due to MCE ground motions of 10% on average across a performance group. Each performance group is required to meet the 10% standard, and any index archetype within a group with a value of 20% is considered an "outlier." Outliers can be negated by the use of a more conservative seismic performance factors or through revisions of the design requirements.

3.7.3 Adjusted Collapse Margin Ratio

The spectral shape significantly influences the calculation of the collapse margin ratio. This is accounted for through the use of the simplified spectral shape factor, SSF, to adjust the collapse margin ratio. The SSF is dependent on fundamental period, period-based ductility, and the applicable SDC.

$$ACMR_i = SSF_i \; x \; CMR_i \qquad (28)$$

Chapter 6 Tables 27 and 28 provide the values of SSF used to adjust the collapse margin ratio. Consideration of the SSF may alter the governing performance group.

3.7.4 Total System Collapse Uncertainty

Large variability in collapse prediction in-turn requires larger collapse margins to ensure acceptable levels of collapse probability. There are four primary sources of collapse response uncertainty and each must be fully evaluated. A review of the four primary sources is as follows:

- Record-to-Record Uncertainty (RTR) - Due to the "variability in the response of index archetypes to different ground motion records." β_{RTR}, is a fixed value of 0.4 for the methodology unless the system has limited period based ductility.
- Design Requirements Uncertainty (DR) - Related to the quality, completeness and robustness, of the design requirements.
- Test Data Uncertainty (TD) - Related to the completeness and robustness of the test data used to define the system.
- (MDL) - Related to quality of index archetype modes.

Total uncertainty is obtained by combining the four primary sources of uncertainty, and influences the shape of the collapse fragility curve. The total system collapse uncertainly (β_{TOT}) is defined as:

$$\beta_{TOT} = \sqrt{\beta_{RTR}^2 + \beta_{DR}^2 + \beta_{TD}^2 + \beta_{MDL}^2} \quad (29)$$

Values for β_{DR}, β_{TD}, and β_{MDL} are provided in Appendix Tables A.2 through A.4. An increase in uncertainty will flatten the curve plotted from IDA. Increased uncertainty in-turn increases the probability of collapse at the MCE intensity, S_{MT}, and affects the CMR.

Total system collapse uncertainty values tabulated in FEMA (2009) are shown in Table 9. The values provided are based on a RTR uncertainty, $\beta_{RTR} = 0.4$.

Table 9: Total System Collapse Uncertainty (β_{TOT}) for Model Quality and Period-based Ductility, $\mu_T \geq 3$

Model Quality (A) Superior				
Quality of Test Data	**Quality of Design Requirements**			
	(A) Superior	**(B) Good**	**(C) Fair**	**(D) Poor**
(A) Superior	0.425	0.475	0.550	0.650
(B) Good	0.475	0.500	0.575	0.675
(C) Fair	0.550	0.575	0.650	0.725
(D) Poor	0.650	0.675	0.725	0.825
Model Quality (B) Good				
(A) Superior	0.475	0.500	0.575	0.675
(B) Good	0.500	0.525	0.600	0.700
(C) Fair	0.575	0.600	0.675	0.750
(D) Poor	0.675	0.700	0.750	0.825
Model Quality (C) Fair				
(A) Superior	0.550	0.575	0.650	0.725
(B) Good	0.575	0.600	0.675	0.750
(C) Fair	0.650	0.675	0.725	0.800
(D) Poor	0.725	0.750	0.800	0.875
Model Quality (D) Poor				
(A) Superior	0.650	0.675	0.725	0.825
(B) Good	0.675	0.700	0.750	0.825
(C) Fair	0.725	0.750	0.800	0.875
(D) Poor	0.825	0.825	0.875	0.950

Acceptable values of adjusted collapse margin ratio are based on the total system collapse uncertainty and the values of acceptable probability. Acceptable performance is defined in FEMA, 2009 with two objectives:

- The probability of collapse for MCE ground motion is approximately 10% or less, on average across a performance group.

$$\overline{ACMR_i} \geq ACMR_{10\%}$$

- The probability of collapse for MCE ground motions is approximately 20% or less, for each index archetype within a performance group.

$$ACMR_i \geq ACMR_{20\%}$$

Acceptable values of adjusted collapse margin ratio are shown in Chapter 6 Table 29 from FEMA (2009) data.

3.7.5 Overstrength and Deflection Amplification Factor Evaluation

The system overstrength factor, Ω_O, should be conservatively increased to be larger than the average value of the calculated archetype overstrength (Ω) from any performance group. The system overstrength must not exceed 1.5 times the response modification factor (R), must be defined in an increment of 0.5, and has a practical maximum limit of 3.0 as shown in Table 12.2-1 of ASCE 7-05.

The deflection amplification factor (C_d) is based on the acceptable R factor and the damping factor (B_I).

$$C_d = \frac{R}{B_I} \tag{30}$$

An assumed value of 5% may be used for damping. Table 18.6-1 in ASCE 7-05 lists the damping coefficients as based on the period (T) and the effective damping (β_I). Effective damping is defined in Section 18.6.2.1 of ASCE 7-05 as the inherent dissipation of

energy by elements of the structure at or just below the effective yield displacement of the seismic-force-resisting system.

Chapter 4: Finite Element Model Analysis Program

This chapter outlines the SDOF shear wall hysteretic models, structural configuration, and kinematic building model assumptions for the finite element model computer program used in this study. The SAPWood computer program was developed as part of the "NEESWood Project funded by the National Science Foundation . … It is a wood-frame analysis program based on the CASHEW and SAWS platforms" (Pei and van de Lindt, 2007). Generalized data is presented in this chapter, and subsequent chapters explain the actual testing and analysis conducted for this study.

4.1 Structural Configuration of Numerical Models

The SAPWood computer program is used for all analytical modeling of the SIP archetypes and equivalent wood-frame archetypes in this study. The program has the capacity to perform static pushover analysis and dynamic response time-history analysis while accounting for strength and stiffness degradations (Pei and van de Lindt, 2007). The components (studs and panels) of the shear wall are modeled as rigid bodies and displace as a rigid body dependent on the restraint of the elements (fasteners) connecting them. The numerical model predicts the equivalent system load-displacement response of the shear wall based on the sheathing-to-framing fastener parameters.

Wall sections are modeled in two distinct ways. First, a Nail Parameter (NP) model, which has 3 DOFs for each stud and panel, is built by systematically defining the location of each component and the location and hysteretic parameters of the connector elements. Alternatively, walls can be defined by the hysteretic parameters obtained from experimental testing. Both approaches are utilized in this study. The structural components are idealized as combinations of beam, plate, and shell elements. The

building structure in each model is composed of rigid horizontal diaphragms and the equivalent nonlinear lateral load resisting shear wall elements. The equivalent wall elements reflect the strength and degrading stiffness behavior of the experimental shear walls, and the 10 parameters defining a component/system, resulting from the load-displacement response of the analysis, simulate the modes of deterioration in the system.

Ten parameters, when calibrated, are used to define the sheathing-to-framing fastener parameters and equivalent nonlinear shear spring elements. The zero height nonlinear springs are used to develop building models. The hysteretic curve used to demonstrate the properties of wood-frame shear walls, as modeled is Figure 11, was developed using a modified Stewart hysteretic model (Pang et al, 2010).

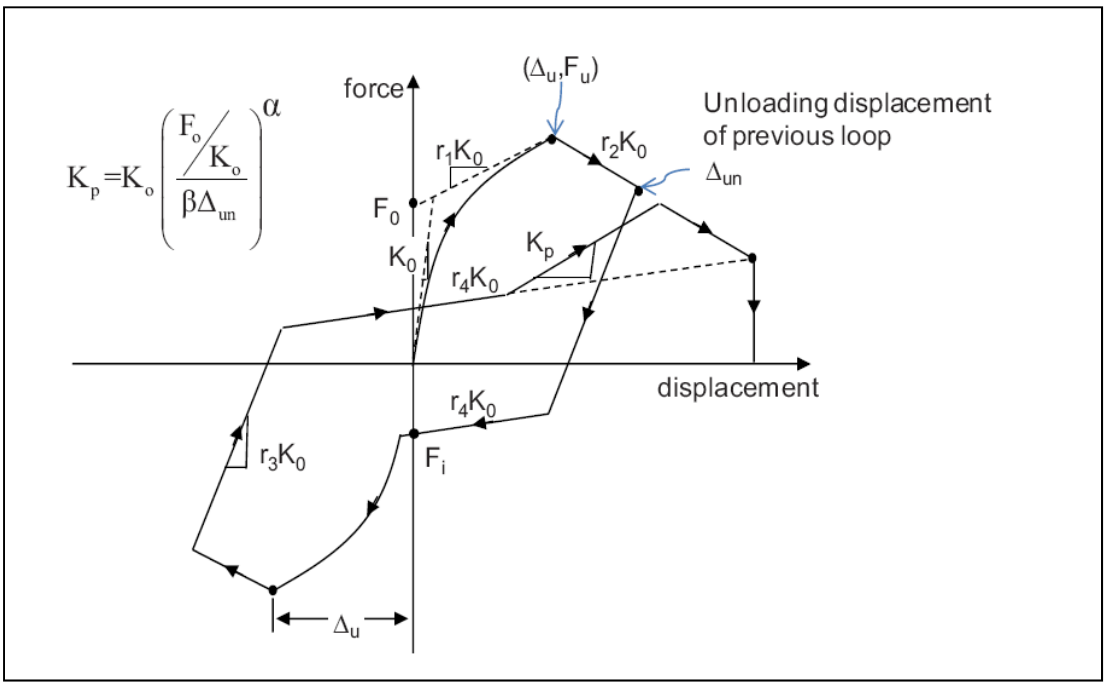

Figure 11: Loading Paths and Parameters of Modified Stewart Hysteretic Model (Source: Pang et at., 2010)

The backbone curve of the shear wall model is defined as follows:

$$F_b(\Delta) = 1 - e^{-\left(\frac{K_0}{F_0}\right)\Delta}(r_1 K_0 \Delta + F_0) \qquad \text{for } \Delta \leq \Delta_u \qquad (31)$$

$$F_b(\Delta) = F_u + r_2 K_0(\Delta - \Delta_0) \qquad \text{for } \Delta > \Delta \qquad (32)$$

The summary of the curve characteristics provided in Table 10 is from the SAPWood User Guide (Pei and van de Lindt, 2007).

Table 10: 10-Paramater Hysteretic Model Characteristics (Source: Pei and van de Lindt, 2007)

Parameter	**Characteristic**
K_0	Initial stiffness
F_0	Resistance force parameter of the backbone
F_1	Pinching residual resistance force
r_1	Stiffness ratio parameter of the backbone, typically a small positive value
r_2	Ratio of the degrading backbone stiffness to K_0, typically a negative value
r_3	Ratio of the unloading path stiffness to K_0, typically close to 1
r_4	Ratio of the pinching load path stiffness to K_0, typically under 0.1
Δ_u	Drift corresponding to the maximum restoring force of the backbone curve
α	Stiffness degradation parameter, usually takes a value between 0.5~0.9
β	Strength degradation parameter, usually takes a value between 1.01~1.5

The kinematic assumptions for the SAPWood building models are based on the formulation developed by Folz and Filiatrault (2004). The building is assumed to be attached to a rigid foundation and each floor/roof section is also assumed to have sufficient in-plane stiffness to be considered rigid. The zero-height nonlinear shear spring elements are then assigned to each floor level. The "planar model does not capture the overturning and flexural response of a structure. However … most wood-frame buildings are low-rise structures so overturning is not typically significant and the deformation mode is primarily one of shear" (Folz and Filiatrault, 2004). The typical

components of a single story wood-frame structure and the equivalent numerical model are shown in Figure 12.

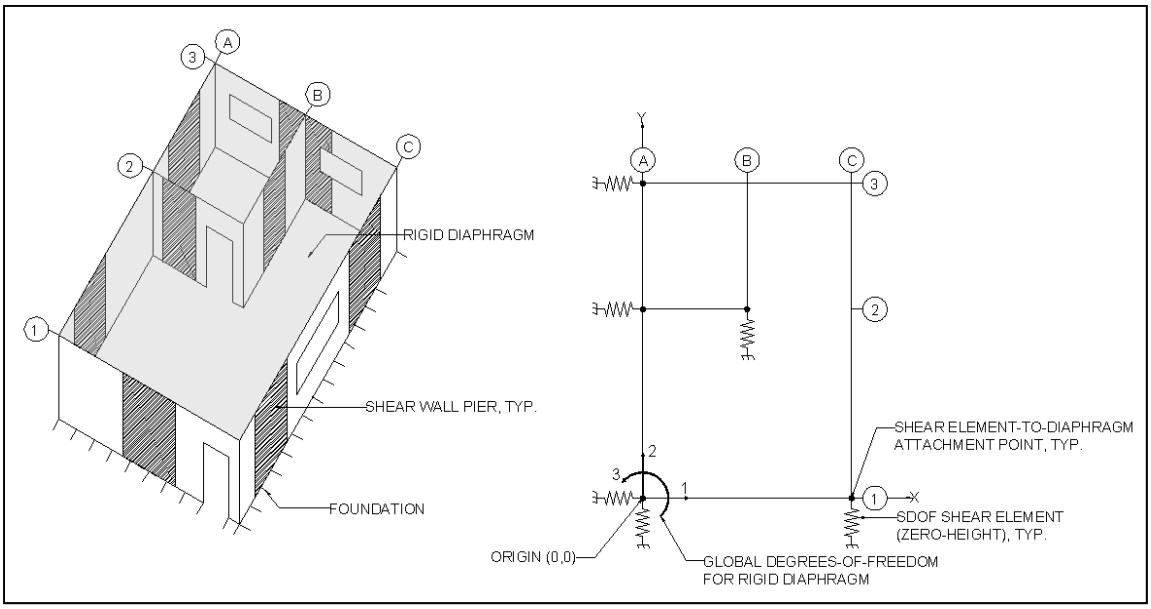

Figure 12: Components and Numerical Model of a Single-Story Structure (After: Folz, 2004)

4.2 SAPWood Components

A review of the SAPWood computer program tools including analysis options, model parameters, and loading protocols will clarify the methods established for the fastener-to-wall and wall-to-building modeling procedures. Multiple "screen shots" of the SAPWood program are shown throughout the chapter to depict the analysis options and output data available to the user.

4.2.1 Loading Protocols

The loading protocols used to develop nonlinear shear wall spring elements in SAPWood are displacement-controlled. The rate of application is not time dependant, but the protocol file is segmented into sub-steps to define the "coarseness" of the analysis. The

same loading protocol can be used with 1 to 100 sub-steps. The larger the quantity of sub-steps used, the longer computation time and the more refined the output will be. Additionally, each protocol can be scaled to a maximum displacement, therefore allowing the utilization of one protocol file for analysis of multiple shear walls containing a broad range of characteristics. Each nonlinear shear wall model was subjected to the monotonic and cyclic loading base protocols provided in Figures 13 and 14, respectively.

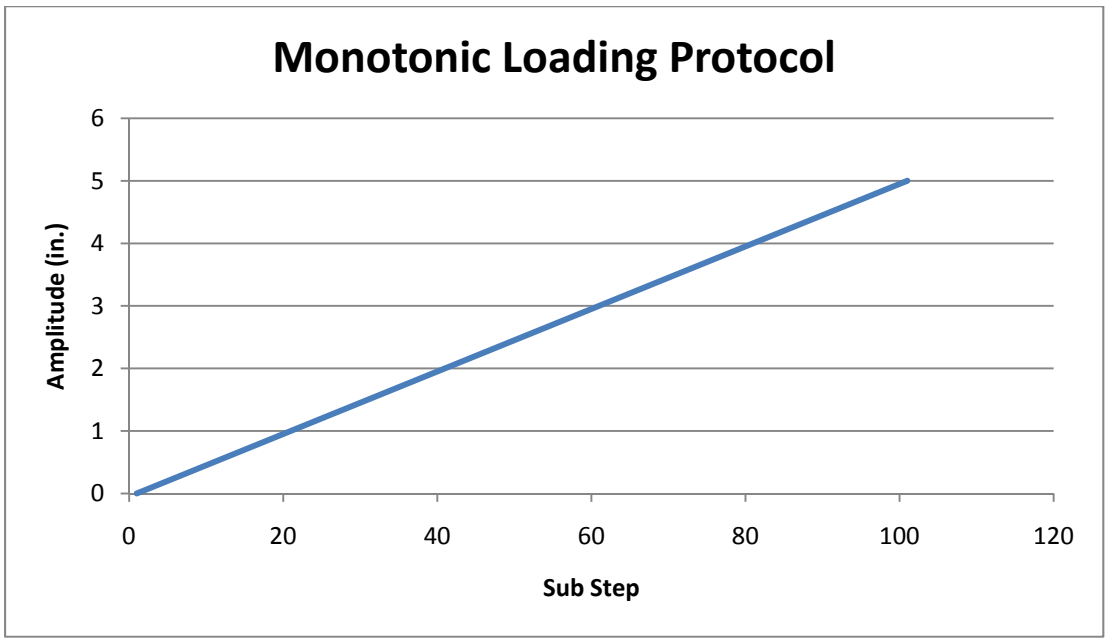

Figure 13: SAPWood Monotonic Loading Protocol

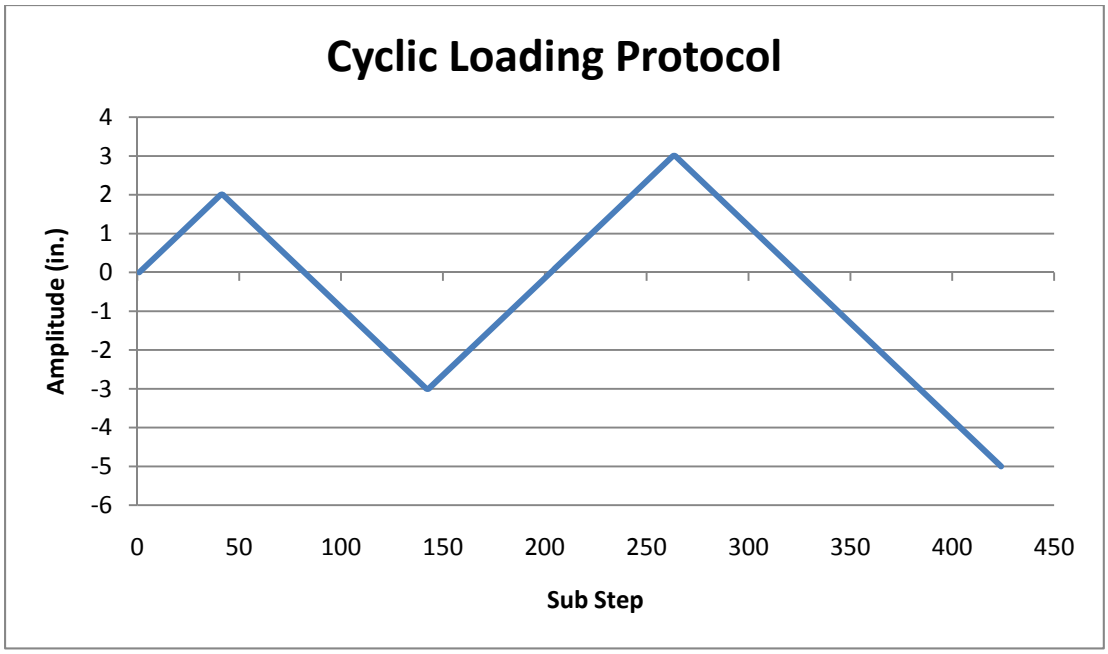

Figure 14: SAPWood Cyclic Loading Protocol

Loading protocols for single earthquake analysis and incremental dynamic analysis can be user-derived or based on pre-recorded ground motions. The input files contain a single column of time and two columns of acceleration data. Each time step corresponds to the acceleration in two directions, perpendicular to one another. The program record scaling is based upon peak ground acceleration (PGA) or Spectral Acceleration (S_a). S_a scaling is dependent on the fundamental period and effective damping of the model and was used in this evaluation to expedite the generation of IDA plots. The graphical representation of a typical earthquake protocol is provided in Figure 15. The data for the earthquake record shown in Figure 15 is provided from the PEER NGA database (PEER, 2006a).

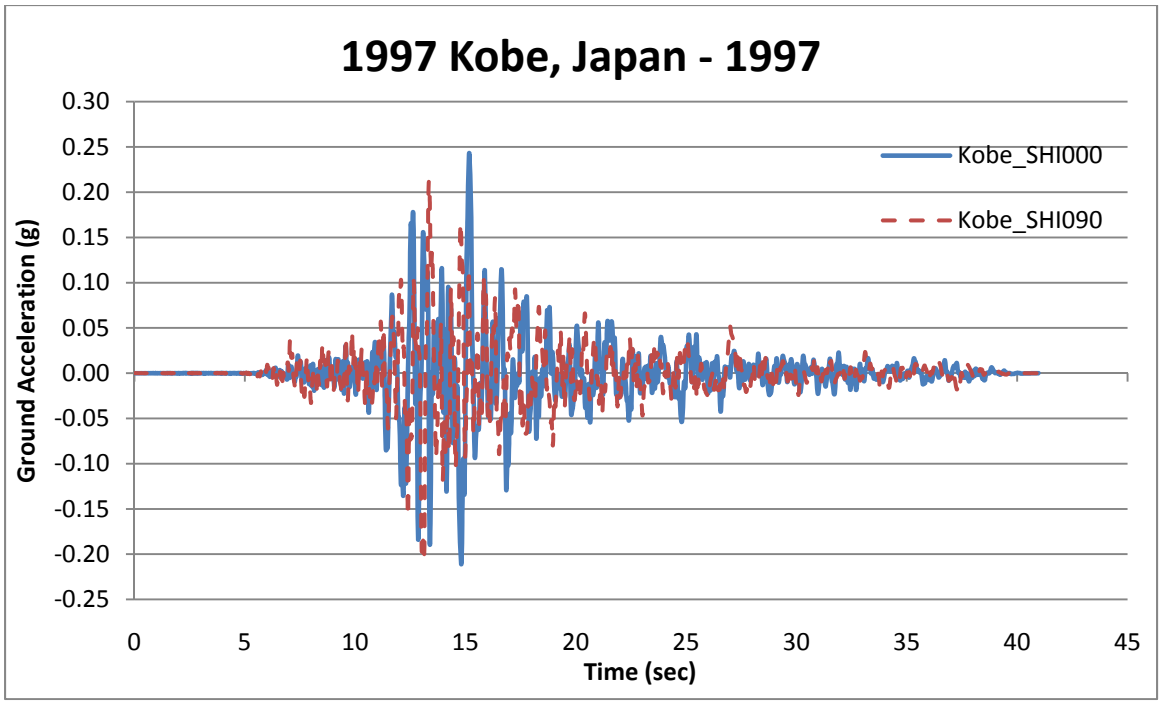

Figure 15: Ground Acceleration Plot; 1997, Kobe, Japan (Source: PEER, 2006a)

4.2.2 Nail Parameter Analysis

Each shear wall defined by individual nail parameters is subjected to the displacement controlled loading protocols in the Nail Parameter (NP) analysis tool. The NP user interface provides a simplistic diagram of the nail locations, loading protocol, and resultant hysteretic output. The output data is used to generate monotonic and cyclic load-displacement curves. Comparison between an experimental monotonic curve and cyclic loading backbone curve, which confines the hysteresis loops, illustrates the reduction in plastic deformation capacity. Figure 16 is a screen shot of the SAPWood NP user interface, and Figures 17 and 18 show plotted analysis results of an 8ft x 8ft shear wall under monotonic and cyclic loading carried out in initial tests of the SAPWood program. The insert in Figure 17 shows the loading deformation mode of the shear wall.

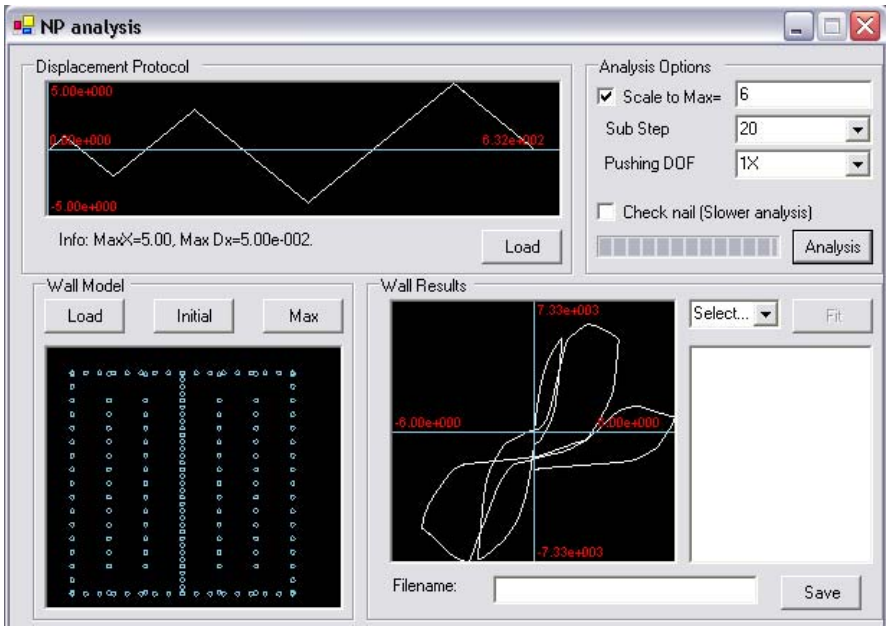

Figure 16: SAPWood NP Analysis Module

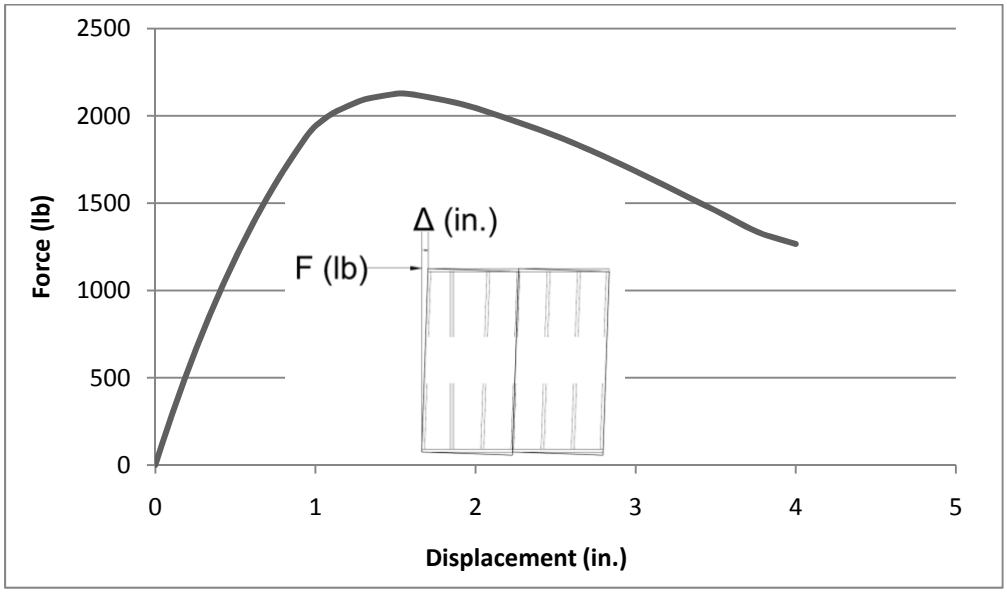

Figure 17: Force vs. Displacement Diagram from Monotonic Load Testing of 8ft x 8ft Shear Wall in SAPWood

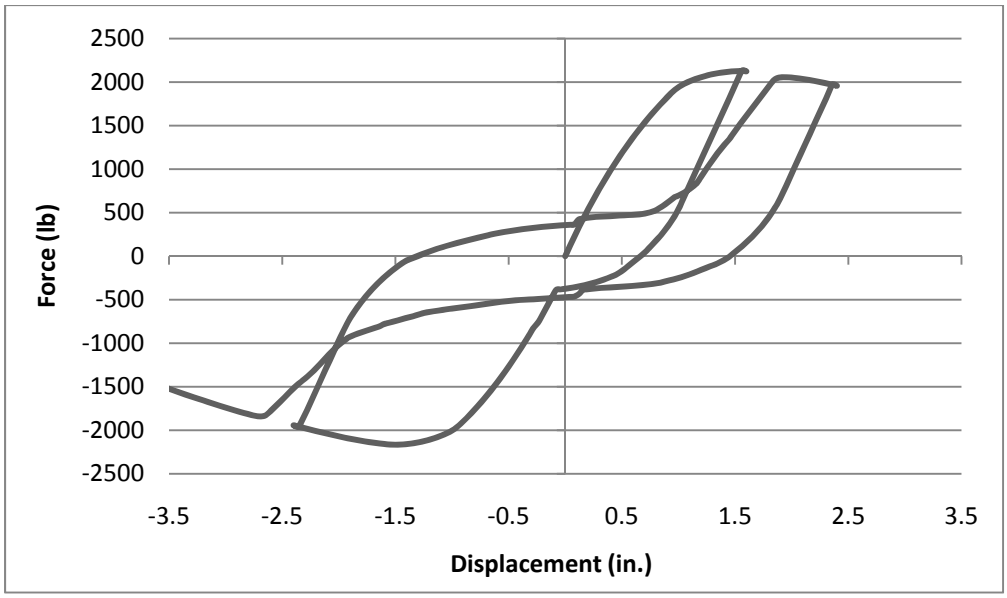

Figure 18: Force vs. Displacement Diagram from Cyclic Load Testing of 8ft x 8ft Shear Wall in SAPWood

4.2.3 Parameter Assignment

SAPWood Manual Fit "provides the user with a tool to determine nonlinear spring model parameters based on an experimental hysteresis or hysteresis results from SDOF identification" (Pei and van de Lindt, 2007). The equivalent SDOF walls segments, defined as piers in the methodology, are assigned parameters based on the resultant load-displacement output. The tool speeds the process of fitting a parameter based curve with that of load-displacement data. The SAPWood Manual Fit tool interface is shown in Figure 19.

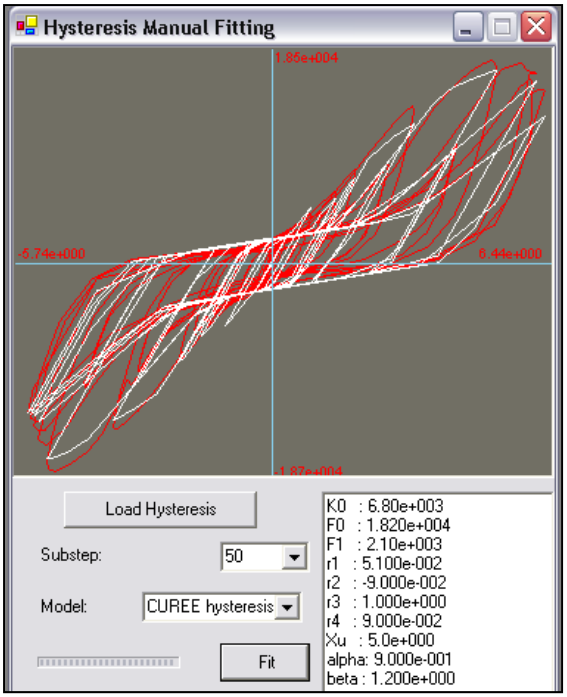

Figure 19: SAPWood Manual Fit Tool

4.2.4 Building Model Development

In alignment with the methodology guidance, each archetype model simulates the specific mode(s) of deterioration from the SDOF piers, and is evaluated through nonlinear static and dynamic analysis. The properties of each model vary dependent upon the range of the archetype design space. The plan dimensions of the two buildings presented in Chapter 6 are used for all evaluations. Figures 20 through 22 demonstrate the typical components of a building for this study and the corresponding SAPWood tools to define the wall properties and building model, respectively.

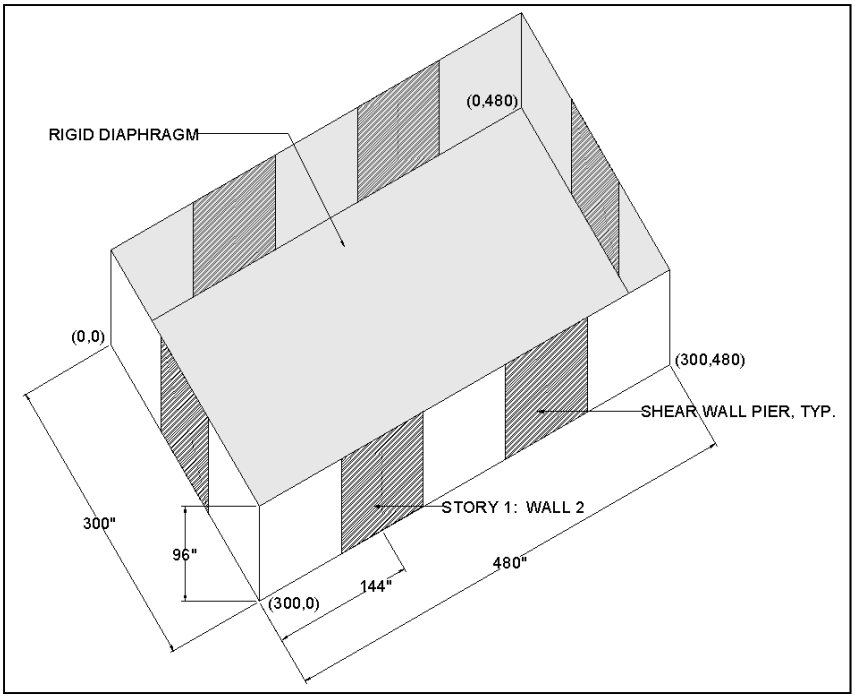

Figure 20: Typical Building Model Pier Orientation

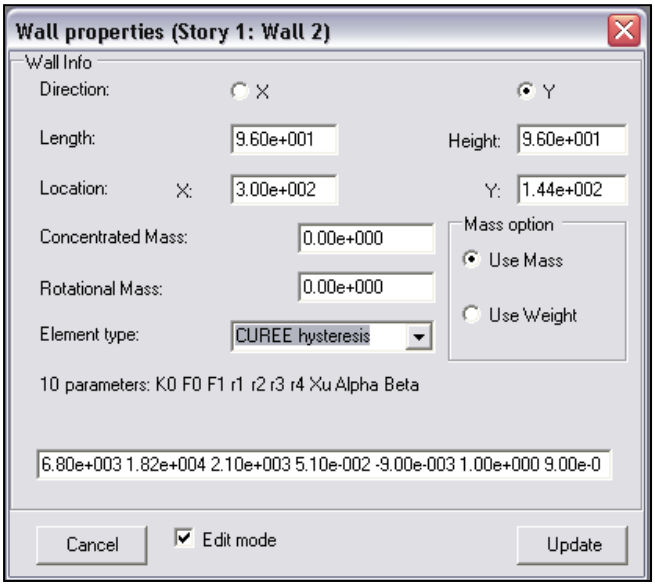

Figure 21: SAPWood Equivalent SDOF Pier Input Data

A fully developed model may be composed of equivalent SDOF piers built from the component level in the NP analysis or from equivalent SDOF piers developed from

experimental tests data. Piers may vary in size, direction, and stiffness within a single archetype model.

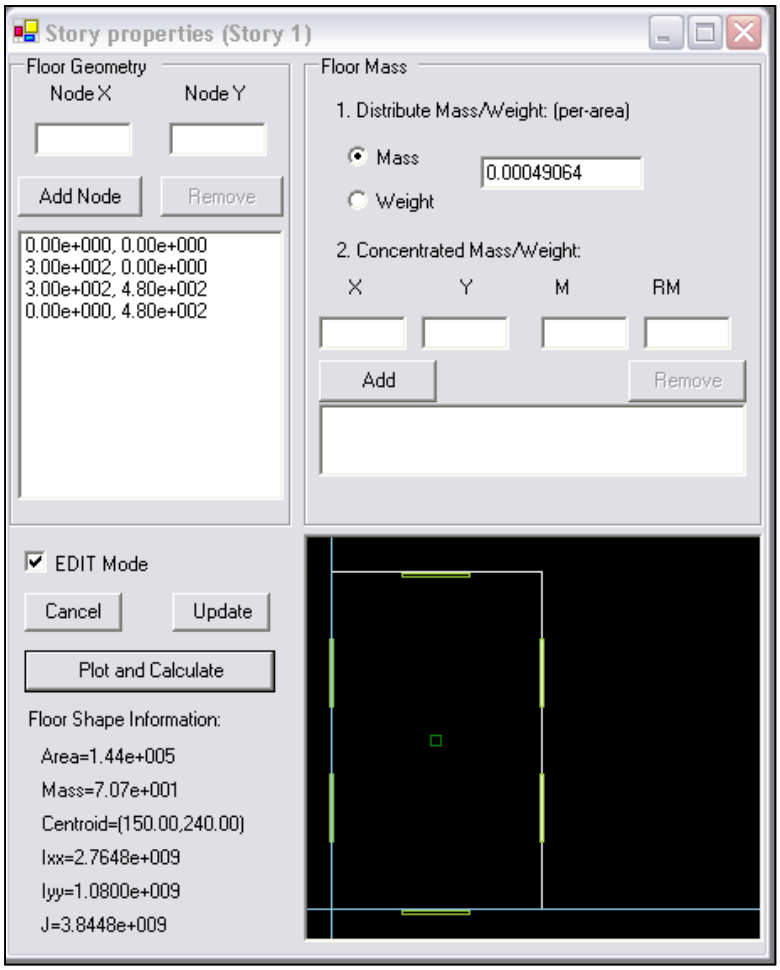

Figure 22: SAPWood Archetype Model User Interface

The distributed masses assigned to a model may vary between individual stories. Additionally, concentrated masses may be added to individual walls or anywhere within the plan of an individual story. Only story level distributed forces were modeled for this study.

4.2.5 Model Assessment

Archetype models are subjected to nonlinear static pushover analysis and incrementally scaled ground motions. The SDOF Identify tool is used for nonlinear static pushover analysis. The tool can only assess the building according to a displacement-based protocol subjected to a single-story height in a single horizontal DOF. Additionally, the analysis output only provides the horizontal force-displacement data for the story assessed. The analysis does consider the stiffness of the piers at and below the point of analysis. Because of this modeling limitation, a multi-step process was established to plot the base shear versus roof level displacement curve. The models are subjected to displacement-controlled protocols, but the process description and corresponding figures are provided in terms of a load-controlled protocol for clarity.

First, the pushover diagrams for each story are obtained by applying an incremental story force at one level until the building collapses. Figure 24 illustrates the story force versus displacement curves for each of the stories in a sample three story building, as shown in Figure 23. The pushover curve for each analysis is assigned a multi-order polynomial equation to define the load-displacement interaction.

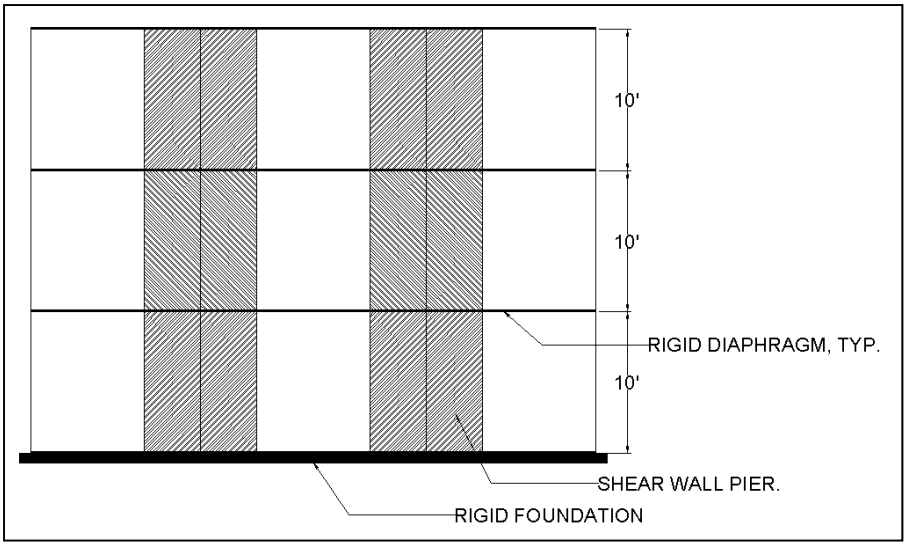

Figure 23: Sample Three Story Building

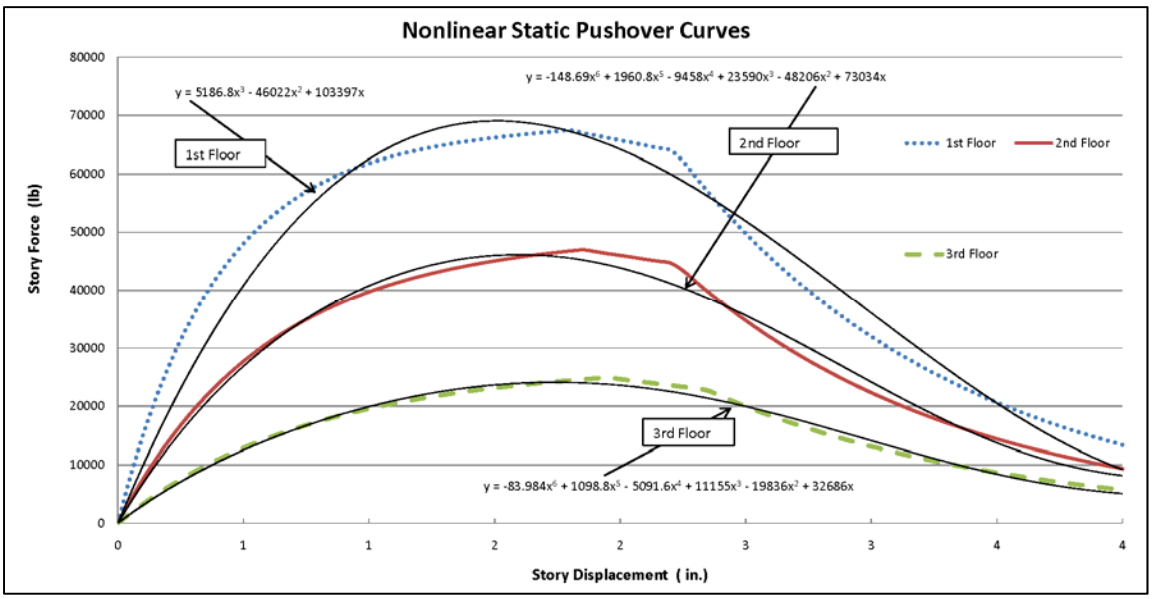

Figure 24: Story Nonlinear Static Pushover Curves

Assessment of each curve in Figure 24 is based on the primary assumption that the principle of superposition applies. The software limitations necessitate the use of this assumption knowing full well that model reacts in a nonlinear manner.

Two methods are readily available to apply these principles. First, a single story force (not to be confused with story shear) can be applied and the corresponding floor displacement can be determined from the individual story pushover curves. The process would be repeated for each story and the cumulative displacement at the roof would be determined. This evaluation method assumes the displacement at the specific level being loaded is equal to displacement in the floors above that level. This assumption is illustrated in Figure 25. The roof displacements correlating to each floor level force are summed and the base shear versus roof displacement can be plotted. However, this method is limited by the ability to assess the post peak response, since the individual story force applied will never exceed the peak base shear.

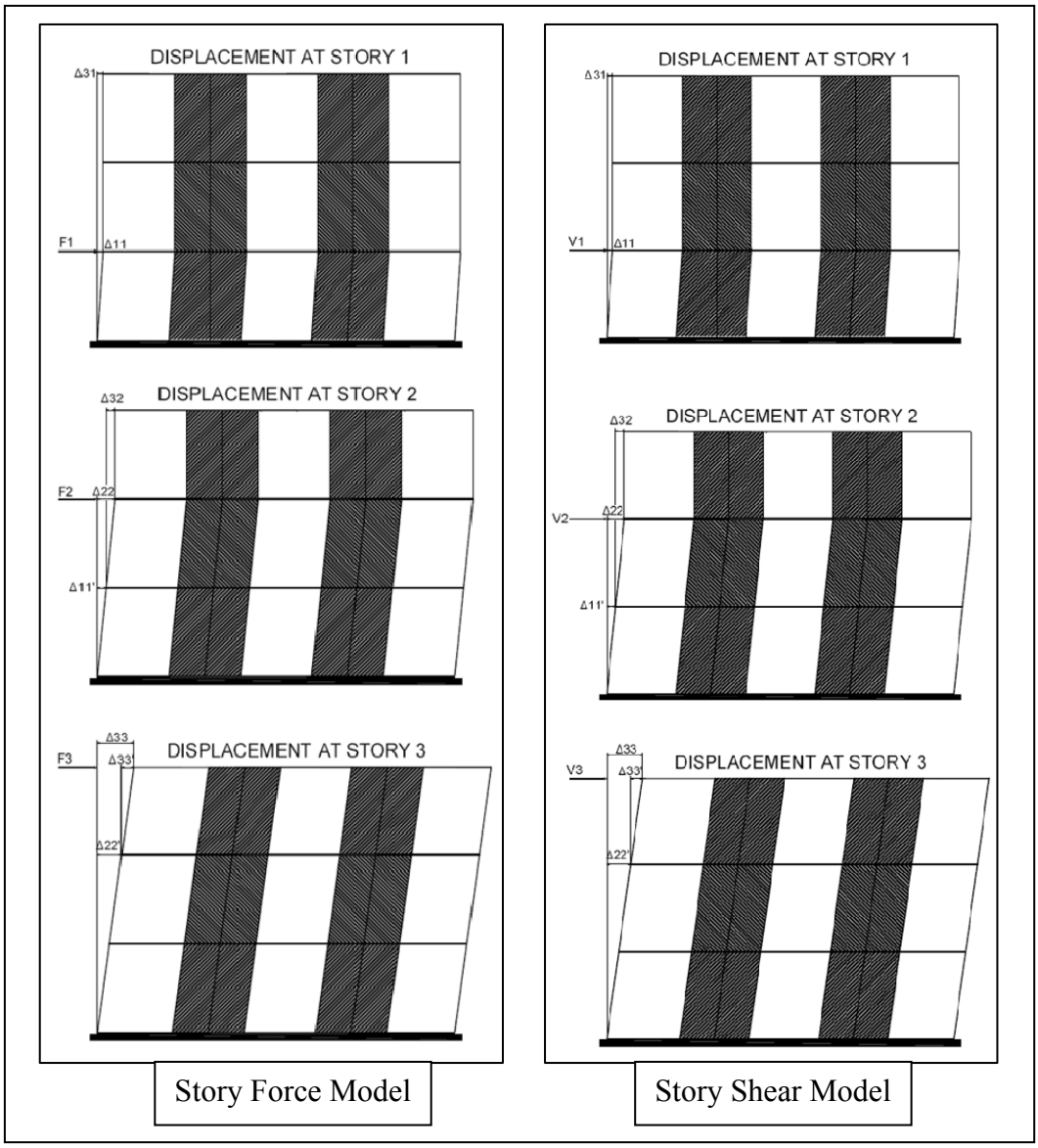

Figure 25: Building Nonlinear Static Pushover Analysis

The second method available is based on applying the story shears to the model to determine the corresponding roof displacement. In this approach, a correction for the displacements that are "double counted" must be provided. Accordingly, the first step is to determine the displacement (Δ_{11}) corresponding to the story shear for the first floor (V_1). V_1 is equal to the total base shear (V_b). Δ_{11} is determined from the first story curve

in Figure 24. The contribution of this displacement to the roof displacements (Δ_{31}) is as follows:

$$\Delta_{31} = \Delta_{11} \quad (33)$$

The second step is to apply the story shear for the second story (V_2) to the second story curve in Figure 24 to determine the correspond displacement (Δ_{22}). The contribution of this displacement to the roof displacement is as follows:

$$\Delta_{32} = \Delta_{22} - \Delta_{11}' \quad (34)$$

Where Δ_{11}' is the displacement at the first story due to the second story shear (V_2) obtained from the first story curve in Figure 24.

The third step is to apply the story shear for the third story (V_3) and determine the displacement at the third story (Δ_{33}) from the third story curve in Figure 24. The contribution of this displacement to the total roof displacement (Δ_{33}') is as follows

$$\Delta_{33}' = \Delta_{33} - \Delta_{22}' \quad (35)$$

Where Δ_{22}' is the displacement at the second story due to the third story shear (V_3) obtained from the second story curve in Figure 24.

The fourth and final step is to determine the total roof displacement (Δ_3) corresponding to the base shear. The equation for Δ_3 is as follows:

$$\Delta_3 = \Delta_{31} + \Delta_{32} + \Delta_{33}' \quad (36)$$

The final base shear versus roof displacement curve is assessed to define the global ductility capacity of the seismic force resisting system.

The SDOF Identify tool interface used to establish the initial story pushover curves is shown in Figure 26.

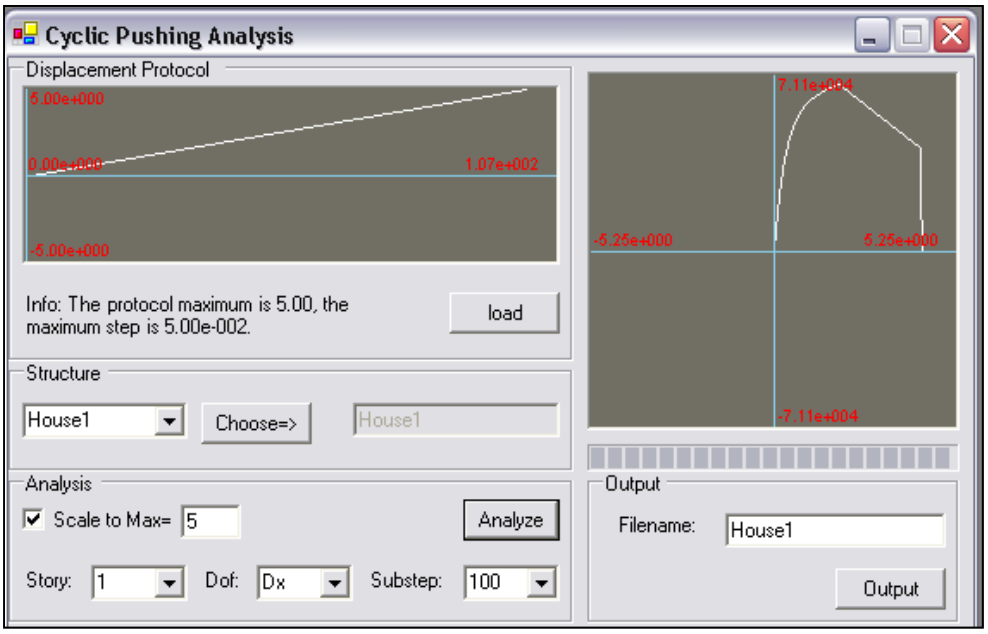

Figure 26: SAPWood SDOF Identify User Interface

In addition to nonlinear pushover analysis, each archetype model was subjected to IDA through the SAPWood IDA or Multi-IDA (MIDA) interfaces. The program enables a single, or multiple buildings, to be subjected to a suite of scaled ground motion records. A screen shot of the SAPWood IDA interface is provided in Figure 27.

The scaling for the methodology specific ground motion records is addressed in Chapter 6.

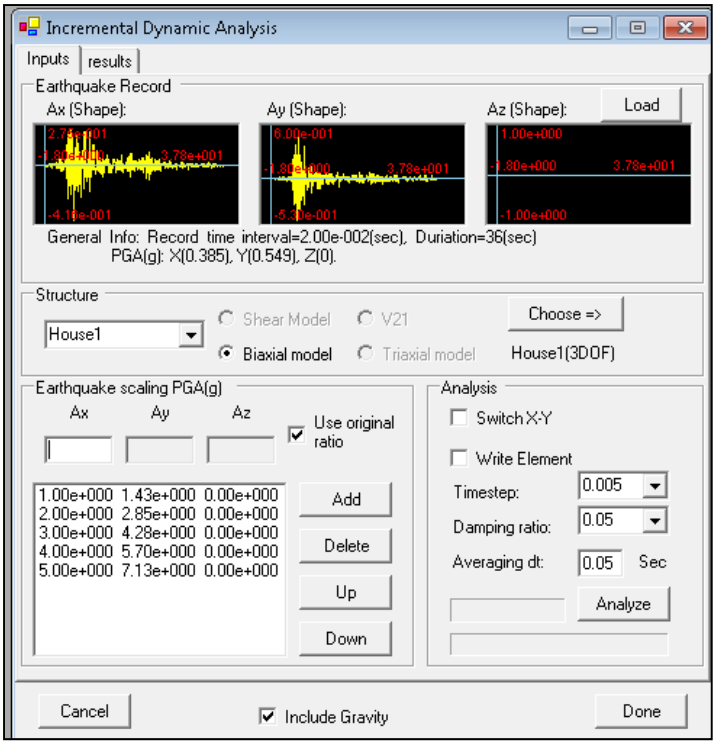

Figure 27: SAPWood Archetype Model Incremental Dynamic Analysis

IDA results comprise of the maximum story drifts and rotations, inter-story drifts and rotation, and story forces for both of the x and y building access. The collapse margin ratio is assessed through analysis of the Sa-versus-inter-story drift plots generated from the analysis data.

The various tools available in the SAPWood program provided an excellent resource for conducting each of the methodology analytical modeling requirements. Chapter 5 assesses the specific data and processes used to develop piers for each of the archetype models. The SAPWood NP and Manual Fit tools were primarily used for this work.

Chapter 5: Nonlinear Shear Wall Development

Analytical studies in the preliminary methodology assessment include one residential dwelling and three light commercial facilities comparable to the wood-frame structures in FEMA P695. Finite element models are used to determine the seismic response of the archetype models when subjected to incrementally scaled ground motions. The nonlinear seismic structural procedures followed are based on the methodology and applicable building code guidance for determining the SPFs for SIPs. Both SIP models and wood-frame models are evaluated to provide a rational basis for comparison. The process of developing shear walls, for the building models, starting from the fastener and experimental data are discussed in this chapter. The NP analysis parameters used for wood-frame and SIP pier development are provided in Table 11 and are obtained from FEMA (2009).

Table 11: Sheathing-to-Framing Connector Hysteretic Parameters Used to Construct Preliminary SIP Shear Elements

Connector Type	K_0 (lbs/in)	F_0 (lbs)	F_1 (lbs)	r_1	r_2	r_3	r_4	Δ_u (in)	α	β
7/16” OSB – 8d common nails	6,643	228	32	0.026	-0.039	1.0	0.008	0.51	0.7	1.2
19/32” Plywood – 10d common nails	7,777	235	39	0.031	-0.056	1.1	0.007	0.49	0.6	1.2

5.1 Wood-frame Pier Development

The wood-frame piers were developed with for two primary reasons. First, the resultant models were compared with public experimental data to determine the accuracy of the SAPWood models. Second, the models were compared with the SIP models and experimental data to evaluate the differences between the systems. Four pier models

intended to represent two 4ft x 8ft sheets of 7/16” OSB backed with vertical studs at 16 in. o.c. and a single top and bottom plate were constructed. The edge nail spacing ranged from 2 in. to 6 in. on center and the field spacing was set at 12 in. on center for each model. A diagram of the sheathing-to-stud nail pattern is provided in Figure 28.

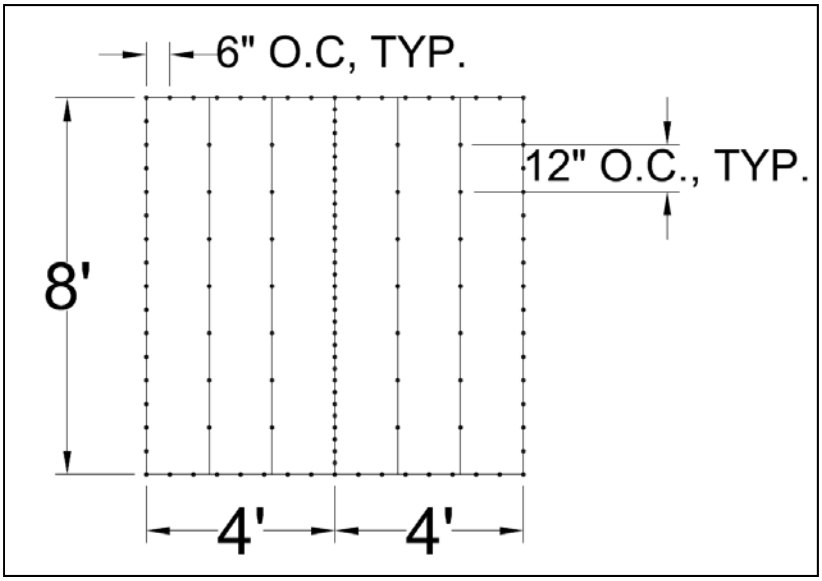

Figure 28: Wood-frame Pier Nailing Pattern

The four models showed excellent correlation to the wood-frame experimental results provided for wood-light frame walls in FEMA P695 (FEMA, 2009). A comparison of monotonic-backbone curves for 8ftx8ft shear wall numerical model and experimental specimens (FEMA, 2009) is provided in Figure 29. The equivalent monotonic-backbone curves for the shear wall models generated in SAPWood are provided in Figure 30.

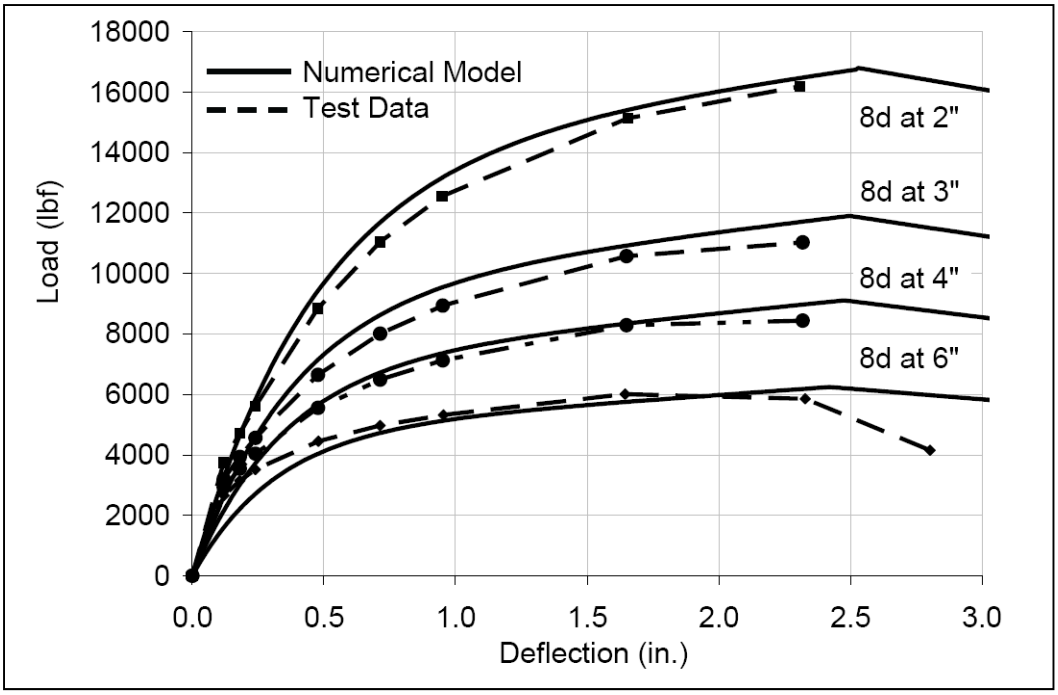

Figure 29: Monotonic Backbone Curves (Source: FEMA, 2009)

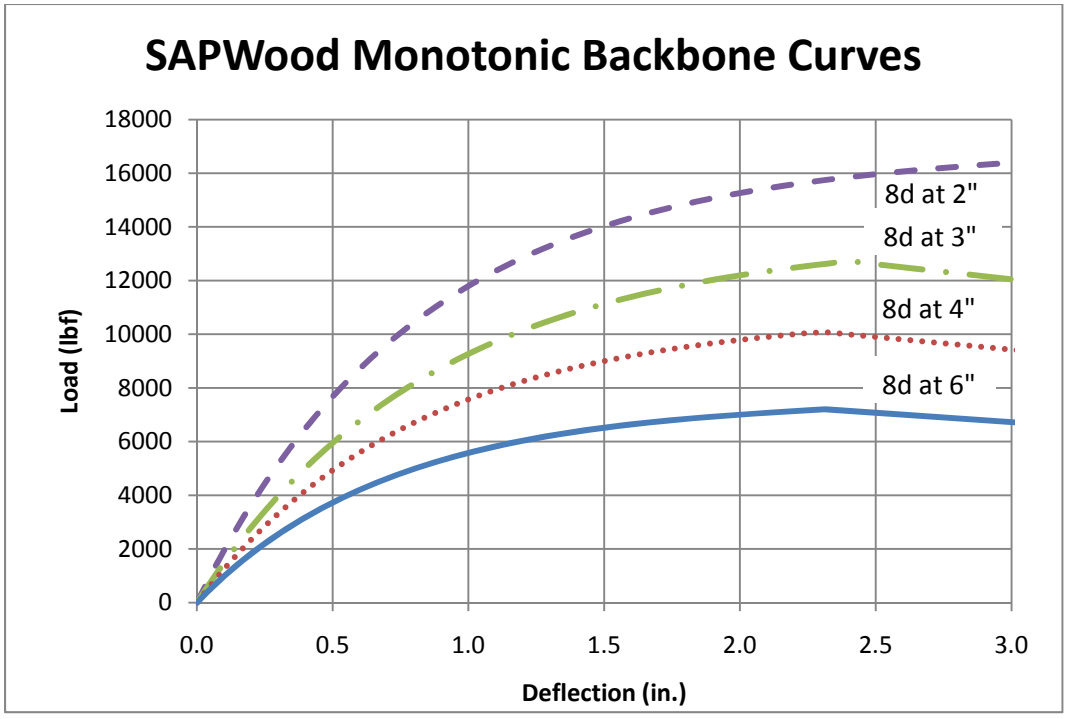

Figure 30: SAPWood Monotonic Backbone Curves

Although the wood-frame pier models compared well with that of experimental data for each of the 8ft piers, experimental data was not readily available for comparison of piers of varied lengths for this study. The extensive wood-frame database in Black (2010) was built in comparison to experimental data for various pier lengths. Therefore, the wood-frame hysteretic parameters from Black (2010), Appendix Table A.7, were used for wood-frame piers with lengths other than 8ft in this study. Additionally, it is important to note that the evaluations for this study proved that the methods used to generate the numerical pier models are appropriate and produce accurate and reliable results. Furthermore, the knowledge gained from the models was invaluable for the development of numerical SIP piers.

5.2 SIP Pier Development

The SIP experimental data used for this study (Terentiuk, 2009) is only representative of 8d nails at 6 in. on center. The following comparison between the experimental data and NP models for 6 in. edge spacing addresses the applicability of using NP based SDOF shear wall models for the SIP building models.

The models were intended to represent 2 - 4ft x 8ft SIPs with vertical studs spaced 48 in. o.c. and a single horizontal top and bottom plate. Only edge nails exist in the SIP model and they are modeled at 3 in. o.c. to represent nails spaced at 6 in. o.c. on the front and rear face of the experimental panel. A diagram of the sheathing-to-stud nail pattern is provided in Figure 31.

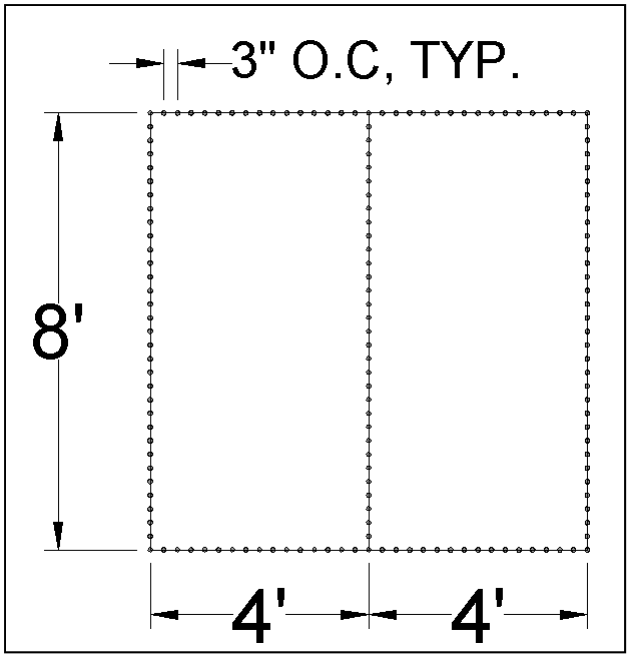

Figure 31: SIP Pier Nailing Pattern

Each nonlinear shear wall model was subjected to the monotonic and cyclic loading protocols provided in Figures 13 and 14, respectively. Each set of cyclic and hysteretic output was calibrated through the SAPWood Manual Fit tool. Typical plots of the monotonic and cyclic output for the 2-panel SIP shear wall, as shown in Figure 31, are provided in Figures 32 and 33.

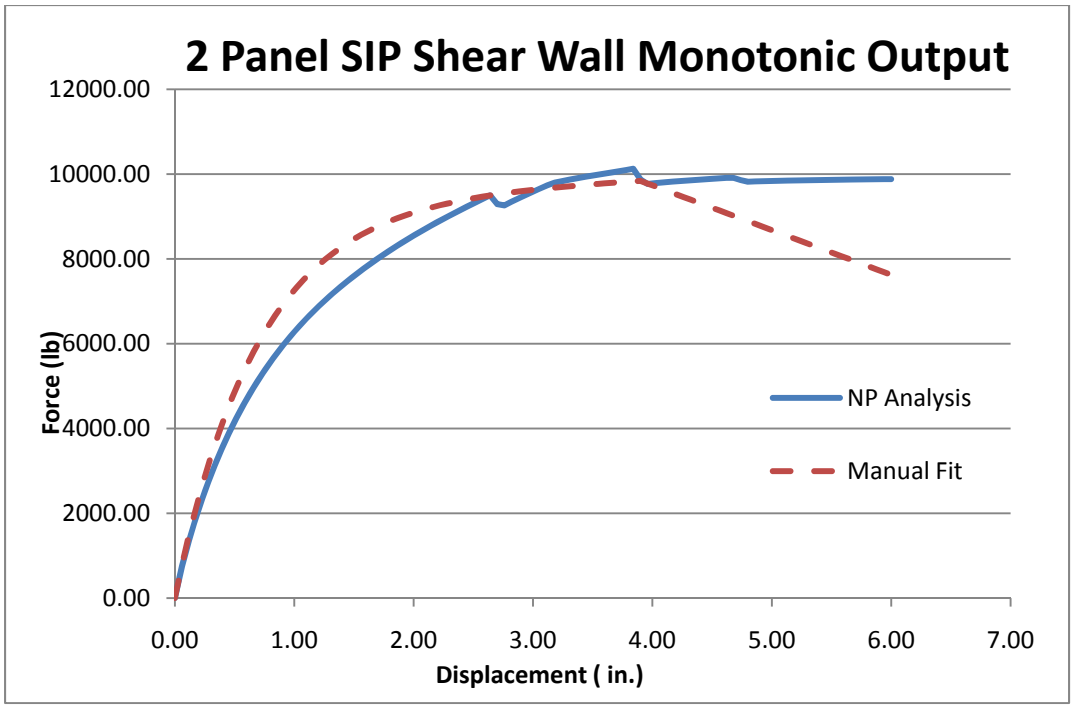

Figure 32: 2 Panel SIP Shear Wall Monotonic Output

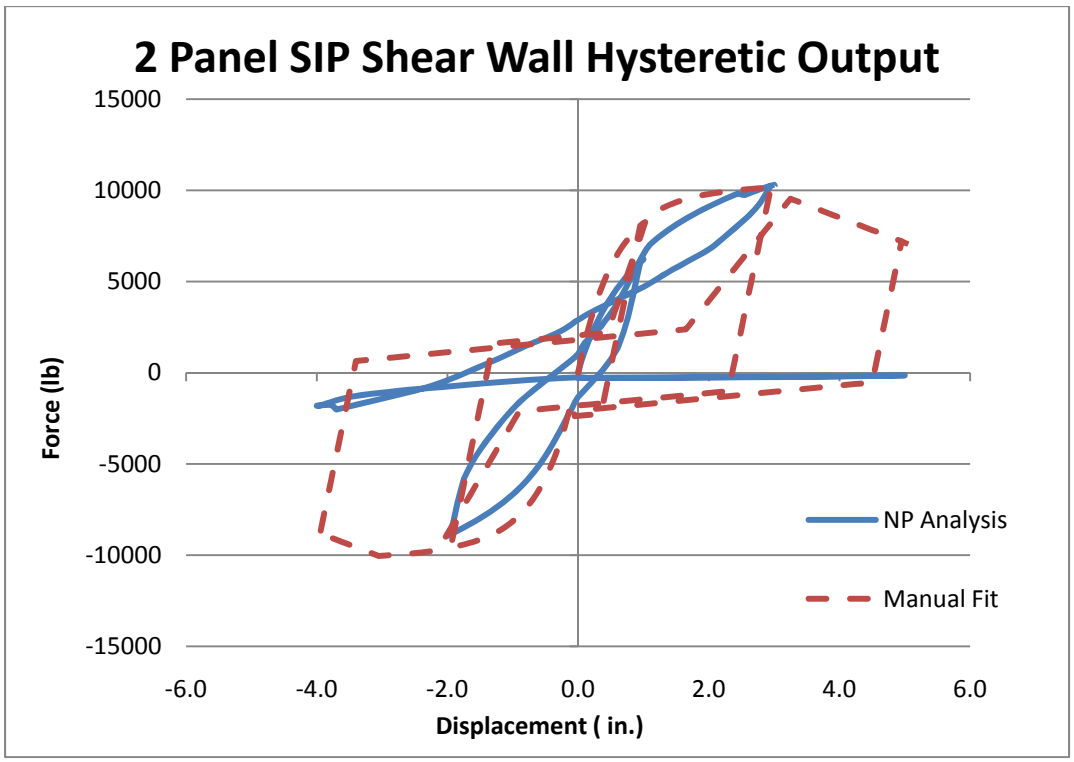

Figure 33: 2 Panel SIP Shear Wall Hysteretic Output

The SIP shear wall manual fit pushover curve, from Figure 32, was overlaid with the curve generated from experimental data from a SIP shear wall loaded monotonically, Terentiuk (2009) test A1-1M, in Figure 34. The experimental wall was composed of 2 - 4ftx8ft panels faced with 7/16" OSB and nailed with 8d nails at 6in o.c. on both side of the panel. A 7/16" OSB center spline was used with the same nailing pattern. The corresponding numerical model had 8d nails spaced at 3in o.c.

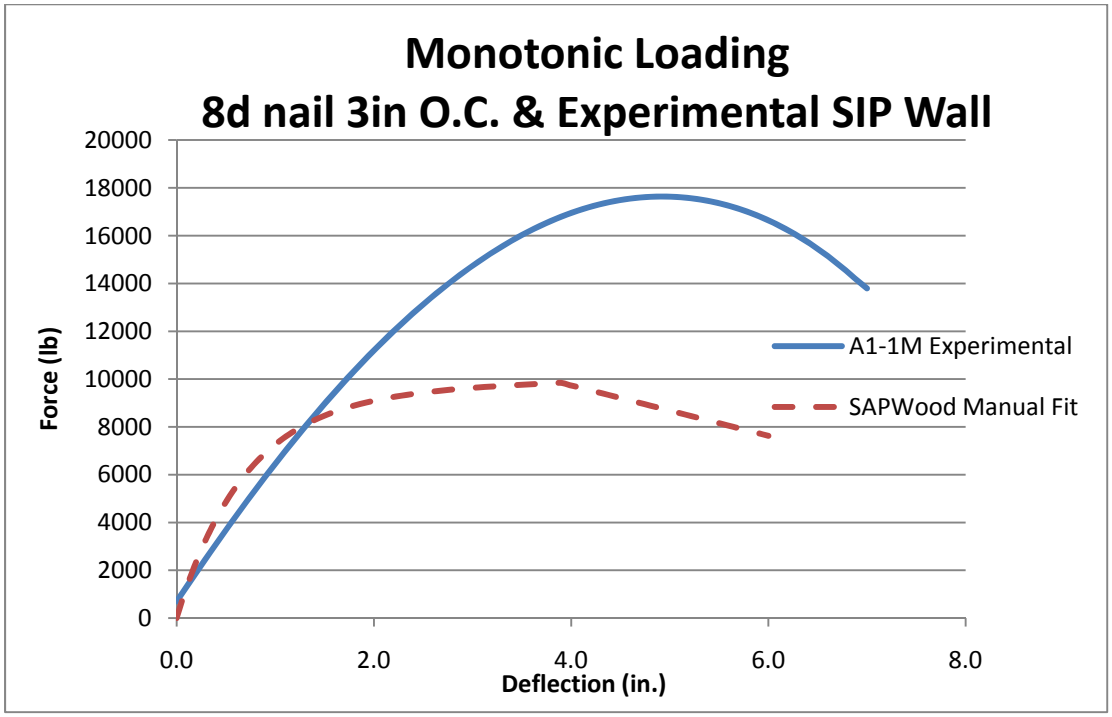

Figure 34: 2 Panel SIP Shear Wall Monotonic Output

Figure 34 clearly shows that the SIP shear wall can resist nearly twice the total shear of the initial SIP numerical model. The backbone produced by the numerical model does not take into account the effect of the 3.5 in. foam core in the SIP experimental panels. The core effectively increases the ultimate strength and provides continuous bracing which allows the panel to reach a larger ultimate displacement than the numerical model.

An equivalent connector was added to the numerical model to account for the contribution of the SIP core. The artificial connectors were modeled as bilinear spring elements to produce a backbone curve similar to that of the A1-1M curve. The monotonic pushover curves of the original numerical model, A1-1M experimental SIP wall, and adjusted numerical model are plotted in Figure 35.

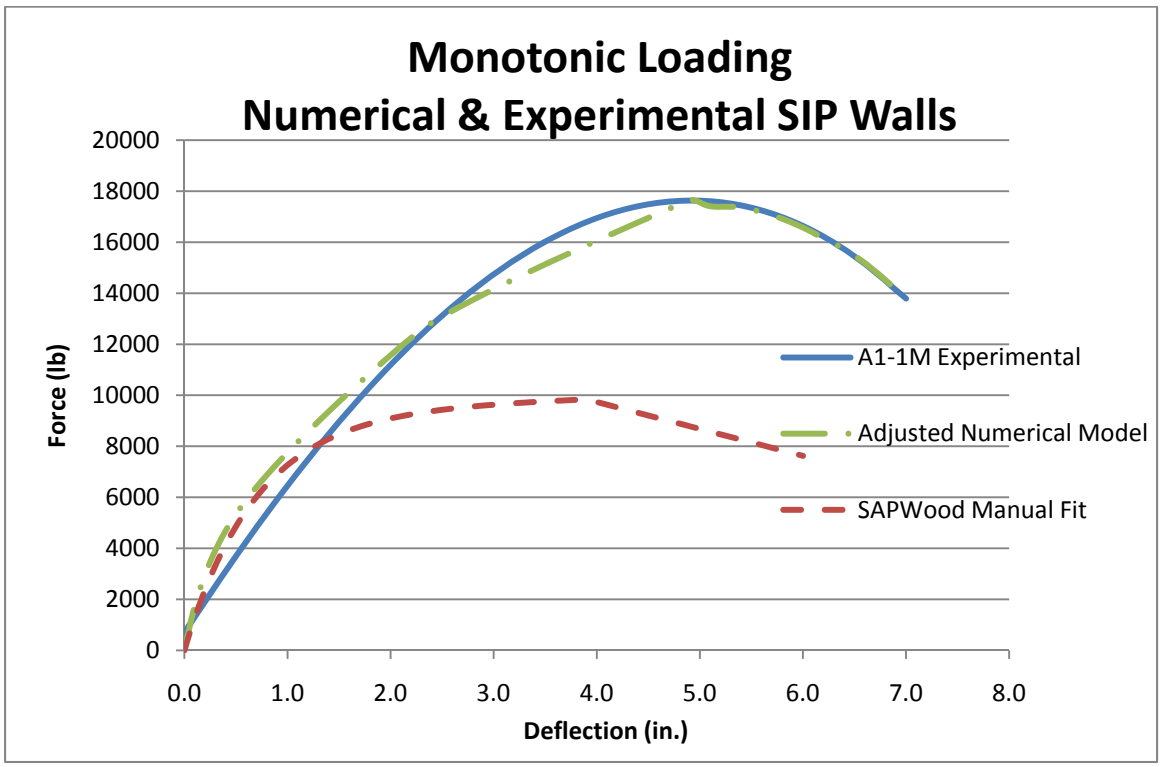

Figure 35: Adjusted Numerical Model & Experimental SIP Shear Wall Monotonic Output

The adjusted numerical model has good correlation to the experimental results. The scaling of this adjusted model to represent various shear wall configurations should not be conducted until additional experimental SIP tests with varied spline, core, fastener, and hold-down configurations are conducted. Equivalent SAPWood NP models of the various SIP tests would more effectively define the contribution of the core, hold-down,

and spline elements within the walls. Therefore, the equivalent nonlinear shear wall spring elements for the SIP archetype models for this report were not generated through NP analysis. The 10 hysteretic parameters of the SIP shear walls were defined through analysis of the monotonic and cyclic SIP experimental data.

Manual Fit plots of the experimental cyclic output for Terentiuk (2009) wall A1-1C is provided in Figure 36. Shear wall A1-1C is equivalent to that of A1-1M, but was subjected to the cyclic CUREE protocol (Krawinklet et al., 2001) instead of a monotonic pushover loading protocol. The SAPWood manual fit tool was used to fit the curve to generate an equivalent 10-parameter hysteretic plot.

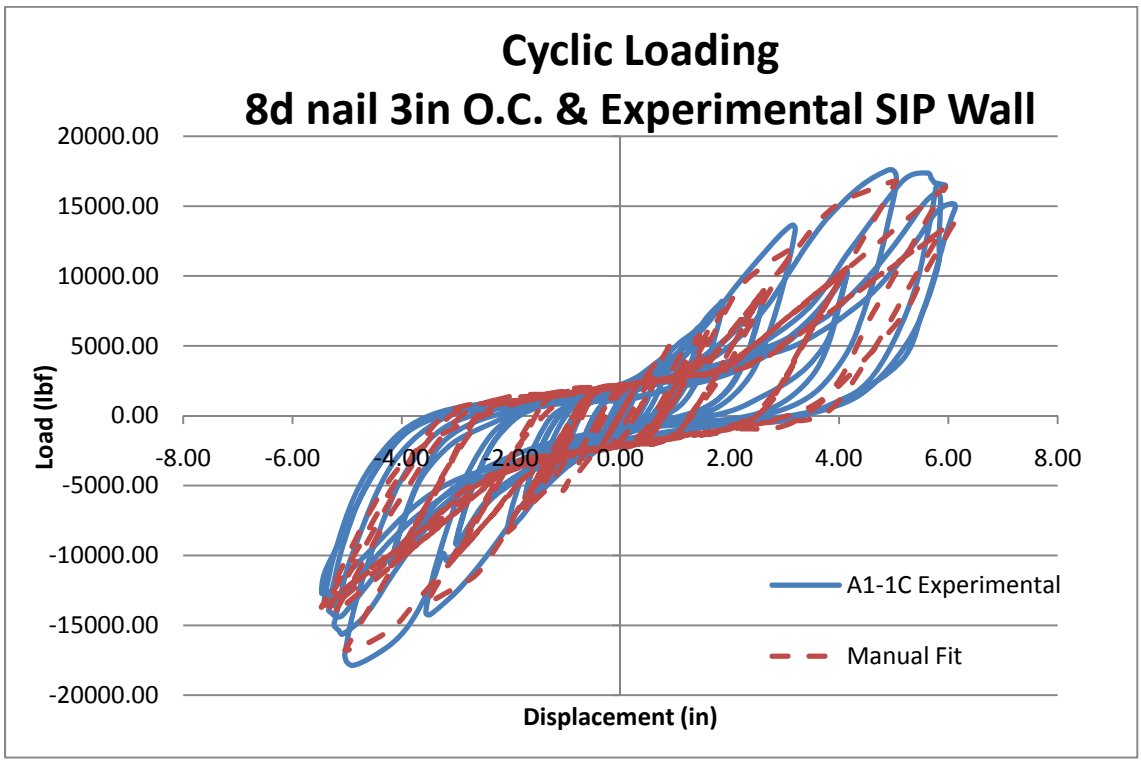

Figure 36: 2 Panel SIP Shear Wall Hysteretic Output

The calibrated output results are provided in Table 12 for comparison against hysteretic output from a comparable wood-frame shear wall (Black, 2010).

Table 12: SIP and Wood-frame Hysteretic 10-Parameter Results

Wall Type	**K_0 (lbs/in)**	**F_0 (lbs)**	**F_1 (lbs)**	**r_1**	**r_2**	**r_3**	**r_4**	**Δ_u (in)**	**α**	**β**
SIP	6,800	18,200	2,100	0.05	-0.090	1.0	0.090	5.0	0.9	1.2
Wood-frame	14,500	6,110	1,020	0.052	-0.065	1.0	0.046	1.480	0.75	1.28

The initial stiffness of the SIP shear wall is less than that of the wood-frame wall, but the SIPs can withstand larger ultimate forces and drifts than the traditional wood-frame wall. The effects of these characteristics as related to collapse evaluation of archetype buildings are presented in Chapter 7.

Chapter 6: FEMA P695 Evaluation

Chapter 6 presents evaluation of the four SIP and wood-frame archetype models selected for this study. Pushover, collapse fragility, and collapse margin ratio diagrams are provided for each of the SIP models. Only the primary values used for assessment of the wood-frame models are presented. The steps outlined in Section 3.1 of this report are followed for the system and individual archetype models.

6.1 System Information

The experimental data and other supporting data were evaluated based on the characterization of monotonic and cyclic behavior of the system. Developing a well-defined seismic force resisting system concept including the configuration, dissipation mechanisms, and application range is the first step in the FEMA P695 methodology. The ability to provide a reliable response prediction is dependent on the compilation of detailed system information. Many of the aspects of SIP assessment mirror the requirements for wood-frame buildings in ASCE 7-05 (2006). The initial assessment for SIP design requirements was based on the parallels between SIPs and wood-frame construction, which has an extensive set of design requirements and testing, and the prescriptive requirements in the IRC. Moderate levels of development but limited lessons learned from major earthquakes justify an initial assessment of the SIP design requirements as "(C) Fair."

The test data was primarily based on the comparison between sheathing-to-framing connections and experimental data. The limited quantity of experimental data contributes to the uncertainty in the overall collapse assessment. Experimental analysis with a wide

range of spline and connector types was conducted by Terentiuk (2009) and wall section equivalent to the most reliable from those tests were used in this pilot study. Alternatively variables such as core type, spline material type, and framing grades continue to generate some uncertainties. Other uncertainties, such as premature failures, are limited through the beneficial traits of panelized manufacturing. Finally, the limited data available for various pier aspect ratios only warrants an initial assessment of "(C) Fair" for system uncertainty.

This preliminary methodology evaluation for SIPs as a seismic force resisting system was conducted in parallel to the wood-frame system presented in FEMA P695. Therefore, the building configurations used for the evaluation were representative of typical residential and commercial buildings. The intended use of the methodology is to verify performance of a class of buildings instead of a specific building, therefore modeling of SIP and wood-frame buildings with the same dimensions and characteristics provided a baseline for comparison for this evaluation. Wall finishes were not addressed in this report, but it is a reasonable assumption that gypsum board will be installed on the interior face of each panel and should be considered in the archetype development of a comprehensive methodology evaluation. Non-structural interior walls were not included.

6.2 Archetype Development

The analytical models of the building archetypes were developed to reflect the system data. The archetype seismic force-resisting systems must be designed to cover the expected range of building sizes, seismic design categories, and gravity loads. However, since this is only a pilot study, only a single SIP pier configuration was used. The collapse assessment provided was created considering this narrow scope. In Filiatrault

and Christovasilis (2008) study, the wood-frame range of parameters included two building configurations, five story heights, two shear wall aspect ratios, and two SDCs. Through systematic reduction, a total of 16 archetypes in four performance groups were used to cover the "current design space for wood light-frame buildings" (Filiatrault and Christovasilis, 2008). The proposed archetype design space for a full SIP study is outlined in Table 13 and is notably based on the wood-frame study in FEMA P695 (2009).

Table 13: Range of Variables Considered for the Definition of SIP Archetype Design Space

Variable	**Range**
Number of stories	1 to 3
Seismic Design Categories (SDC)	D_{max} and D_{min}
Story Height	8 ft
Interior and exterior nonstructural wall finishes	Not considered
Wood shear wall pier aspect ratios	High / Low

The program for this report includes only four SIP building models, equal in plan, weight, and SDC to the models evaluated for the wood-frame system. Figure 37 depicts the plan dimensions of the each building type (FEMA, 2009).

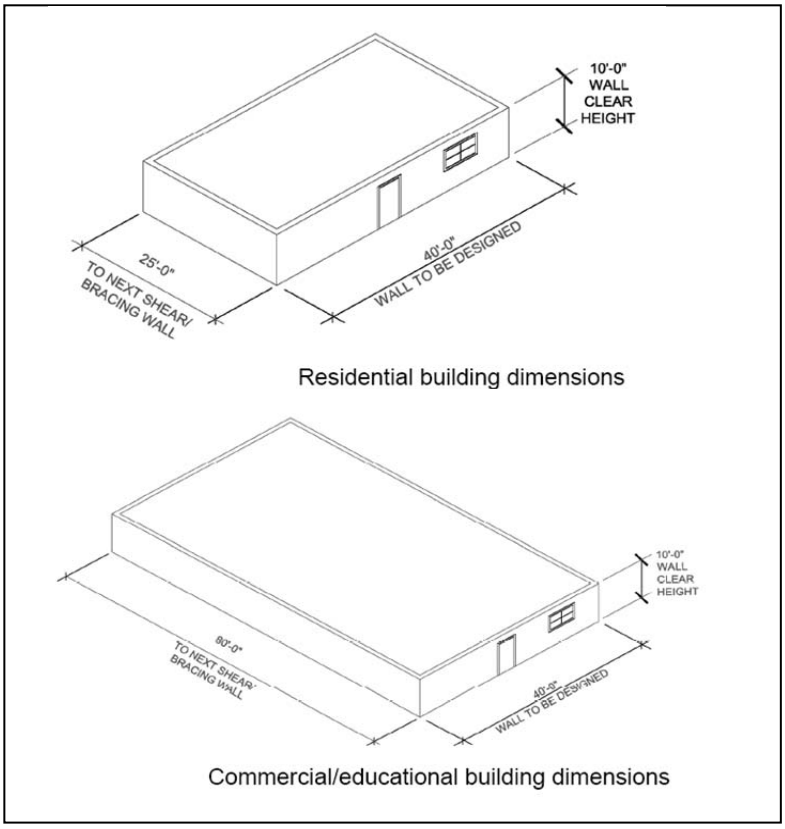

Figure 37: Archetype Building Dimensions (Source: FEMA, 2009)

In accordance with the established archetype design space and guidance from the FEMA P695 wood-frame example, the performance groups were established and systematically adjusted to create the minimum set of models necessary to represent the full range of characteristics. The performance groups are summarized in Table 14, and are identified by three numbers for the number of archetypes. The *x / y / z* numbering is representative of: *x* = number of wood-frame buildings analyzed for FEMA P695; *y* = number of buildings proposed for a full SIP methodology evaluation; *z* = number of wood-frame and SIP buildings analyzed for this preliminary study. If the parameters between all systems are identical, then only one identifier is provided. In other words, if a

comprehensive study was to be undertaken for SIPs, the number of buildings to be modeled would be identified by y. For this pilot project, however, only a subset represented by z is modeled. If the wood-frame parameter differs from the SIP parameter used for this study a fourth identifier is added to describe the wood-frame parameter used for this study.

Table 14: Performance Group Matrix Used in the Evaluation of Structural Insulated Panel Buildings (After: FEMA, 2009)

Performance Group Summary					
Group Number	**Grouping Criteria**				**Number of Archetypes (*x / y / z*)**
	Basic Structural Configuration	**Design Load Level**		**Period Domain**	
		Gravity	**Seismic**		
PG-1	Low Wall Aspect Ratio	High (Nominal)	SDC D_{max}	Short	3 / 3 / 2
PG-2				Long	0 / 0 / 0
PG-3			SDC D_{min}	Short	0 / 0 / 0
PG-4				Long	1 / 1 / 1
PG-5		Low (NA)	SDC D_{max}	Short	0 / 0 / 0
PG-6				Long	
PG-7			SDC D_{min}	Short	
PG-8				Long	
PG-9	High Wall Aspect Ratio	High (Nominal)	SDC D_{max}	Short	5 / 3 / 0
PG-10				Long	0 / 0 / 0
PG-11			SDC D_{min}	Short	4 / 4 / 1
PG-12				Long	3 / 1 / 0
PG-13		Low (NA)	SDC D_{max}	Short	0 / 0 / 0
PG-14				Long	
PG-15			SDC D_{min}	Short	
PG-16				Long	

Low aspect ratio walls range from 1:1 to 1.43:1 and a high aspect ratio walls range from 2.70:1 to 3.33:1 are proposed for the full program. Tables 15 and 16 define the specific characteristic variations that define each archetype model. Only archetypes based on model #1, 4, 5, and 11 were assessed in this preliminary evaluation. Only information for 12 models is provided, in comparison to the 16 suggested for the wood light frame

system. This adjustment is due to a reduction in assessed story heights from five to three for the SIP seismic force resisting system. The twelve models listed in Tables 15 and 16 would be appropriate for a comprehensive evaluation of SIPs in follow-up studies.

Table 15: Index Archetype Configurations for Structural Insulated Panel Shear Wall Systems (After: FEMA P695)

Model No.	No. of Stories	Tributary Width for Seismic Weight (ft)	Floor/Roof Tributary Seismic Weight (kips)	Shear Wall Aspect Ratio	Occupancy
1	1	40	41/0	Low	Commercial
2	1	12.5	13.65/0	High	1 & 2 Family
3	1	40	41/0	High	Commercial
4	1	12.5	13.65/0	High*	1 & 2 Family
5	2	40	82/41	Low	Commercial
6	2	12.5	17.31/13.65	High	1 & 2 Family
7	2	40	82/41	High	Commercial
8	2	12.5	17.31/13.65	High	1 & 2 Family
9	3	40	82/41	Low	Commercial
10	3	12.5	27.3/13.65	High	Multi-Family
11	3	40	82/41	Low	Commercial
12	3	12.5	27.3/13.65	High	Multi-Family

Shear wall nailing data for 8ft wide piers with 8d nails at 6 in. on center is the most appropriate experimental data currently available for SIP shear walls. Therefore, all SIP models were constructed with multiple 8ft piers to achieve a total pier length similar to the corresponding wood-frame model. This modification effectively changed model #4 from a high to low aspect ratio classification only for this study. The same *x / y / z* parameter labeling format used for Table 14 is also used in Table 16 for the number of piers, pier length, and shear wall nailing. The shear wall nailing is representative of the nails at the perimeter of the panel. The field nailing for each wood-frame pier was standardized at 12 in. on center. SIPs do not have any field nailing. The "No. of Piers"

column defines the total number of piers in a single shear wall line. Only the 40ft perimeter walls were analyzed for the residential and commercial facilities.

Table 16: Index Archetype Designs for Structural Insulated Panel Shear Wall Systems (after FEMA, 2009

Model No.	No. of Stories	No. of Piers	Pier Length (ft)	Shear Wall Nailing
1	1	2 / 2 / 2	9.0 / 9.0 / 8.0	8d at 6”
2	1	4 / 4 / 0	3.0 / 3.0 / 0	8d at 6” / 8d at 6” / 0
3	1	4 / 4 / 0	3.0 / 3.0 / 0	8d at 6” / 8d at 6” / 0
4	1	2 / 2 / 1 / 2	3.0 / 3.0 / 8.0 / 4.0 & 2.0	8d at 6”
5	2	3 / 3 / 3	8.0 / 8.0 / 8.0	8d at 4” / 8d at 4” / 8d at 6” / 8d at 4”
	1	3 / 3 / 3	8.0 / 8.0 / 8.0	8d at 2” / 8d at 2” / 8d at 6” / 8d at 2”
6	2	5 / 5 / 0	3.0 / 3.0 / 0	8d at 6” / 8d at 6” / 0
	1	5 / 5 / 0	3.0 / 3.0 / 0	8d at 3” / 8d at 3” / 0
7	2	5 / 5 / 0	3.0 / 3.0 / 0	8d at 4” / 8d at 4” / 0
	1	5 / 5 / 0	3.0 / 3.0 / 0	8d at 2” / 8d at 2” / 0
8	2	2 / 2 / 0	3.0 / 3.0 / 0	8d at 6” / 8d at 6” / 0
	1	2 / 2 / 0	3.0 / 3.0 / 0	8d at 4” / 8d at 4” / 0
9	3	3 / 3 / 0	10.0 / 10.0 / 0	8d at 6” / 8d at 6” / 0
	2	3 / 3 / 0	10.0 / 10.0 / 0	8d at 2” / 8d at 3” / 0
	1	3 / 3 / 0	10.0 / 10.0 / 0	10d at 2” / 8d at 2” / 0
10	3	6 / 6 / 2 / 6	3.0 / 3.0 / 8.0 / 4.0 & 2.0	8d at 6” / 8d at 6” / 0
	2	6 / 6 / 2 / 6	3.0 / 3.0 / 8.0 / 4.0 & 2.0	8d at 2” / 8d at 3” / 0
	1	6 / 6 / 2 / 6	3.0 / 3.0 / 8.0 / 4.0 & 2.0	10d at 2” / 8d at 2” / 0
11	3	2 / 2 / 2	7.0 / 7.0 / 8.0	8d at 6”
	2	2 / 2 / 2	7.0 / 7.0 / 8.0	8d at 3” / 8d at 3” / 8d at 6” / 8d at 3”
	1	2 / 2 / 2	7.0 / 7.0 / 8.0	8d at 2” / 8d at 2” / 8d at 6” / 8d at 2”
12	3	3 / 3 /	3.0 / 3.0 / 0	8d at 6” / 8d at 6” / 0
	2	3 / 3 /	3.0 / 3.0 / 0	8d at 3” / 8d at 3” / 0
	1	3 / 3 /	3.0 / 3.0 / 0	8d at 2” / 8d at 2” / 0

Each archetype model was numerically modeled as a three dimensional structure in SAPWood, but only the primary shear walls used for collapse analysis were evaluated. The quantity of piers for the 25ft wall and 80ft walls for the residential and commercial facilities, respectively, were selected proportionally to the ratio of pier length to wall length in the primary wall direction. Plan sketches of a typical floor of the wood-frame and SIP models assessed in this study are provided in Figures 38 through 40.

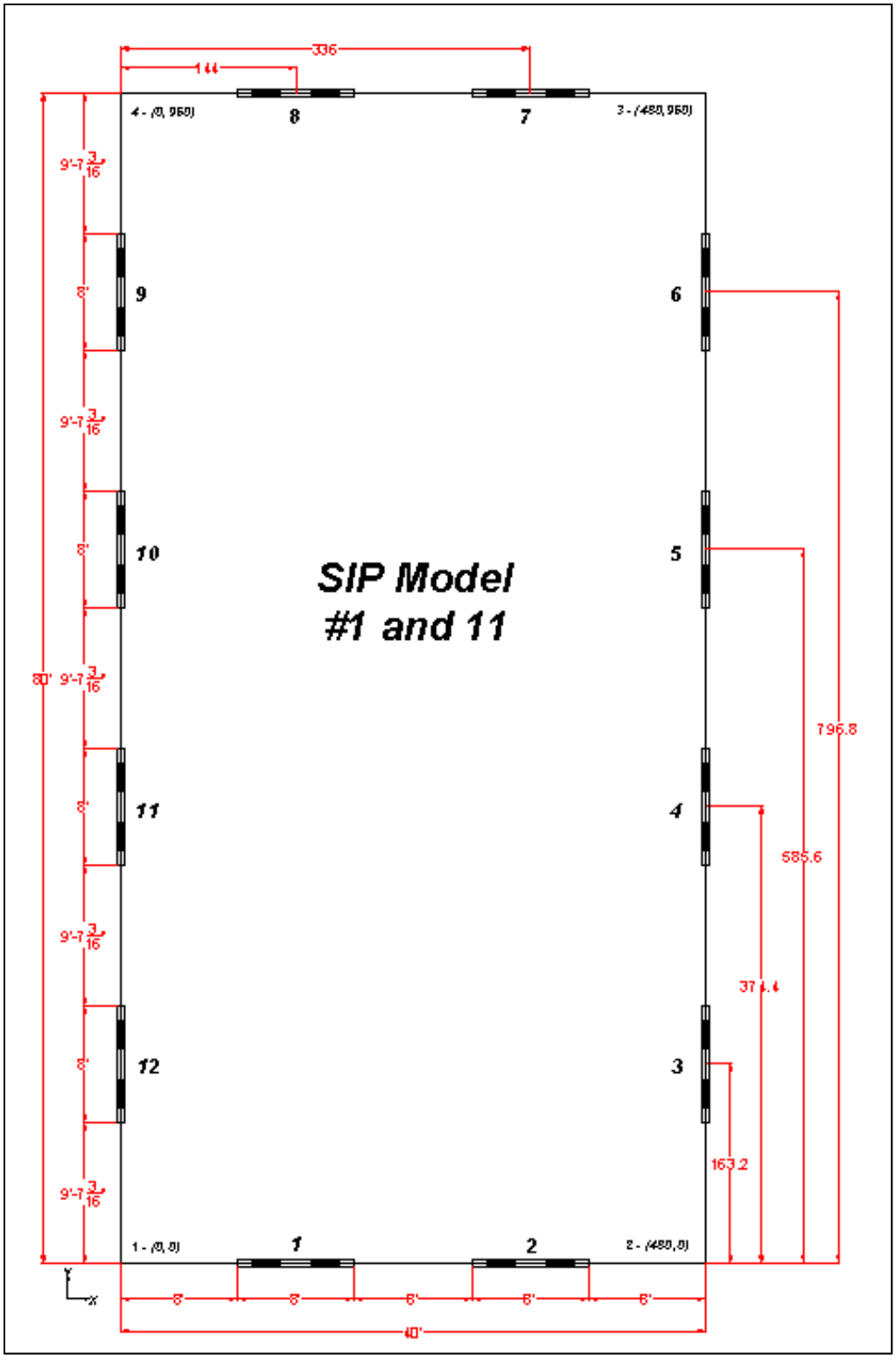

Figure 38: SIP Archetype Model #1 and 11 Plan View

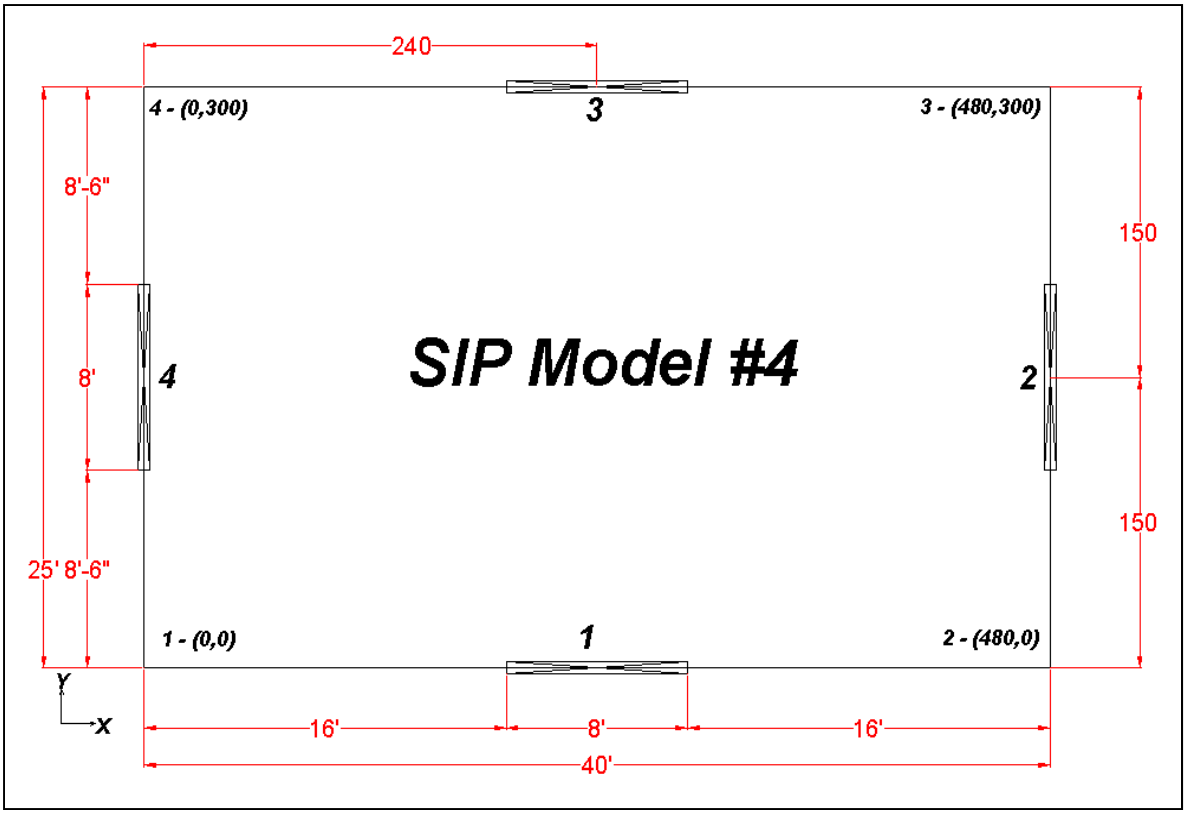

Figure 39: SIP Archetype Model #3 Plan View

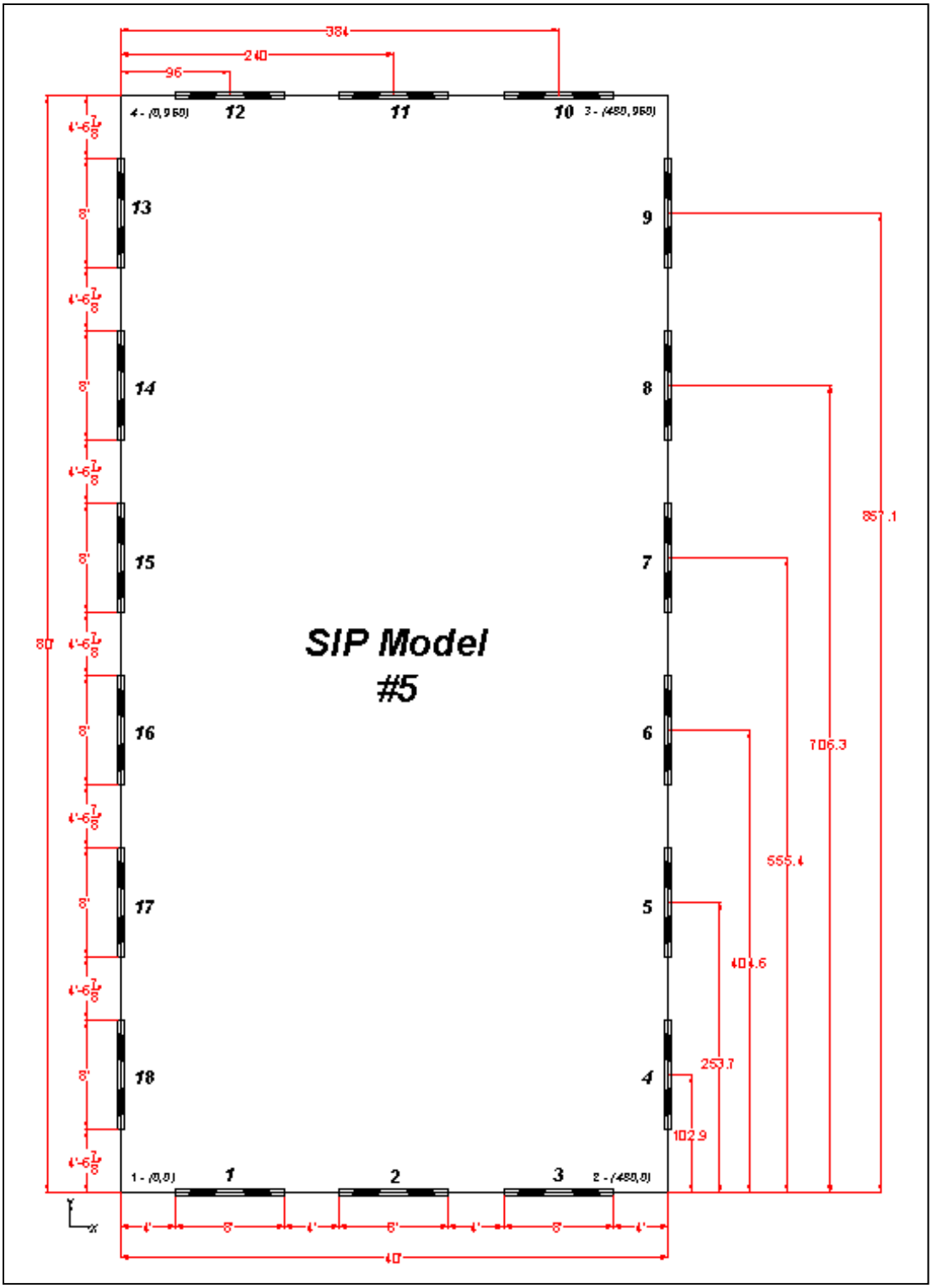

Figure 40: SIP Archetype Model #5 Plan View

As defined by the methodology and outlined in Section 3.4 of this report, the gravity loads used for nonlinear analysis are not equal to those used for gravity load design (FEMA, 2009). The tributary area and distributed loads used for nonlinear analysis for each SIP model matched that of the corresponding wood-frame model.

The structural modeling of the individual archetype models using SIP panels reflected the primary behavioral aspects of the physical shear walls. However, alternate modes of collapse, defined as non-simulated collapse (NSC), may have exceeded the computational ability of the computer modeling program. A NSC mode typically is associated with component failure, and its timing presumes it will lead to the collapse of the system. A NSC limit state, such as failure of tie-downs in wood-frame shear walls, can occur prior to the point corresponding to the deformation at peak strength that is simulated in the computer model (FEMA, 2009). This additional variability in collapse is factored into the system performance evaluation. Therefore, the initial uncertainty due to model quality was assessed as "(C) Fair."

6.3 Nonlinear Analysis

Each archetype building model was subjected to nonlinear static pushover analysis to determine the overstrength factor and characterize the system ductility. The equivalent lateral force (ELF) procedure was used for the development of all index archetype designs in this study. The methodology uses Site Class D (stiff soil) for all archetype designs. It also defines S_s =1.1g and S_1 = 0.6g as the maximum values of spectral acceleration in SDC D. The full range of short-period spectral acceleration and 1-second spectral acceleration values used for methodology is provided in the Tables 17 and 18.

Table 17: Summary of Mapped Values of Short-Period Spectral Acceleration, Site Coefficients and Design Parameters for Seismic Design Categories, B, C, and D (FEMA, 2009)

Seismic Design Category		**Maximum Considered Earthquake**			**Design**
Maximum	**Minimum**	**S_S (g)**	**F_a**	**S_{MS} (g)**	**S_{DS} (g)**
D		1.5	1.0	1.5	1.0
C	D	0.55	1.36	0.75	0.50
B	C	0.33	1.53	0.50	0.33
	B	0.156	1.6	0.25	0.167

Table 18: Summary of Mapped Value of 1-Second Spectral Acceleration, Site Coefficients and Design Parameters for Seismic Design Categories, B, C, and D (FEMA, 2009)

Seismic Design Category		**Maximum Considered Earthquake**			**Design**
Maximum	**Minimum**	**S_1 (g)**	**F_v**	**S_{M1} (g)**	**S_{D1} (g)**
D		0.60	1.50	0.90	0.60
C	D	0.132	2.28	0.30	0.20
B	C	0.083	2.4	0.20	0.133
	B	0.042	2.4	0.10	0.067

Seismic load combinations are defined in accordance with Section 12.4 of ASCE 7-05 (2006) and the methodology. Index archetype designs reflect the trial value of R and the inherent overstrength from the design requirements. The performance group design variations include SDC, gravity load, and building height variations. Index archetypes are designed for the minimum and maximum spectral intensities of the highest considered SDC. Therefore, analysis was conducted for spectral acceleration values SDC D_{min} /C_{max} and SDC D_{max}. The following is the step-by-step ELF procedure labeled by the associated ASCE 7-05 section, figure, and equation numbers with consideration given to the methodology guidance (ASCE, 2006) for archetype model #11 evaluated for SDC D_{min}.

11.4.1 Obtain mapped maximum considered earthquake spectral response acceleration at short periods, S_s, and 1-Second Period, S_1, from Figures 22-1 and 22-2.

Figure 22-1 S_s = 55%g (SDC D_{min})

Figure 22-2 S_1 = 13.2%g (SDC D_{min})

In accordance with the methodology summarized S_s and S_1 values provided as provided in Tables 17 and 18.

11.4.2 Site Class: The site shall be classified as shown in Table 20.3-1, where soil properties are known in sufficient detail to determine the site class.

Methodology guidance states site class D shall be used.

11.4.3 Site coefficients and adjusted maximum considered earthquake spectral response acceleration parameters

Equation 11.4-1: $S_{MS} = F_a S_s$ F_a = Table 11.4-1 site coefficient

Table 11.4-1 (SDC D_{min}) with $S_s = 0.55 \Rightarrow F_a = 1.36$

$$S_{MS} = F_a S_s = 1.36 * 0.55 = 0.75$$

Equation 11.4-2: $S_{M1} = F_v S_1$ F_v = Table 11.4-2 site coefficient

Table 11.4-2 (SDC D_{min}) with $S_1 = 0.132 \Rightarrow F_V = 2.28$

$$S_{M1} = F_v S_1 = 2.28 * 0.132 = 0.30$$

11.4.4 Design Spectral Response Acceleration Parameters at short Periods (S_{DS}) and 1-second periods (S_{D1}) for 5% damping:

Equation 11.4-3: $S_{DS} = 2/3\ S_{MS}$

(SDC D_{min}) with $S_{MS} = 0.75$

$$S_{DS} = 2/3\ S_{MS} = 2/3 * 0.75 = 0.5$$

Equation 11.4-4: $S_{D1} = 2/3\ S_{M1}$

(SDC D_{min}) with $S_{M1} = 0.3$

$$S_{D1} = 2/3\ S_{M1} = 2/3 * 0.3 = 0.2$$

11.5 Occupancy Category (O.C.) and Importance Factors: Each structure shall be assigned an occupancy category as in Table 1-1 and importance factor (I) as in Table 11.5.

Table 1-1: O.C I: Low hazard to human life (e.g. agricultural facilities)
O.C II: Structures not assigned to O.C. III of IV

Methodology guidance state O.C. I or II shall be used for analysis. O.C. I does not apply this study, therefore O.C. II shall be selected.

Table 11.5-1: I = 1.0

11.6 Seismic Design Category (SDC)

Table 11.6-1 $S_{DS} = 0.5g$ and O.C. = II => SDC = D_{min}

Table 11.6-2 $S_{D1} = 0.2g$ and O.C. = II => SDC = D_{min}

In accordance with Table 11.6-1, 2 and methodology guidance, SDC D_{max} and SDC D_{min} / SDC C_{max} shall be assigned for the models.

12.6 Analysis Procedures: Section 5.2.1 of the methodology guidance states the Equivalent Lateral Force (ELF) Method defined in Section 12.8 of ASCE 7-05 shall be used unless limited by the guidance in ASCE 7-05 Table 12.6-1.

Table 12.6-1 The ELF procedure is permitted for structures of light-framed construction not exceeding 3 stories in height, O.C. II, and located in SDC D and C.

6.3.1 Equivalent Lateral Force Procedure

12.8: Equivalent Lateral Force Procedure: W = Effective seismic weight

12.8.1: Seismic Base Shear: The base shear (V) equation, containing the Seismic Response Coefficient (C_s) and the effective seismic weight (W), is the basis of defining the forces for the ELF procedure.

Equation 12.8-1: $V = C_S W$

Equation 12.8-2: $C_s = \frac{S_{DS}}{(\frac{R}{I})}$

Table 19: Excerpt from ASCEC 7-05 Table 12.2-1 (after ASCE, 2005)

Seismic Force-Resisting System	**ASCE 7 Section where Detailing Requirements are Specified**	**Response Modification Coefficient, R**	**System Over-strength Factor, Ω_0**	**Deflection Amplification Factor, C_d**	**Structural System Limitations and Building Height (ft) Limit**				
					Seismic Design Category				
					B	**C**	**D**	**E**	**F**
Bearing Wall Systems									
13. Light-framed walls sheathed with wood structural panels rated for shear resistance or steel sheets	14.1, 14.1.4.2, and 14.5	6.5	3	4	NL	NL	65	65	65

The IRC guidance for Structural Insulated Panels does not provide a suggested R value, therefore R = 6 shall be used as the trial value to correspond to the wood-frame system in the FEMA P695 example.

$C_s = 0.5 / (6/1) = 0.083$ (SDC D_{min})

C_s computed in Equation 12.8-2 should not exceed Equation 12.8.3 and 12.8.4.

Equation 12.8-3: $C_s = \frac{S_{D1}}{T\,(R/I)}$ for $T \leq T_L$

Equation 12.8-4: $C_s = \frac{S_{DS}\,T_L}{T^2\,(R/I)}$ for $T > T_L$

ASCE 7-05 Section 11.4.5: T_L = long-period transition period(s) shown in Figures 22-15 through 22-20. Values of T_L range from 4 to 16 seconds, but the methodology limits the fundamental period to less than 4 seconds. Therefore, the C_S shall not be reduced in accordance with Equation 12.8-4.

C_s computed in Equation 12.8-2 shall not be less than Equation 12.8-5.

Equation 12.8-5: $C_S = 0.01$

12.8.2: Approximate Fundamental Period

Equation 12.8-7: $T_a = C_t\,h_n^x$ h_n = building height in feet

Table 20: Excerpt from ASCEC 7-05 Table 12.8-2 (Source: ASCE, 2006)

Structure Type	**C_t**	**x**
All other structural systems	0.02	0.75

The story height of each building is based on equivalent assumptions provided in Pang (2009) that each story is eight feet tall, floor diaphragms are 10 in. tall, and the roof diaphragm is 15 in. tall. The building height for one, two, and three story buildings is summarized in Table 21.

Table 21: Building Heights

Number of Stories	Building Height (ft)
1	8ft + (15 in./2) = 8.6 ft
2	8ft +10 in. + 8ft + (15 in./2) = 17.5 ft
3	8ft +10 in. + 8ft +10 in. + 8ft + (15 in./2) = 26.3 ft

$T_a = C_t h_n^x = 0.02 * 26.3 \text{ ^ } (0.75) = 0.23$ sec

Table 22: Excerpt from ASCEC 7-05 Table 12.8-1, Coefficient for Upper Limit of Calculated Period (Source: ASCE, 2006)

Design Spectral Response Acceleration Parameter at 1 s, S_{D1}	Coefficient C_u
≥ 0.4	1.4
0.3	1.4
0.2	1.5
0.15	1.6
≤ 0.1	1.7

Section 12.8-2: $T < C_u T_a$ $S_{D1} = 0.2 \Rightarrow C_u = 1.5$ (SDC D_{min})

$T = C_u T_a = 1.5 * 0.23 = 0.35$ sec

Section 5.2.5 of FEMA P695 (2009) specifies the fundamental period (T) must be great than 0.25 seconds.

All values of T are ≤ 1.0, therefore Equation 12.8-2 will control over Equation 12.8-3.

The transition period, T_s, is defined as the "boundary between the region of constant acceleration and the region of constant-velocity of the design response spectrum" (FEMA, 2009).

Section 5.2.3 (FEMA, 2009): $T_s = \frac{S_{D1}}{S_{DS}} = \frac{S_{M1}}{S_{MS}}$

(SDC D_{min}); $T_s = 0.2 / 0.5 = 0.4$

Where $T \leq T_s$ the seismic coefficient is defined as:

Section 5.2.4 (FEMA, 2009): $C_S = \frac{S_{DS}}{R}$

(SDC D_{min}); $C_s = 0.5 / 6 = 0.083$

And when $T > T_s$, C_s is defined as: $C_S = \frac{S_{DS}}{T\,R} \geq 0.44\,S_{DS}$

The ELF procedure calculations covered for the other 11 SIP models are summarized in Table 23.

Table 23: ELF Calculations for SIP Archetype Models

Archetype ID	No. of Stories	Building Configuration	SDC	S_S (g)	F_a	$S_{MS} = S_S * F_a$	S_1 (g)	F_v	$S_{M1} = S_1 * F_v$	$S_{DS} = 2/3 * S_{MS}$	$S_{D1} = 2/3 * S_{M1}$	Trial R Value	I	$C_s = S_{DS} / (R/I)$	C_t	x	h_n (ft)	T_a (sec) = $C_t * h_n^x$	C_u	T (sec) = $C_u * T_a$	T ≥ 0.25 sec	$T_s = S_{D1} / S_{DS}$	$T<T_s$; $C_s = S_{DS} / R$
Performance Group No. PG-1 (Short Period, Low Aspect Ratio)																							
1	1	Commercial	D_{max}	1.5	1.0	1.5	1	1.5	0.9	1.0	0.6	6	1.0	0.167	0.02	0.75	8.6	0.10	1.4	0.14	0.25	0.6	0.167
5	2	Commercial	D_{max}	1.5	1.0	1.5	1	1.5	0.9	1.0	0.6	6	1.0	0.167	0.02	0.75	17.5	0.17	1.4	0.24	0.25	0.6	0.167
9	3	Commercial	D_{max}	1.5	1.0	1.5	1	1.5	0.9	1.0	0.6	6	1.0	0.167	0.02	0.75	26.3	0.23	1.4	0.33	0.33	0.6	0.167
Performance Group No. PG-9 (Short Period, High Aspect Ratio)																							
2	1	1 & 2 Family	D_{max}	1.5	1.0	1.5	1	1.5	0.9	1.0	0.6	6	1.0	0.167	0.02	0.75	8.6	0.10	1.4	0.14	0.25	0.6	0.167
6	2	1 & 2 Family	D_{max}	1.5	1.0	1.5	1	1.5	0.9	1.0	0.6	6	1.0	0.167	0.02	0.75	17.5	0.17	1.4	0.24	0.25	0.6	0.167
10	3	Multi-Family	D_{max}	1.5	1.0	1.5	1	1.5	0.9	1.0	0.6	6	1.0	0.167	0.02	0.75	26.3	0.23	1.4	0.33	0.33	0.6	0.167
Partial Performance Group No. PG-4 (Long Period, Low Aspect Ratio)																							
11	3	Commercial	D_{min}	0.55	1.4	0.75	0	2.28	0.30	0.50	0.20	6	1.0	0.083	0.02	0.75	26.3	0.23	1.5	0.35	0.35	0.4	0.083
Performance Group No. PG-11 (Long Period, High Aspect Ratio)																							
3	1	Commercial	D_{min}	0.55	1.4	0.75	0	2.28	0.30	0.50	0.20	6	1.0	0.083	0.02	0.75	8.6	0.10	1.5	0.15	0.25	0.4	0.083
4	1	1 & 2 Family	D_{min}	0.55	1.4	0.75	0	2.28	0.30	0.50	0.20	6	1.0	0.083	0.02	0.75	8.6	0.10	1.5	0.15	0.25	0.4	0.083
7	2	Commercial	D_{min}	0.55	1.4	0.75	0	2.28	0.30	0.50	0.20	6	1.0	0.083	0.02	0.75	17.5	0.17	1.5	0.26	0.26	0.4	0.083
8	2	1 & 2 Family	D_{min}	0.55	1.4	0.75	0	2.28	0.30	0.50	0.20	6	1.0	0.083	0.02	0.75	17.5	0.17	1.5	0.26	0.26	0.4	0.083
Performance Group No. PG-12 (Long Period, High Aspect Ratio)																							
12	3	Multi-Family	D_{min}	0.55	1.4	0.75	0	2.28	0.30	0.50	0.20	6	1.0	0.083	0.02	0.75	26.3	0.23	1.5	0.35	0.35	0.4	0.083

Seismic Base Shear: Model #11: 3 Story Commercial

The tributary loads for seismic design for a single 40ft wall and distributed loads for all wood-frame and SIP models is defined as follows:

Residential Models

Tributary area: 12.5 ft x 40 ft = 500 ft^2

Tributary Weight: 1 & 2 Family: Floor: 17.2k x 1000 / 500 ft^2 = 34.4 psf
Roof: 13.65k x 1000 / 500 ft^2 = 27.3 psf

Multi-Family: Floor: 27.3k x 1000 / 500 ft^2 = 54.6 psf
Roof: 13.65k x 1000 / 500 ft^2 = 27.3 psf

Commercial Models

Tributary area: 40’ x 40’ = 1600 ft^2

Tributary Weight: Floor: 82k x 1000 / 1600 ft^2 = 51.3 psf
Roof: 41k x 1000 / 1600 ft^2 = 25.6 psf

Model #11: W = (3200 ft^2 * 51.3psf)*2 +3200 ft^2 *25.6psf = 410,000 lb

(SDC D_{min}); V = C_s * W = 0.083 * 410,000lb = 34,076 lb

The vertical distribution of seismic forces is defined Section 12.8.3. This method was selected over the distribution of forces based on the fundamental ordinate mode and story mass as defined in Equation 12 in Section 3.5 of this report. The lateral seismic force at any level is defined by equations12.8-11 and 12.8-12.

Equation 12.8-11: $F_x = C_{vx} V$

Equation 12.8-12: $C_{vx} = \frac{w_x h_x^k}{\sum_{1=1}^{n} w_i h_i^k}$

C_{vx}: The vertical distribution factor

w_i and w_x : The portion of the total effective seismic weight (lb) at level *i* or *x*

h_i and h_x: Equal to the height (ft) from the base to level *i* or *x*

k: Exponent related to the building period, and is set to a value of 1.0 for all models with a period of less than 0.5 second.

Model #11: $C_{v,floor\ 1} = \frac{164{,}000 * 8.42^{1.0}}{164{,}000*8.42^{1.0}+164{,}000*17.25^{1.0}+82{,}000*26.29^{1.0}} = 0.21$

$$C_{v,floor\ 2} = \frac{164{,}000 * 17.25^{1.0}}{164{,}000*8.42^{1.0}+164{,}000*17.25^{1.0}+82{,}000*26.29^{1.0}} = 0.44$$

$$C_{v,Roof} = \frac{82{,}000 * 26.29^{1.0}}{164{,}000*8.42^{1.0}+164{,}000*17.25^{1.0}+82{,}000*26.29^{1.0}} = 0.35$$

The vertical distribution factors for the other 11 models are presented in Table 24.

Table 24: Base Shear Calculations for SIP Archetype Models

Archetype ID	No. of Stories	Building Configuration	Floor Distributed Load (psf)	Roof Distributed Load (psf)	Effective Seismic Weight (lb)	$V = C_s * W = V_b$	$C_{v,floor1}$	$C_{v,floor2}$	$C_{v,Roof}$
Performance Group No. PG-1 (Short Period, Low Aspect Ratio)									
1	1	Commercial	--	25.6	82,000	13,667	--	--	1.0
5	2	Commercial	51.3	25.6	246,000	41,000	0.49	--	0.51
9	3	Commercial	51.3	25.6	410,000	68,333	0.22	0.44	0.34
Performance Group No. PG-9 (Short Period, High Aspect Ratio)									
2	1	1 & 2 Family	--	27.3	27,300	4,550	--	--	1.0
6	2	1 & 2 Family	34.4	27.3	61,700	10,283	0.38	--	0.62
10	3	Multi-Family	54.6	27.3	136,500	22,750	0.22	0.44	0.34
Partial Performance Group No. PG-4 (Long Period, Low Aspect Ratio)									
11	3	Commercial	51.3	25.6	410,000	34,076	0.22	0.44	0.34
Performance Group No. PG-11 (Long Period, High Aspect Ratio)									
3	1	Commercial	--	25.6	82,000	6,815	--	--	1.0
4	1	1 & 2 Family	--	27.3	27,300	2,269	--	--	1.0
7	2	Commercial	51.3	25.6	246,000	20,445	0.49	--	0.51
8	2	1 & 2 Family	34.4	27.3	61,700	5,128	0.38	--	0.62
Performance Group No. PG-12 (Long Period, High Aspect Ratio)									
12	3	Multi-Family	54.6	27.3	136,500	11,345	0.22	0.44	0.34

Input Ground Motions: For short-period archetypes ($T \leq T_S$), the MCE ground motion intensity, S_{MT}, is defined as: $S_{MT} = S_{MS}$

(SDC D_{max}); $S_{MS} = 1.5$ (SDC D_{min}); $S_{MS} = 0.75$

The results of the ELF procedure were used for the nonlinear static analysis of the models and selection/evaluation of the SPFs for SIPs. The process outlined in Chapter 4 of this

study was used to develop the roof drift versus base shear pushover curves for each model. The period based ductility was also determined from the pushover curves.

6.4 Nonlinear Dynamic Analysis

Each building model was subjected to nonlinear dynamic analysis using the 22 pairs of predetermined ground motion records addressed in Section 3.6 and presented in Table 25.

Table 25: PEER NGA Database Far-Field Ground Motion Set and Normalization Factors (Source: FEMA, 2009)

ID No.	Earthquake			Recording Station		Normalization Factor
	M	Year	Name	Name	Owner	
1	6.7	1994	Northridge	Beverly Hills – Hulhol	USC	0.65
2	6.7	1994	Northridge	Canyon Country – WLC	USC	0.83
3	7.1	1999	Duzce, Turkey	Bolu	ERD	0.63
4	7.1	1999	Hector Mine	Hector	SCSV	1.09
5	6.5	1979	Imperial Valley	Delta	UNAMUCSD	1.31
6	6.5	1979	Imperial Valley	El Centro Array #11	USGS	1.01
7	6.9	1995	Kobe, Japan	Mishi-Akashi	CUE	1.03
8	6.9	1995	Kobe, Japan	Shin-Osaka	CUE	1.1
9	7.5	1999	Kocaeli, Turkey	Duzce	ERD	0.69
10	7.5	1999	Kocaeli, Turkey	Arcelik	KOERI	1.36
11	7.3	1992	Landers	Yermo Fire Station	CDMG	0.99
12	7.3	1992	Landers	Coolwater	SCE	1.15
13	6.9	1989	Loma Prieta	Capitola	CDMG	1.09
14	6.9	1989	Loma Prieta	Gilroy Array #3	CDMG	0.88
15	7.4	1990	Manjil, Iran	Abbar	BHRC	0.79
16	6.5	1987	Superstition Hills	El Centro Imp. Co.	CDMG	0.87
17	6.5	1987	Superstition Hills	Poe Road (temp)	USGS	1.17
18	7	1992	Cape Mendocino	Rio Dell Overpass	CDMG	0.82
19	7.6	1999	Chi-Chi, Taiwan	CHY101	CWB	0.41
20	7.6	1999	Chi-Chi, Taiwan	TCU045	CWB	0.96
21	6.6	1971	San Fernando	LA – Hollywood Stor	CDMG	2.1
22	6.5	1976	Friuli, Italy	Tolmezzo	--	1.44

The ground motions were incrementally scaled and evaluated at the point where half of the ground motions caused collapse of the archetype. A preliminary assessment of SIP archetype model #1 was conducted in SAPWood to determine the necessary range of ground motion scaling for IDA assessment. The model was subjected to each of the 22 sets of far-field ground motions and scaled incrementally. The initial range of necessary scaling to reach the median collapse capacity was unknown. Methodology scaling is dependent on the fundamental period (T) and SDC selected for analysis. Therefore, a initial run with each archetype model was conducted to determine the fundamental period of the model (T_1), as determined by eigenvalue analysis in SAPWood (FEMA, 2009). The normalization and scaling of the ground motion records was based on T_1 and the SDC for the archetype model. Normalization factors are provided in Table 25 and scaling factors are provided in the Table 26.

Table 26: Median 5%-Damped Spectral Accelerations of Normalized Far-Field Set and Scaling Factor (Source: FEMA, 2009)

Period $T = C_u T_a$ (sec.)	Scaling Factors for Anchoring Far-Field Record Set to MCE Spectral Demand			
	SDC D_{max}	SDC C_{max} / SDC D_{min}	SDC B_{max} / SDC C_{min}	SDC B_{min}
0.25	1.93	0.96	0.64	0.32
0.3	1.94	0.97	0.65	0.32
0.35	1.97	0.99	0.66	0.33
0.4	2.00	1.00	0.67	0.33
0.45	2.00	0.89	0.59	0.30
0.5	2.04	0.82	0.54	0.27
0.6	2.49	0.83	0.55	0.28
0.7	2.40	0.80	0.53	0.27
0.8	2.50	0.83	0.56	0.28
0.9	2.50	0.83	0.56	0.28
1	2.59	0.86	0.58	0.29
1.2	2.49	0.83	0.55	0.28
1.4	2.51	0.84	0.56	0.28
1.6	2.70	0.90	0.60	0.30
1.8	2.98	0.99	0.66	0.33
2	3.05	1.02	0.68	0.34
2.2	3.08	1.03	0.68	0.34
2.4	3.18	1.06	0.71	0.35
2.6	3.28	1.09	0.73	0.36
2.8	3.53	1.18	0.79	0.39
3	3.75	1.25	0.83	0.42
3.5	4.10	1.37	0.91	0.46
4	4.29	1.43	0.95	0.48
4.5	4.34	1.45	0.96	0.48
5	4.43	1.48	0.98	0.49

The minimum scaling factor for SDC D_{min} is 0.96 and the maximum scale factor for SDC D_{max} is 2.60, corresponding to the minimum and maximum fundamental periods of the SIP buildings as determined through the ELF procedure and SAPWood, respectively. Additionally, the wood-frame methodology IDA example plot provided in FEMA P695 (2009) ranges from 0 to 7.0 for S_a (g). After a few iterative trials, the preliminary IDA

analysis was conducted with S_a (g) values ranging from 0.1 (g) to 5.0 (g) and with increments of 0.1 (g). Incremental Dynamic Analysis used each of the 22 Far-Field record sets, which include component pairs of horizontal ground motions from sites located greater than or equal to 10km (FEMA, 2009). The point on the "intensity-drift IDA plot having a nearly horizontal slope but without exceeding a peak inter-story drift of 7% in any wall of the model" was defined as the intensity of the ground motion causing collapse of the model (ASCE, 2008c). IDA results confirm that the extreme minimum and maximum values of Sa are well beyond the range necessary for collapse evaluation. S_a (g) values ranging from 0.1 (g) to 5.0 (g) increased in increments of 0.1 (g) as determined from the preliminary test results proved satisfactory for analysis, and adjustment was not needed for additional models. The CMR is the ratio of the median collapse intensity to the MCE intensity and was determined based on the IDA results.

The CMR must be adjusted for spectral shape factor (SSF), which is based on its global ductility capacity obtained from the pushover curve. The SSF values, provided in Table 27 and 28, are selected based on the SDC, fundamental period, and period-based ductility for a single archetype model.

Table 27: Spectral Shape Factor (SSF) for Archetypes Designed for SDC B, SDC C, or SDC, Dmin (Source: FEMA, 2009)

T (sec.)	**Period-Based Ductility, μ_T**							
	1.0	**1.1**	**1.5**	**2**	**3**	**4**	**6**	**≥ 8**
≤ 0.5	1.0	1.02	1.04	1.06	1.08	1.09	1.12	1.14
0.6	1.0	1.02	1.05	1.07	1.09	1.11	1.13	1.16
0.7	1.0	1.03	1.06	1.08	1.10	1.12	1.15	1.18
0.8	1.0	1.03	1.06	1.08	1.11	1.14	1.17	1.20
0.9	1.0	1.03	1.07	1.09	1.13	1.15	1.19	1.22
1.0	1.0	1.04	1.08	1.10	1.14	1.17	1.21	1.25
1.1	1.0	1.04	1.08	1.11	1.15	1.18	1.23	1.27
1.2	1.0	1.04	1.09	1.12	1.17	1.20	1.25	1.30
1.3	1.0	1.05	1.10	1.13	1.18	1.22	1.27	1.32
1.4	1.0	1.05	1.10	1.14	1.19	1.23	1.30	1.35
≥ 1.5	1.0	1.05	1.11	1.15	1.21	1.25	1.32	1.37

Table 28: Spectral Shape Factor (SSF) for Archetypes Designed using SDC Dmax (Source: FEMA, 2009)

T (sec.)	**Period-Based Ductility, μ_T**							
	1.0	**1.1**	**1.5**	**2**	**3**	**4**	**6**	**≥ 8**
≤ 0.5	1.0	1.05	1.10	1.13	1.18	1.22	1.28	1.33
0.6	1.0	1.05	1.11	1.14	1.20	1.24	1.30	1.36
0.7	1.0	1.06	1.11	1.15	1.21	1.25	1.32	1.38
0.8	1.0	1.06	1.12	1.16	1.22	1.27	1.35	1.41
0.9	1.0	1.06	1.13	1.17	1.24	1.29	1.37	1.44
1.0	1.0	1.07	1.13	1.18	1.25	1.31	1.39	1.46
1.1	1.0	1.07	1.14	1.19	1.27	1.32	1.41	1.49
1.2	1.0	1.07	1.15	1.20	1.28	1.34	1.44	1.52
1.3	1.0	1.08	1.16	1.21	1.29	1.36	1.46	1.55
1.4	1.0	1.08	1.16	1.22	1.31	1.38	1.49	1.58
≥ 1.5	1.0	1.08	1.17	1.23	1.32	1.40	1.51	1.61

The ACMR is computed for the archetype design as a multiple of the SSF and CMR. The Adjusted CMR (ACMR) was evaluated with the total system collapse uncertainty (β_{TOT}) against methodology defined acceptance criteria.

The composite system uncertainty (β_{TOT}) for SIPs as a lateral force resisting system is as follows:

SIP Design Requirements Uncertainty (β_{DR}): (C) Fair = 0.35

SIP Data Uncertainty (β_{TD}): (C) Fair = 0.35

SIP Modeling Uncertainty (β_{MDL}): (C) Fair = 0.35

Record-to-record variability (β_{RTR}) = 0.4

$\beta_{TOT} = \sqrt{0.35^2 + 0.35^2 + 0.35^2 + 0.40^2}$ = 0.727

The methodology objectives for collapse prevention probability are 20% for each archetype model and 10% for the average of the performance groups. Unacceptable values of ACMR fail the acceptance criteria of the methodology and the system design or the R value must be adjusted and reevaluated. The composite uncertainty for a system significantly affects the final evaluation therefore justifying the necessity of a comprehensive peer review process to develop each of the uncertainty variables. The acceptable values of ACMR are presented in Table 29.

Table 29: Acceptable Values of Adjusted Collapse Margin Ration (ACMR10% and ACMR20%) (Source: FEMA, 2009)

Total System Collapse Uncertainty	Collapse Probability				
	5%	10% ($ACMR_{10\%}$)	15%	20% ($ACMR_{20\%}$)	25%
0.275	1.57	1.42	1.33	1.26	1.20
0.300	1.64	1.47	1.36	1.29	1.22
0.325	1.71	1.52	1.40	1.31	1.25
0.350	1.78	1.57	1.44	1.34	1.27
0.375	1.85	1.62	1.48	1.37	1.29
0.400	1.93	1.67	1.51	1.40	1.31
0.425	2.01	1.72	1.55	1.43	1.33
0.450	2.10	1.78	1.59	1.46	1.35
0.475	2.18	1.84	1.64	1.49	1.38
0.500	2.28	1.90	1.68	1.52	1.40
0.525	2.37	1.96	1.72	1.56	1.42
0.550	2.47	2.02	1.77	1.59	1.45
0.575	2.57	2.09	1.81	1.62	1.47
0.600	2.68	2.16	1.86	1.66	1.50
0.625	2.80	2.23	1.91	1.69	1.52
0.650	2.91	2.30	1.96	1.73	1.55
0.675	3.04	2.38	2.01	1.76	1.58
0.700	3.16	2.45	2.07	1.80	1.60
0.725	3.30	**2.53**	2.12	**1.84**	1.63
0.750	3.43	2.61	2.18	1.88	1.66
0.775	3.58	2.7	2.23	1.92	1.69
0.800	3.73	2.79	2.29	1.96	1.72
0.825	3.88	2.88	2.35	2.00	1.74
0.850	4.05	2.97	2.41	2.04	1.77
0.875	4.22	3.07	2.48	2.09	1.80
0.900	4.39	3.17	2.54	2.13	1.83
0.925	4.58	3.27	2.61	2.18	1.87
0.950	4.77	3.38	2.68	2.22	1.90

6.5 SIP Archetype Model

The figures provided in this section are for each of the four SIP archetype models evaluated for this study. Each plotted collapse margin ratio is not adjusted for the

beneficial effects of spectral shape. The analysis results are compared to the corresponding wood-frame archetypes in Section 6.6. Figure 41 is provided as reference for the primary values obtained from each nonlinear static pushover plot. As provided in equation 15, the effective yield roof drift displacement, $\delta_{y\,eff}$, is a calculated value and not a valued obtained from the plot.

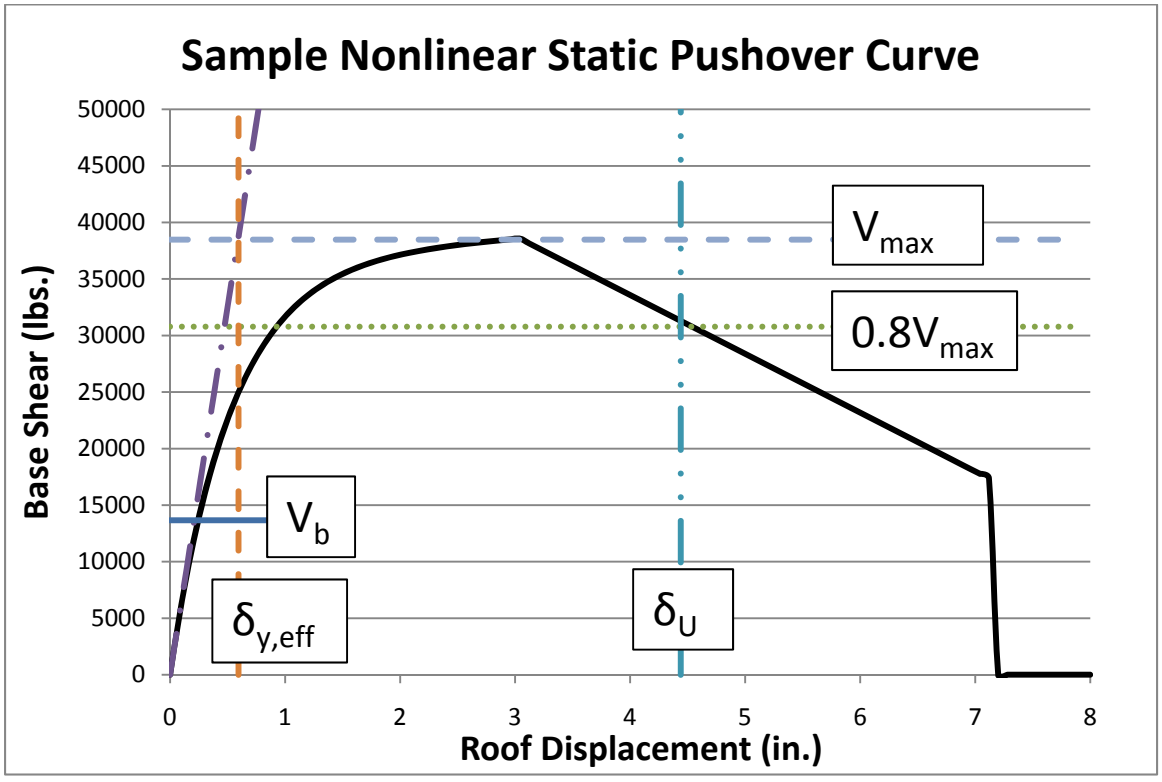

Figure 41: Sample Nonlinear Static Pushover Curve

6.5.1 SIP Archetype Model #1

SIP archetype model #1 consists of a one-story commercial building 40ft x 80ft in plan. Two 8ft x 8ft piers are included on each of the 40ft walls and four 8ft x 8ft piers are included on each of the 80ft walls. The nonlinear pushover curve for the one-story

building is provided in Figure 42. The results of incremental dynamic analysis and associated collapse fragility curve for the model #1 are provided in figures 43 and 44.

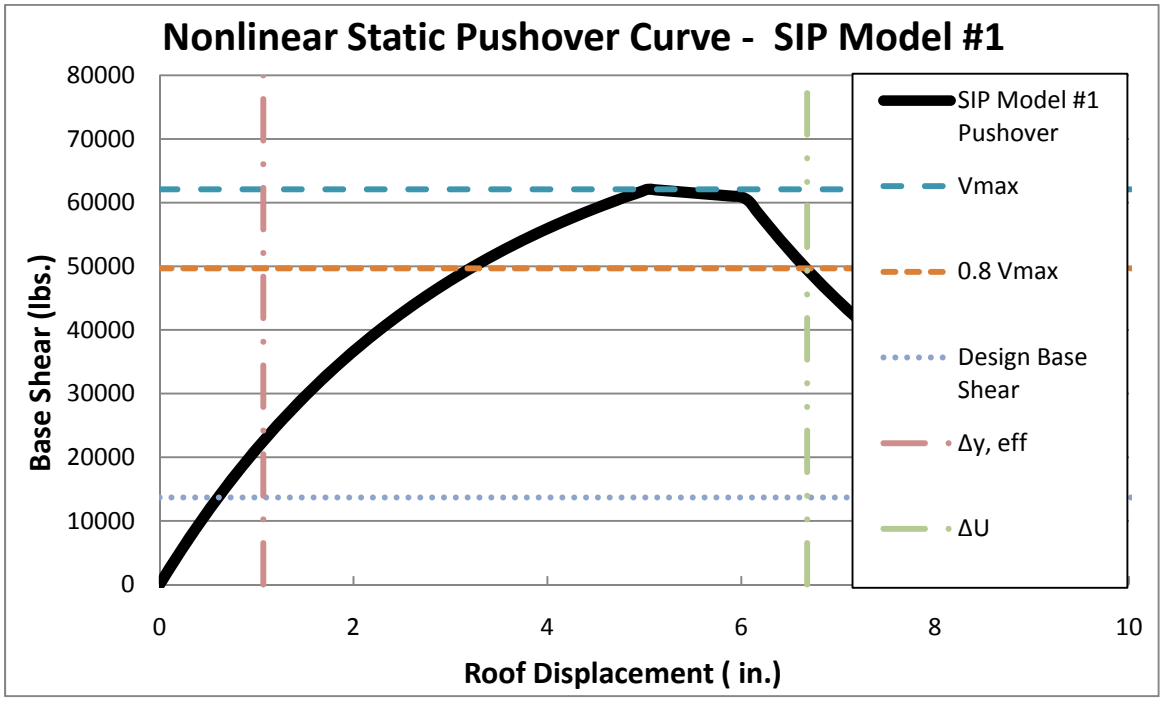

Figure 42: Nonlinear Static Pushover Curve, SIP Model #1

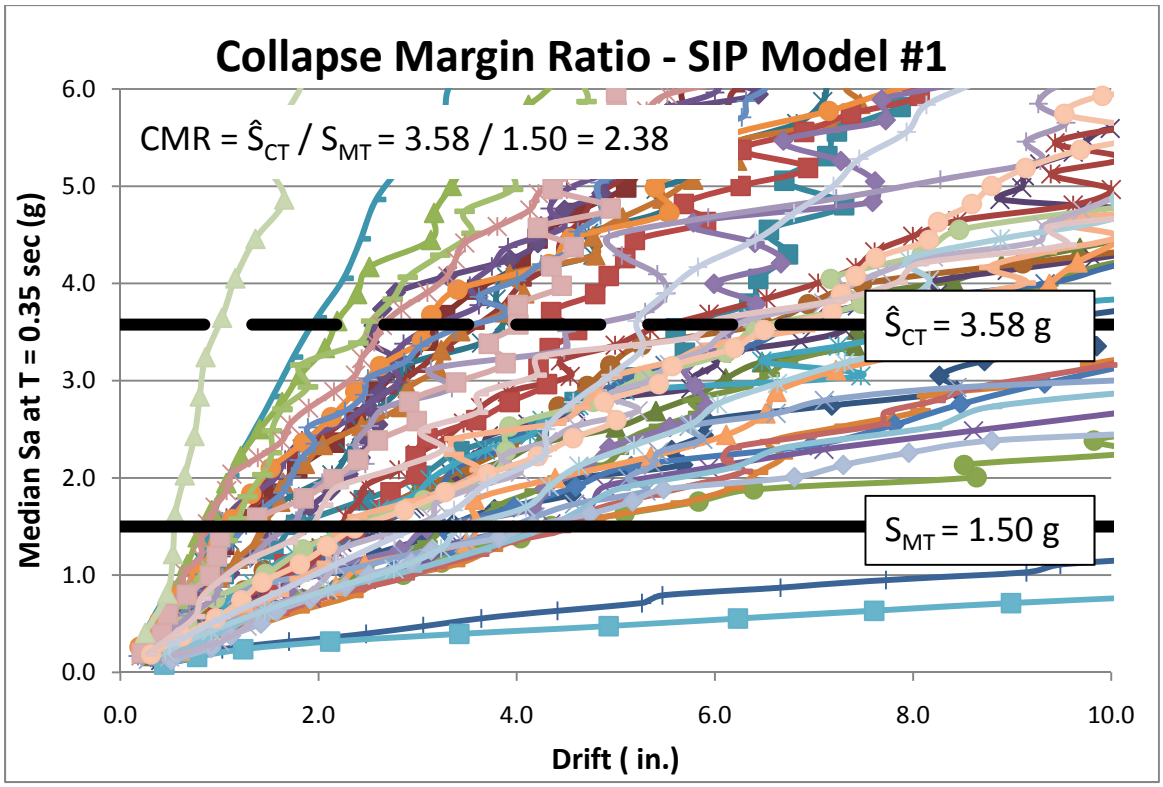

Figure 43: Collapse Margin Ratio, SIP Model #1

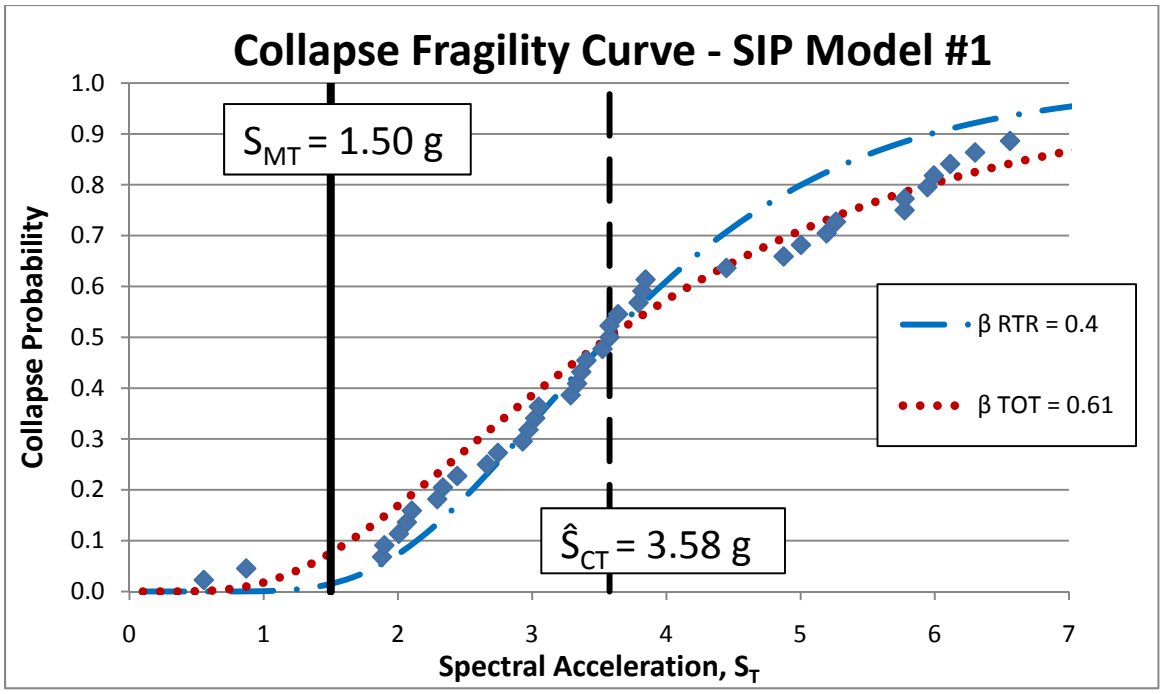

Figure 44: Collapse Fragility Curve, SIP Model #1

6.5.2 SIP Archetype Model #4

SIP archetype model #4 consists of a one-story 1 and 2 family residential building 40ft x 25ft in plan. One 8ft x 8ft pier is included on each the perimeter walls. The nonlinear pushover curve for the one-story building is provided in Figure 45. The results of incremental dynamic analysis and associated collapse fragility curve for the model #4 are provided in figures 46 and 47.

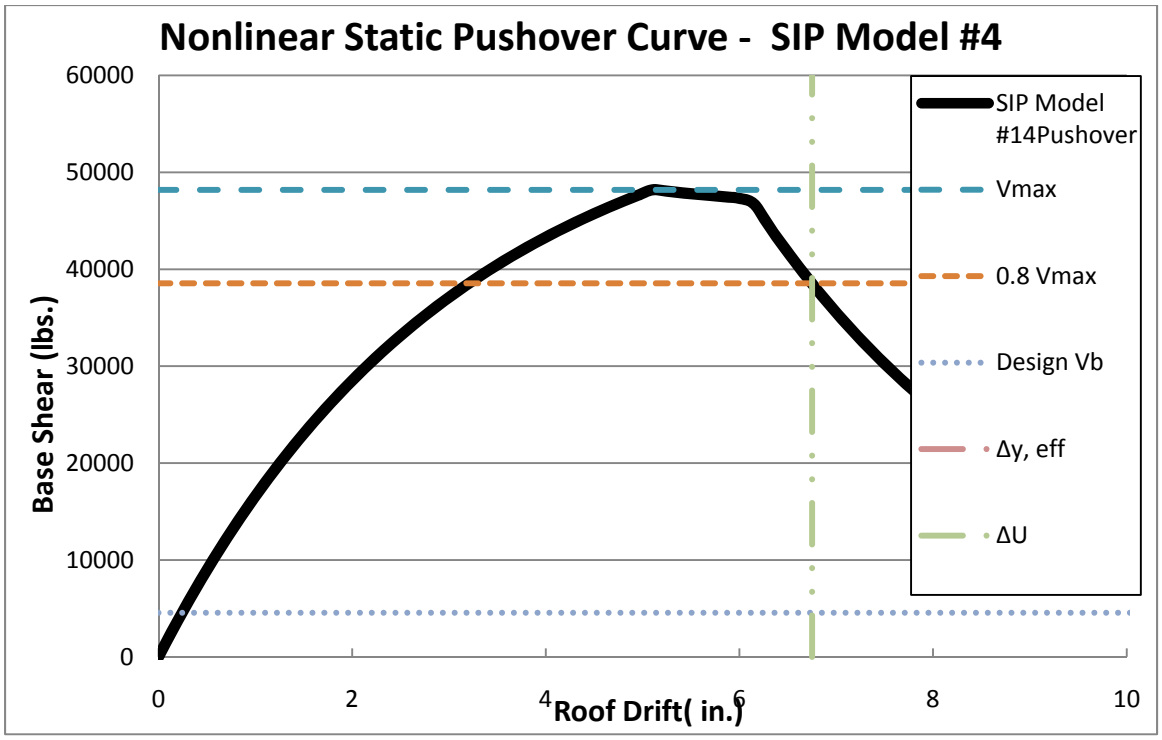

Figure 45: Nonlinear Static Pushover Curve, SIP Model #4

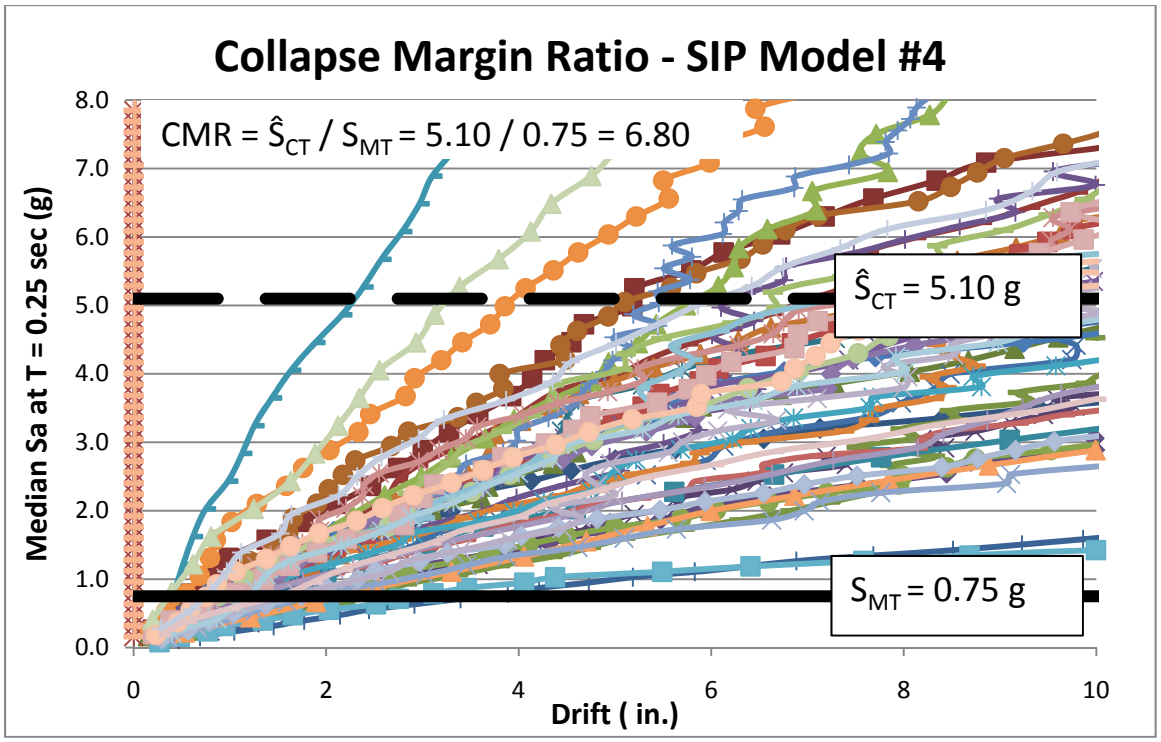

Figure 46: Collapse Margin Ratio, SIP Model #4

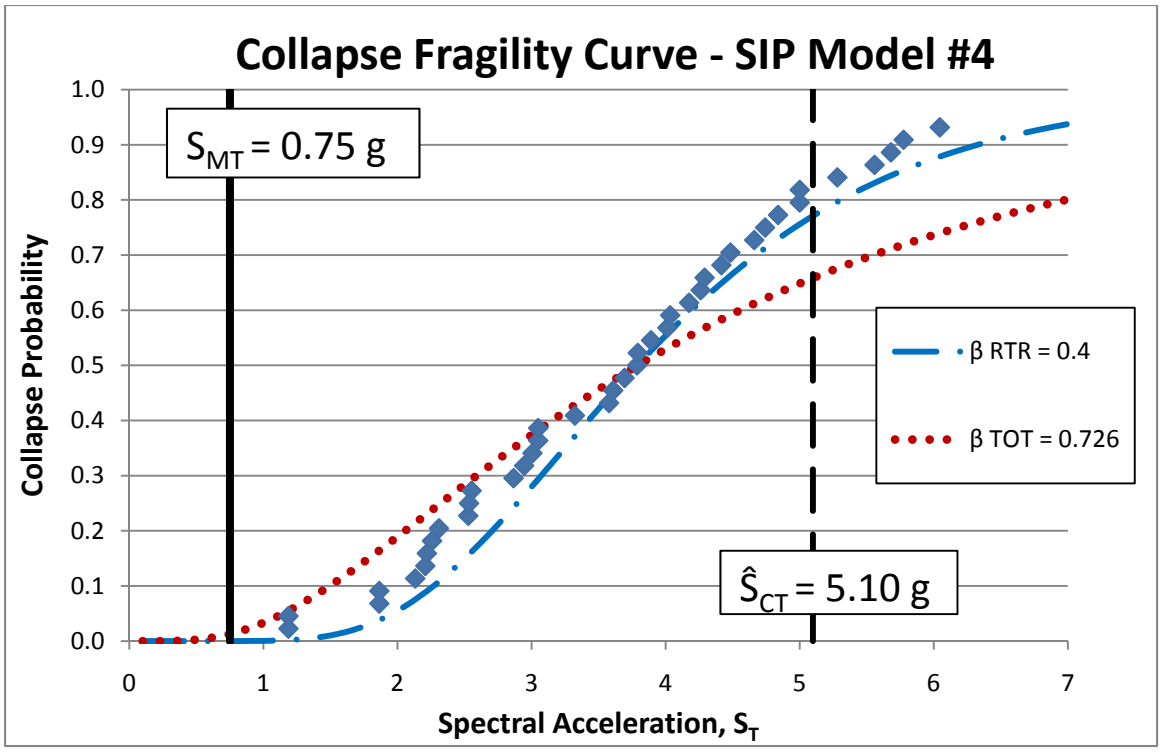

Figure 47: Collapse Fragility Curve, SIP Model #4

6.5.3 SIP Archetype Model #5

SIP archetype model #5 consists of a two-story commercial building 40ft x 80ft in plan. Three 8ft x 8ft piers are included on each the 40ft walls and six 8ft x 8ft piers are included on each of the 80ft walls. The story nonlinear pushover curves for the two-story building are provided in Figure 48, and the resultant roof drift versus base shear pushover curve is provided in Figure 49. The results of incremental dynamic analysis and associated collapse fragility curve for the model #5 are provided in figures 50 and 51.

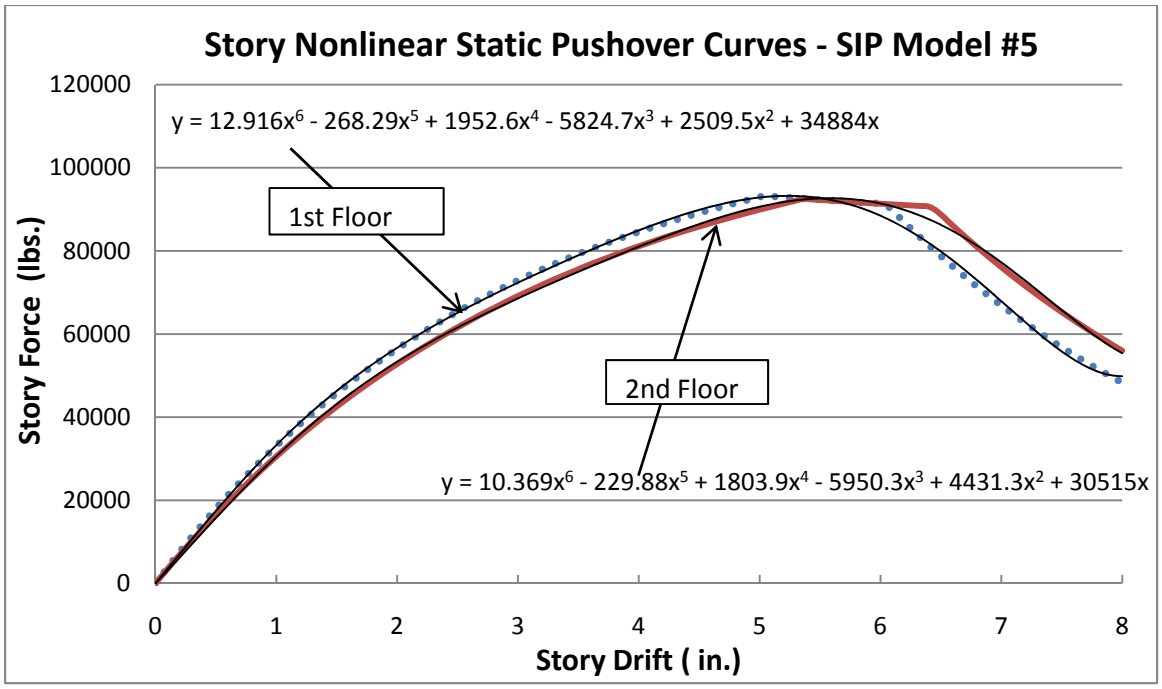

Figure 48: Story Nonlinear Static Pushover Curves, SIP Model #5

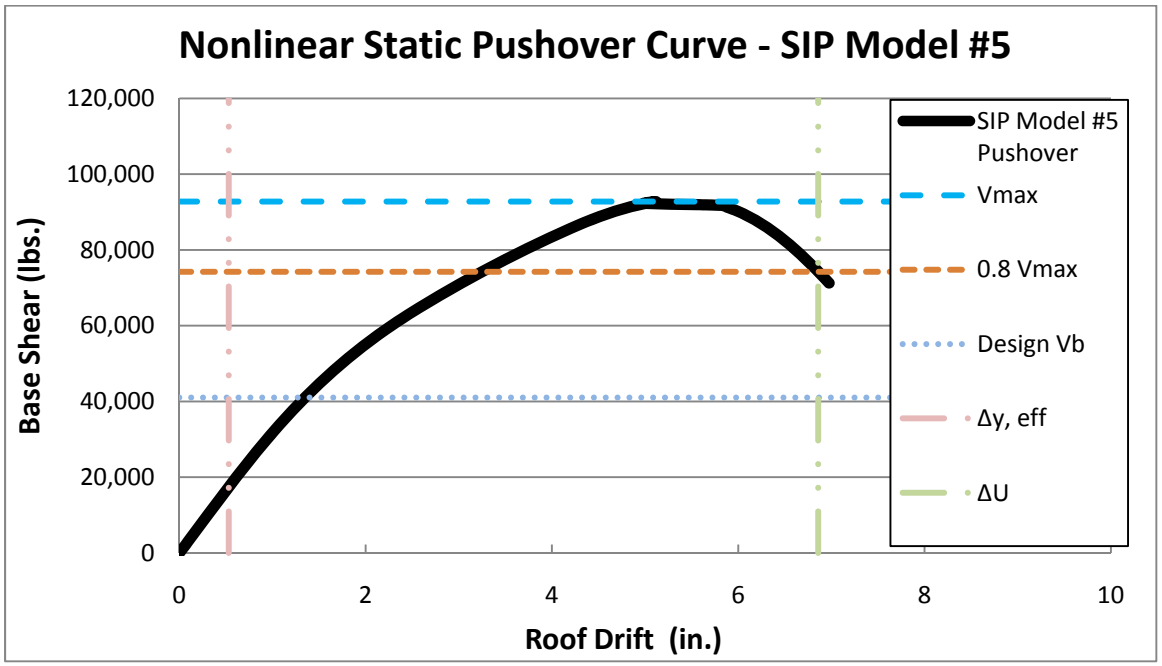

Figure 49: Nonlinear Static Pushover Curve, SIP Model #5

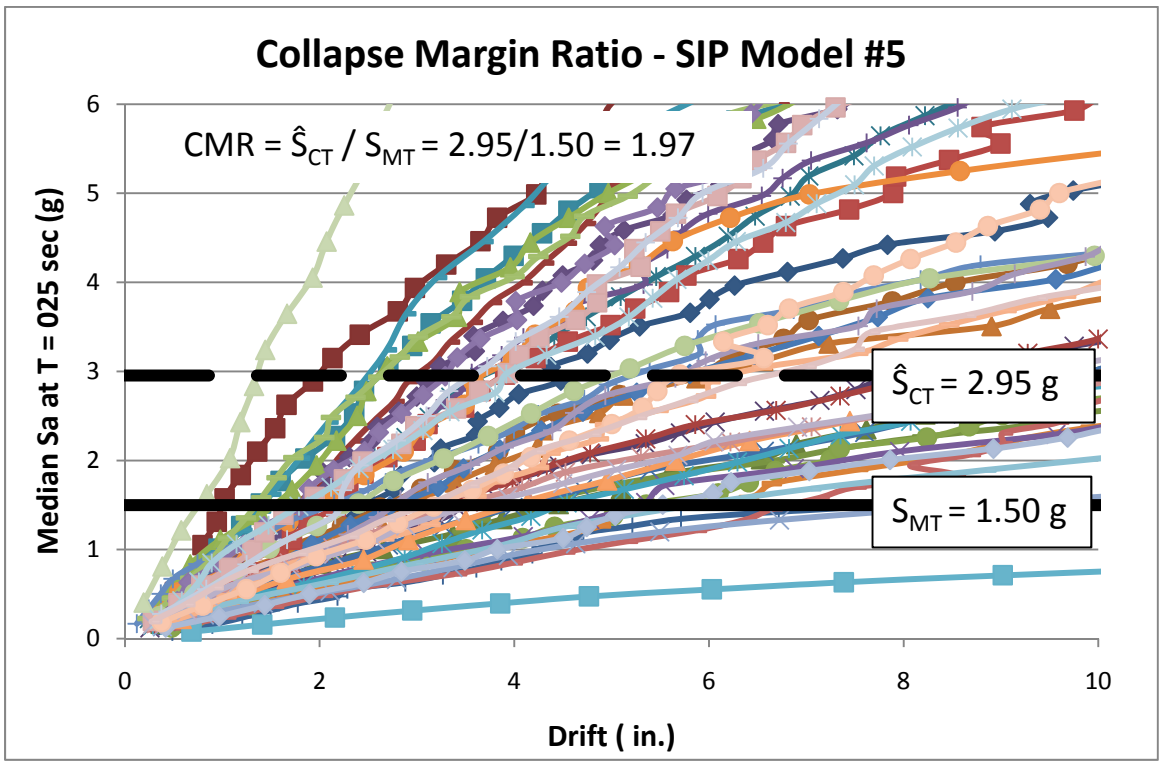

Figure 50: Collapse Fragility Curve, SIP Model #5

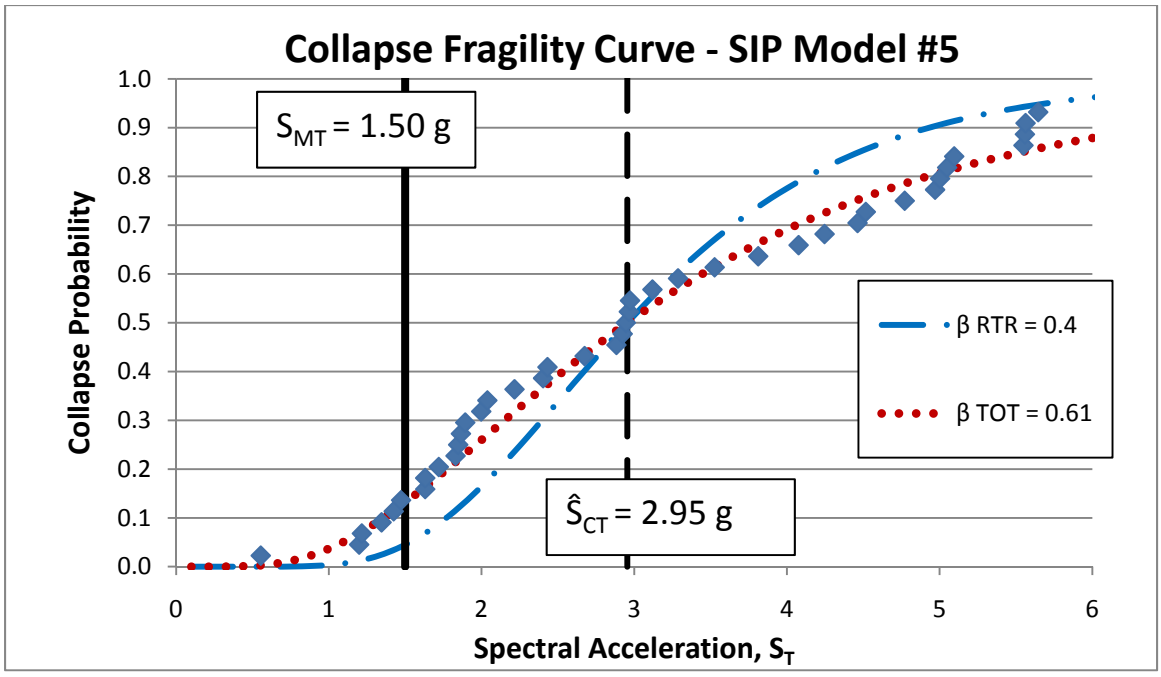

Figure 51: Collapse Fragility Curve, SIP Model #5

6.5.4 SIP Archetype Model #11

SIP archetype model #11 consists of a three-story commercial building 40ft x 80ft in plan. Two 8ft x 8ft piers are included on each the 40ft walls and four 8ft x 8ft piers are included on each of the 80ft walls. The story nonlinear pushover curves for the three-story building is provided in Figure 52, and the resultant roof drift versus base shear pushover curve is provided in Figure 53. The results of incremental dynamic analysis and associated collapse fragility curve for the model #11 are provided in figures 54 and 55.

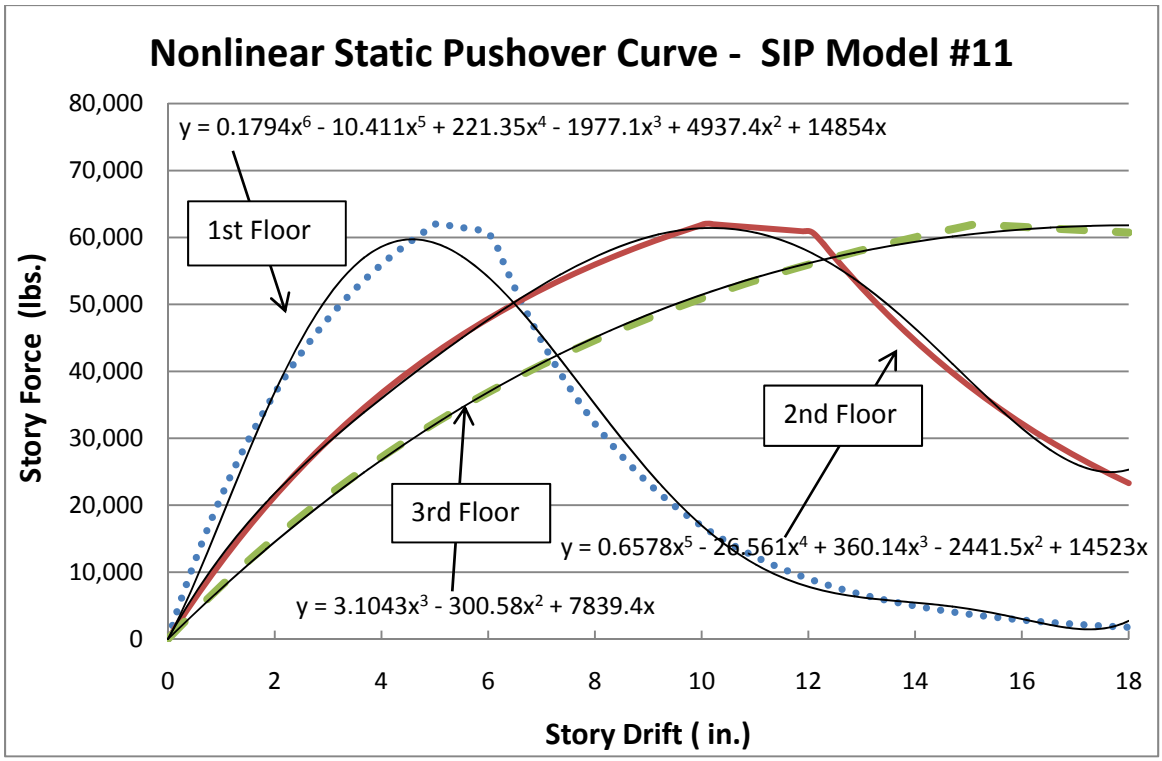

Figure 52: Story Nonlinear Static Pushover Curves, SIP Model #11

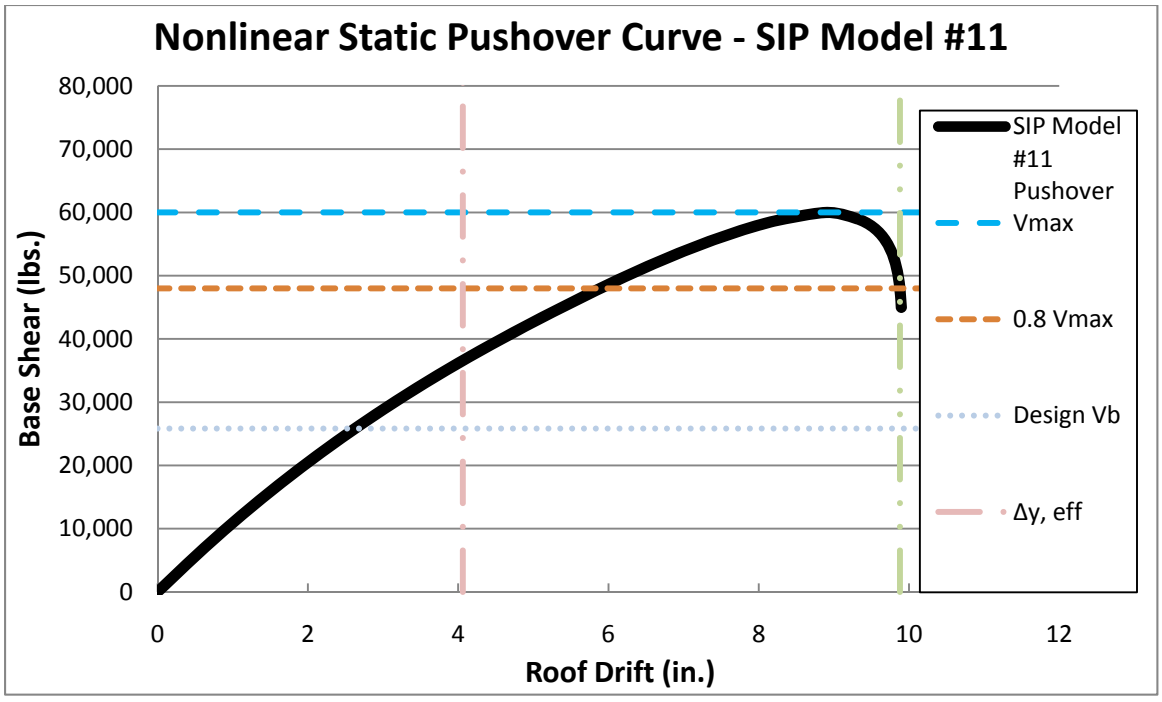

Figure 53: Nonlinear Static Pushover Curve, SIP Model #11

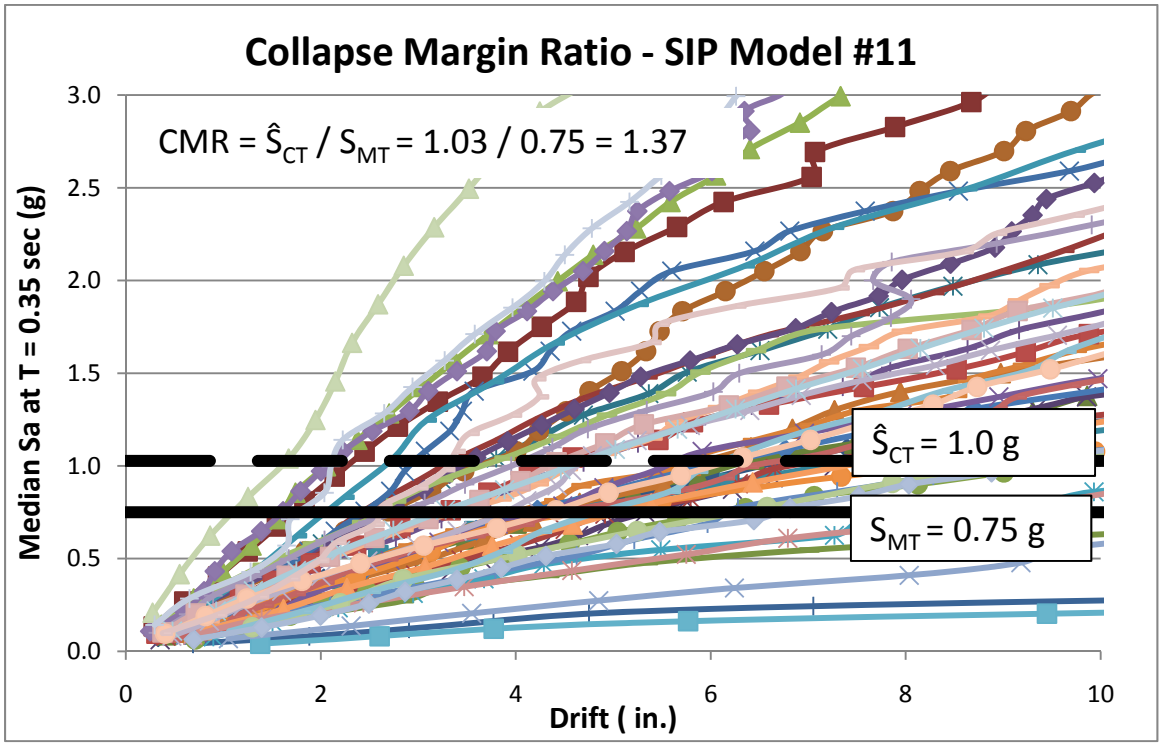

Figure 54: Collapse Fragility Curve, SIP Model #11

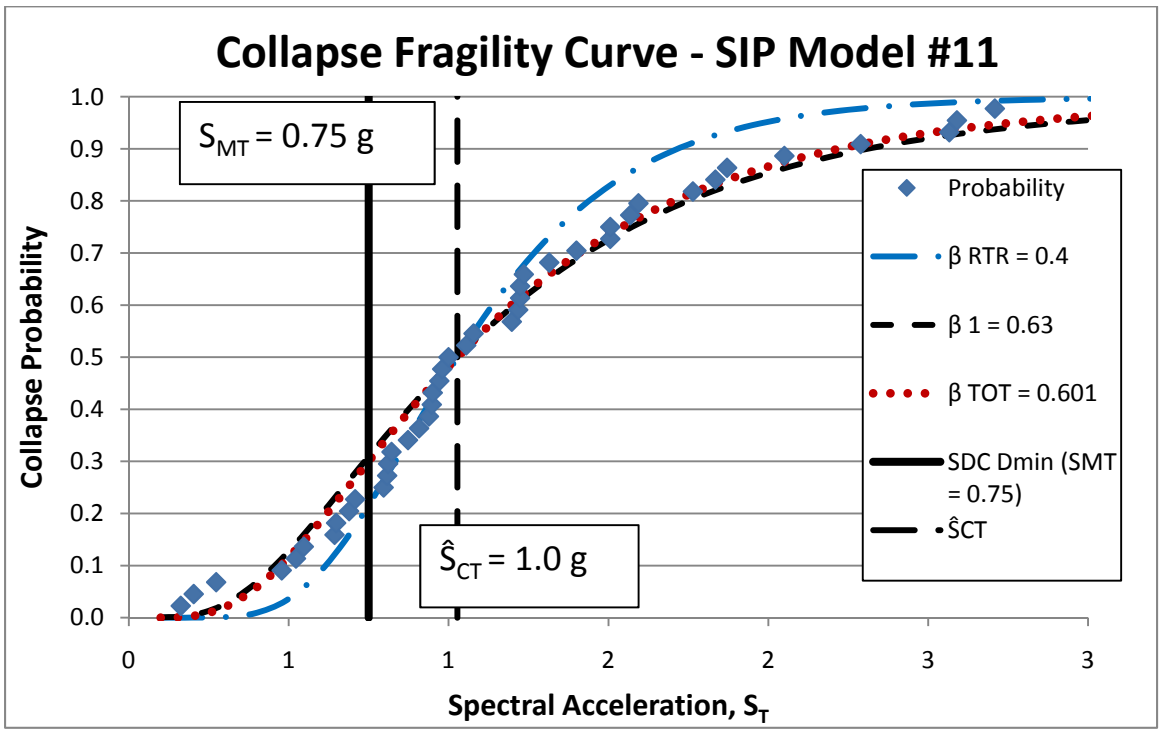

Figure 55: Collapse Fragility Curve, SIP Model #11

6.6 SIP Archetype Model Assessment

The collapse margin ratios provided in Figures 42, 45, 49, and 53 do not take into account the spectral shape factor, SSF. As addressed in Section 3.6, 3.7 and Chapter 6 Tables 27 and 28. The appropriate SSF is selected based on the period based ductility, μ_T, as calculated from the pushover curves provided in Figures 42, 45, 49, and 53. The adjusted collapse margin ratio, ACMR, is then computed as the product of the CMR and SSF. The collapse assessment parameters from the figures presented for each model and corresponding parameters used to define the values are summarized in Table 30.

Table 30: SIP Nonlinear Analysis Values

Archetype ID	V_{max} (lbs.)	0.8 V_{max} (lbs.)	δ_U (in.)	Design V_b (lbs.)	$\delta_{y,\,eff}$ (in.)
Performance Group No. PG-1 (Short Period, Low Aspect Ratio)					
1	62,101	49,681	6.68	13,667	1.07
5	92,750	74,200	6.86	41,000	0.53
Partial Performance Group No. PG-4 (Long Period, Low Aspect Ratio)					
11	60,000	48,000	9.98	34,076	4.06
Performance Group No. PG-11 (Long Period, High Aspect Ratio)					
4	48,192	38,554	6.75	4,550	18.69

The collapse assessment parameters obtained from the figures presented for each archetype model and corresponding parameters used to assess the values are summarized in Table 31.

Table 31: SIP Collapse Assessment Parameters

System Type	Archetype ID	S_{MT} [T] (g)	$\hat{S}_{CT}$ [T] (g)	$\Omega = V_{max} / V_b$	CMR	SSF	ACMR	10% ACMR	20% ACMR	Pass / Fail
Performance Group No. PG-1 (Short Period, Low Aspect Ratio)										
SIP	1	1.50	3.58	4.54	2.39	1.28	3.05	2.53	1.84	Pass
L-F Wood	1	1.50	2.01	2.00	1.34	1.33	1.78	1.90	1.52	Pass
SIP	5	1.50	2.95	2.26	1.97	1.33	2.62	2..53	1.84	Pass
L-F Wood	5	1.50	2.23	2.50	1.45	1.31	1.95	1.90	1.52	Pass
Partial Performance Group No. PG-4 (Long Period, Low Aspect Ratio)										
SIP	11	0.75	1.03	1.76	1.37	1.07	1.47	2.53	1.84	Fail / Fail
L-F Wood	11	0.75	1.98	2.10	2.64	1.13	2.98	1.90	1.52	Pass
Performance Group No. PG-11 (Long Period, High Aspect Ratio)										
SIP	4	0.75	5.10	10.59	6.80	1.00	6.80	2.53	1.84	Pass
L-F Wood	4	0.75	2.09	5.40	2.78	1.14	3.16	2.38	1.76	Pass

The four models assessed for this study performed well for the limited amount of data available to construct each numerical model. The one and two-story buildings passed the acceptance criteria, but SIP Model #3, the three-story commercial building, did not pass. Models #2 and #3 were composed of three stories of equal strength and stiffness. Alternatively, each of the stories in the wood-frame archetypes was modeled with increasing strength and stiffness from top to bottom of the building, respectively. It can also be observed that SIP Model #5, the two-story commercial building was only slightly above the $ACMR_{10\%}$. The strength limitations in the lower levels of the multi-story buildings expedited the collapse of each building. The primary conclusions drawn from this evaluation are presented in Chapter 7.

Chapter 7: Summary, Conclusions, and Recommendations

The assessment conducted for this report provides a solid foundation for a full FEMA P695 based methodology assessment of structural insulated panels as a seismic-force-resisting system. A proposed range of 12 building models, including the associated nail spacing and pier aspect ratios, was established for the SIP system and variations on four of the building models were tested in accordance with methodology guidance. Three of the four building models passed acceptance criteria, and the limited data available to model unacceptable building clearly nullify its' failure. The SAPWood computer program was used for analytical testing of the residential and light commercial structures. The models analyzed were comparable to the buildings assessed in the wood-frame portion of the FEMA P695 (2009) project. Wood-frame archetypes and their corresponding SIP archetypes showed good comparison, but the comparative analysis was limited by the available data to develop SIP archetype models. The SAPWood computer modeling program was established as an excellent tool available for the modeling of SIP piers and building models. Artificial fasteners were added to the SIP shear walls to represent the SIP core's contribution to lateral stiffness.

Comparative analysis of wood-frame and SIP shear walls clearly demonstrates that the initial stiffness of a SIP shear wall is less than that of the equivalent wood-frame wall, but the SIPs can withstand larger ultimate forces and drifts than the traditional wood wall. Additionally, previous research has shown that the sheathing-to-framing fastener connection is critical to the performance of the shear wall. Therefore it can be determined that the core of the SIP acts as a mechanism to redistribute the load path of

the shear wall. The initial stiffness of the SIP is primarily based on the fasteners contribution with minimal stiffening effect by the core prior to end stud-to-core contact. However, when larger displacement occur and the end studs start to bear against the core, the core supplements stiffness and strength to the degraded fasteners for lateral force resistance. The redistribution of forces clarifies how the stiffness increases as testing progresses. The core enhances the shear wall performance by modifying the load path so that a portion of the forces are transmitted through the core rather than only the sheathing nails. This redistribution of forces is analogous to an internalized brace in brace in a light-frame or timber frame shear wall. The SIP performs distinctly different that a traditional wood-frame wall, and therefore further justifies the use of the adjusted numerical model for SIP building analysis.

An initial assessment of SIPs as a seismic-performance-resisting system with R=6 is strongly optimistic based on the performance of the four building models, but a conclusive value determination for the system overstrength factor, Ω, for the SIP system is not achievable with the available data from this study. Excluding the results from Model #11, for reasons addressed in Chapter 6, based on the results of the study it can be determine that the overstrength factor for the SIP system will likely match the maximum allowable value of 3.0 as assigned to wood-frame systems.

Experimental testing with broad range of fastener spacing, pier aspect ratios, and spline configurations must be conducted for a comprehensive evaluation of the SIP system and rational determination of seismic performance factors. Additionally, a full methodology assessment requires the entire process to be evaluated by a peer review panel consisting of members qualified to critically evaluate the development of the proposed system.

The completed research project has provided an extensive amount of information regarding the quantification of SPFs for SIP wall systems. The background information and comparative wood-frame to SIP shear wall analysis will provide a strong basis for the Structural Insulated Panel Association's efforts, in follow-up studies, to move closer to code approval beyond that introduced in Section R614 of the 2007 IRC Supplement. This report is meant to be used as the basis of study for a comprehensive evaluation of the methodology for structural insulated panels.

References

American National Standards Institute and American Forest and Paper Association (2005). *National Design Specifications for Wood Construction*, ANSI/AF&PA NDS-2005, Washington, D.C.

American Society for Testing and Materials, (2006). "Standard Practice for Static Load Test for Shear Resistance of Vertical Elements of Framed Walls for Buildings," ASTM E564-06, *ASTM Annual Book of Standards*, West Conshohocken, Pennsylvania.

American Society for Testing and Materials, (2009). "Standard Test Methods for Cyclic (Reversed) Load Test for Shear Resistance of Vertical Elements of the Lateral Force Resisting Systems for Buildings," ASTM E2126-09, *ASTM Annual Book of Standards*, West Conshohocken, Pennsylvania.

American Society of Civil Engineers, (2006). *Minimum Design Loads for Buildings and Other Structures*, ASCE Standard – ASCE/SEI 7-05, Reston, Virginia.

American Society of Civil Engineers, (2006b). *Seismic Rehabilitation of Existing Buildings*, ASCE Standard - ASCE/SEI 41-06, Reston, Virginia.

Applied Technology Council, (1978). ATC-3-06, *Tentative Provisions for the Development of Seismic Regulations for Buildings*, Applied Technology Council (ATC), Redwood City, California.

Applied Technology Council, (1995). ATC-19, *Structural Response Modification Factors*, Applied Technology Council (ATC), Redwood City, California.

Ayoub, A., (2007). "Seismic Analysis of Wood Building Structures," *Engineering Structures*, Vol. 29, pp. 213-223.

Black, Gregory O., (2009). *Development and Application of an Empirical Loss Analysis for Wood-frame Buildings Subject to Seismic Events*, A thesis submitted to the Faculty of the University of Delaware in partial fulfillment of the requirements for the degree of Master of Civil Engineering, Newark, Delaware.

Chehab, M., (1982). *Seismic Analysis of a Two-Story Wood-frame House Using the Response Spectrum Technique*, Master of Science Thesis, Oregon State University, Corvallis, Oregon.

Davenne, L., Daudeville, L., Ricahrd, N., Kawai, N. and Yasumura, M. (1998) "Modeling of Timber Shear Walls with Nailed Joints Under Cyclic Loading," *Proceedings of the Fifth World Conference on Timber Engineering*, Lausanne, Switzerland, Vol. 1, pp.353-360.

Deierlein, G.G., Liel, A. B., Haselton, C.B., Kircher, C.A., (2008). "ATC 63 Methodology for Evaluating Seismic Collapse Safety of Archetype Buildings", *Proceedings of the ASCE Structures Congress 2008*, April 24-28, 2008, Vancouver, British Columbia, Canada, CD-Rom, 10 pages.

Dolan, J.D., (1998). "*The Dynamic Response of Timber Shear Walls*," Doctor of Philosophy Dissertation, University of British Columbia, Vancouver, Canada.

Dolan, J.D., Foschi, R.O., (1991). "Structural Analysis Model for Static Loads on Timber Shear Walls," *J. Structural Engineering*, Vol. 117, No. 3, pp. 851–861.

Dolan, J.D. and Nadsen, B., (1992). "Monotonic and Cyclic Tests of Timber Shear Wall," *Can. J. Civ. Eng.*, 19(4), 415-422.

Falk, R.H. and Itani, R.Y., (1989) "Finite Element Modeling of Diaphragms," *J. Structural Engineering*, Vol. 115, No. 3, pp. 543-559.

Federal Emergency Management Agency (FEMA), (2004). *Recommended Provisions for Seismic Regulations for New Buildings and Other Structure*, FEMA 450-1/2003 Edition, Part 1: Provisions, Washington, D.C.

Federal Emergency Management Agency (FEMA), (2004b). *NEHRP Recommended Provisions for Seismic Regulations for New Buildings and Other Structure*, FEMA 450-2/2003 Edition, Part 2: Commentary, Washington, D.C.

Federal Emergency Management Agency (FEMA), (2009). *Quantification of Building Seismic Performance Factors*, FEMA P695, Washington, D.C.

Federation of American Scientists (FAS), (2010), *Analysis of the Seismic Performance of SIPs: A White Paper*, 15 January 2010, http://www.fas.org/programs/energy/btech/advanced%20technologies/seismic%20SIPs%20white%20paper.pdf

Filiatrault A., (1990). "Static and Dynamic Analysis of Timber Shear Walls," *Canadian Journal of Civil Engineering*, Vol. 17 No. 4, pp. 643–651.

Filiatrault, A. and Christovasilis, I.P., (2008). "Example Evaluation of the ATC-63 Methodology for Wood Light-Frame System," *Proceedings of the ASCE Structures*

Congress 2008, April 24-28, 2008, Vancouver, British Columbia, Canada, CD-Rom 10 pages.

Folz, B. and Filatrault, A., (2001). "Cyclic Analysis of Wood-frame shear walls ." *J. Structural Engineering*, Vol. 127, No. 4, pp. 433-441.

Folz, B., and Filatrault, A., (2004a). "Seismic Analysis of Wood-frame Structures. I: Model Formulation." *J. Structural Engineering*, Vol. 130, No. 8, pp. 1353-1360.

Folz, B., and Filatrault, A., (2004b). "Seismic Analysis of Wood-frame Structures. II: Model Implementation and Verification." *J. Structural Engineering*, Vol. 130, No. 8, pp.1361-1370.

Foschi, R.O., (1995). Diaphragm Analysis Program 3D--User's Manual. University of British Columbia, Vancouver, British Columbia, 1995.

Foschi, R.O., (2000). "Modeling the Hysteretic Response of Mechanical Connections for Wood Structures," *World Conference on Timber Engineering*, Vancouver, British Columbia.

Gupta, A.K. and Kuo, G.P., (1987). "Modeling of a Wood-Framed House," *J. Structural Engineering*, Vol. 113, No. 2, pp. 260–278.

Gupta, A.K. and Kuo, G.P., (1985). "Behavior of Wood-Framed Shear Walls," *J. Structural Engineering*, Vol. 111, No. 8, pp. 1722–1733.

Gupta, A.K. and Kuo, G.P., (1987). "Modeling of a Wood-Framed House," *J. Structural Engineering*, Vol. 113, No. 2, pp. 260-278.

He, M., Lam, F., and Foschi, R.O., (2001). "Modeling Three-Dimensional Timber Light-Frame Buildings," *J. Structural Engineering*, Vol. 127, No. 8, pp. 901–913.

Ibarra, L.F., Medina, R.A., and Krawinkler, H. (2005). "Hysteretic Models that Incorporate Strength and Stiffness Deterioration." *Earthquake Engineering and Structural Dynamics*, Vol. 34, pp.1489-1511.

International Code Council (ICC), (2009). "AC 130 – Acceptance Criteria for Prefabricated Wood Shear Panel," *ICC Evaluation Service, Inc.,* Whittier, California.

Itani R.Y., Cheung, C.K., (1984). "Nonlinear Analysis of Sheathed Wood Diaphragms," *J. Structural Engineering*, Vol. 110, No. 9, pp. 2137-2147.

Jamison, J.B., (1997). *Monotonic and Cyclic Performance of Structurally Insulated Panel Shear Walls*, Thesis submitted in partial fulfillment of the Master of Science Degree at the Virginia Polytechnic Institute and State University, Blacksburg, Virginia.

Johnston, A.R., Denn, P.K., and Shenton III, H.W., (2006). "Effects of Vertical Load and Hold-Down Anchors on the Cyclic Response of Wood-frame Shear Walls," *J. Structural Engineering*, Vol. 132, No. 9, pp. 1426-1434.

Kasal, B. and Leichti, R.J., (1992). "Nonlinear Finite Element Model for Light-Frame Stud Walls," *J. Structural Engineering*, Vol. 118, No. 11, pp.3124–3135.

Kasal, B., Leichti, R.J., and Itani, R.Y., (1994). "Nonlinear Finite Element Model of Complete Wood-frame Structures," *J. Structural Engineering*, Vol. 120, No. 1, pp. 100-119.

Kircher, C.A., Heintz, J.A., (2008). "Overview and Key Concepts of the ATC-63 Methodology," *Proceedings of the ASCE Structures Congress 2008*, April 24-28, 2008, Vancouver, British Columbia, Canada, CD-Rom 10 pages.

Krawinkler, H., Parisi, F., Ibarra, L., Ayoub, A., and Medina, R., (2001). "Development of a Testing Protocol for Wood-frame Structures," *CUREE-Caltech Wood-frame Project Rep. No. W-02*, Stanford University, Stanford, California.

Lebeda, D.J., Gupta, R., Rosowsky, D.V., and Dolan, J.D., (2005). "Effect of Hold-Down Misplacement on Strength and Stiffness of Wood-frame shear walls ," *Practice Periodical on Structural Design and Construction*, Vol. 10, No.2, pp. 79-87.

Mosalam, K.M., Hagerman, J. and Kelly, H. (2008). "Seismic Evaluation of Structural Insulated Panels," *5th International Engineering and Construction Conference*, Irvine, CA Aug.

Pacific Earthquake Engineering Research Center (PEER), (2006). PEER NGA Database, University of California, Berkeley, CA, Available at http"/peer.berkeley.edu/nga/.

Pang, W., Rosowsky, D.V., Pei, S., and van de Lindt, J.W., (2008). "Simplified Direct Displacement Design of Six-Story Woodframe Building and Pretest Seismic Performance Assessment," *J. Structural Engineering*, Vol. 136, No. 7, pp. 813-825.

Pei, S. and van de Lindt, J.W., (2007). *User's Manual for SAPWood for Windows: Seismic Analysis Package for Woodframe Structures*, Colorado State University, Fort Collins, CO.

Porter, M.L., (1987). "Sequential Phased Displacement (SDP) Procedure for TCCMAR Testing," *Proceedings of the 3rd Meeting of the Joint Technical Coordinating Committee on Masonry Research*, U.S.-Japan Coordinated Earthquake Research Program, Tomamu, Japan.

Stewart, W.G., (1987). *The Seismic Design of Plywood Sheathed Walls*, Doctor of Philosophy Thesis, University of Canterbury, New Zealand.

Terentiuk, Stefanie, (2009). *Parametric Study of Structural Insulated Panels Under Monotonic and Cyclic Loading*, Submitted in Partial Fulfillment of the Requirements for the Proposal for the Degree of Master of Science, State College, Pennsylvania.

Terentiuk, S. and Memari, A. M., (2011). "Seismic Evaluation of Structural Insulated Panels through Full-scale Racking Load Testing," *Journal of Architectural Engineering*, In press.

Toothman, A.D., (2003). *Monotonic and Cyclic Performance of Wood-frame shear Walls with Various Sheathing Materials*, Thesis submitted in partial fulfillment of the Master of Science Degree at the Virginia Polytechnic Institute and State University, Blacksburg, Virginia.

Vamvatsikos, D. and C. Allin Cornell (2002). "Incremental Dynamic Analysis," *Earthquake Engineering and Structural Dynamics*, Vol. 31, Issue 3, pp.491-514.

White, M.W. and Dolan, J.D., (1995). "Nonlinear Shear Wall Analysis," *J. Structural Engineering*, Vol. 121, No. 11, pp. 1629–1635

Appendix

Table A.1: SIP and Wood-frame Analysis Summary

System Type	Archetype ID	S_{MT} [T] (g)	$\Omega = V_{max} / V_b$	$\mu_T = \delta_U / \delta_{y,eff}$	$\hat{S}_{CT}$ [T] (g)	β_{TOT}	CMR	SSF	ACMR	10% ACMR	20% ACMR	Pass / Fail
Performance Group No. PG-1 (Short Period, Low Aspect Ratio)												
SIP	1	1.5	4.54	6.24	3.58	0.762	2.39	1.28	3.05	2.53	1.84	Pass
L-F Wood	1	1.5	2	10	2	0.5	1.3	1.3	1.8	1.9	1.52	Pass
SIP	5	1.5	2.26	12.94	2.95	0.762	1.97	1.33	2.62	2..53	1.84	Pass
L-F Wood	5	1.5	2.5	7	2.23	0.5	1.5	1.31	2.0	1.9	1.52	Pass
Partial Performance Group No. PG-4 (Long Period, Low Aspect Ratio)												
SIP	11	0.75	1.76	2.46	1.03	0.762	1.37	1.07	1.47	2.53	1.84	Fail / Fail
L-F Wood	11	0.75	2.1	7	1.98	0.5	2.64	1.1	3.0	1.9	1.52	Pass
Performance Group No. PG-11 (Long Period, High Aspect Ratio)												
SIP	4	0.75	10.59	1	5.1	0.762	6.8	1	6.8	2.53	1.84	Pass
L-F Wood	4	0.75	5.4	10	2.0	0.7	2.8	1.1	3.2	2.38	1.76	Pass

Table A.2: Quality Rating of Design Requirements (Source: FEMA, 2009)

Completeness and Robustness	**Confidence in Basis of Design Requirements**		
	High	**Medium**	**Low**
High. Extensive safeguards against unanticipated failure modes. All important design and quality assurance issues are addressed.	(A) Superior $\beta_{DR} = 0.10$	(B) Good $\beta_{DR} = 0.20$	(C) Fair $\beta_{DR} = 0.35$
Medium. Reasonable safeguards against unanticipated failure modes. Most of the important design and quality assurance issues are addressed.	(B) Good $\beta_{DR} = 0.20$	(C) Fair $\beta_{DR} = 0.35$	(D) Poor $\beta_{DR} = 0.50$
Low. Questionable safeguards against unanticipated failure modes. Many important design and quality assurance issues are not addressed.	(C) Fair $\beta_{DR} = 0.35$	(D) Poor $\beta_{DR} = 0.50$	--

Table A.3: Quality Rating of Test Data from an Experiment Investigation Program (Source: FEMA, 2009)

Completeness and Robustness	**Confidence in Test Results**		
	High	**Medium**	**Low**
High. Material, component, connection, assembly, and system behavior well understood and accounted for. All, or nearly all, important testing issues addressed.	(A) Superior $\beta_{TD} = 0.10$	(B) Good $\beta_{TD} = 0.20$	(C) Fair $\beta_{TD} = 0.35$
Medium. Material, component, connection, assembly, and system behavior generally understood and accounted for. Most important testing issues addressed.	(B) Good $\beta_{TD} = 0.20$	(C) Fair $\beta_{TD} = 0.35$	(D) Poor $\beta_{TD} = 0.50$
Low. Material, component, connection, assembly, and system behavior fairly understood and accounted for. Several important testing issues not addressed.	(C) Fair $\beta_{TD} = 0.35$	(D) Poor $\beta_{TD} = 0.50$	--

Table A.4: Quality Rating of Index Archetype Models (Source: FEMA, 2009)

Representation of Collapse Characteristics	**Accuracy and Robustness of Models**		
	High	**Medium**	**Low**
High. Index models capture the full range of the archetype design space and structural behavioral effects that contribute to collapse	(A) Superior $\beta_{MDL} = 0.10$	(B) Good $\beta_{MDL} = 0.20$	(C) Fair $\beta_{MDL} = 0.35$
Medium. Index models are generally comprehensive of the design space and behavioral effects that contribute to collapse.	B) Good $\beta_{MDL} = 0.20$	(C) Fair $\beta_{MDL} = 0.35$	(D) Poor $\beta_{MDL} = 0.50$
Low. Significant aspects of the design space and/or collapse behavior are not captured in the index models.	(C) Fair $\beta_{MDL} = 0.35$	(D) Poor $\beta_{MDL} = 0.50$	--

Table A.5: Seismic Behavioral effects and Related Design Considerations (Source: FEMA, 2009

Behavioral Issue	**Related Design Considerations**
Strength	• Minimum design member forces • Calculated member forces • Capacity design requirements • Component overstrength
Stiffness	• Design member forces • Drift Limits • Plan and elevation configuration • Calculated inter-story drifts • Diaphragm stiffness • Foundation stiffness
Inelastic-deformation capacity	• Component detailing requirements • Member geometric proportions • Capacity design requirements • Calculated member forces • Redundancy of the seismic force-resisting system
Seismic Design Category	• Design ground motion intensity • Special design/detailing requirements
Inelastic-system mobilization	• Building height and period • Diaphragm strength and stiffness • Permitted strength and stiffness irregularities • Capacity design requirements

Table A.6: Configuration Design Variables and Related Physical Properties (Source: FEMA, 2009)

Design Variable	**Related Physical Properties**
Occupancy and Use	• Typical framing layout • Distribution of seismic-force-resisting system components • Gravity load intensity • Component overstrength
Elevation and Plan Configuration	• Typical framing layout • Distribution of seismic-force-resisting components • Permitted vertical (strength and stiffness) irregularities • Beam spans, number of framing bays, system regularity • Wall length, aspect ratio, plan geometry, wall coupling • Braced bay size, number of braced bays, bracing configuration • Diaphragm proportions, strength, and stiffness • Ratio of seismic mass to seismic-force-resisting components • Ratio of tributary gravity load to seismic load
Building Height	• Story height • Number of stories
Structural Component Type	• Moments frame connection types • Bracing component types • Shear wall sheathing and fastener types • Isolator properties and types
Seismic Design Category	• Design ground motion intensity • Special design/detailing requirements • Application limits
Gravity Load	• Gravity load intensity • Typical framing layout • Ratio of tributary gravity load to seismic load • Component overstrength

Table A.7: Wood Light Frame Hysteretic Parameters (Source: Black, 2010)

Nail Type & Sheathing Thickness (in.)	Nail Pattern	Wall Length	K_0	F_0	F_1	R_1	R_2	R_3	R_4	Δ_u	α	β
10d common; 5/8	2/12	2ft	3,150	3,850	709	0.045	-0.160	0.70	0.032	5.355	0.58	1.23
		4ft	14,000	8,400	1,630	0.055	-0.165	0.65	0.032	2.900	0.58	1.20
		8ft	39,000	18,000	3,360	0.030	-0.105	0.75	0.027	2.250	0.64	1.26
	3/12	2ft	2,700	2,350	522	0.060	-0.120	0.70	0.028	4.900	0.60	1.26
		4ft	11,500	5,500	1,200	0.060	-0.120	0.65	0.025	2.655	0.60	1.24
		8ft	27,000	12,000	2,370	0.040	-0.090	0.82	0.028	2.280	0.57	1.28
	4/12	2ft	2,100	1,950	388	0.040	-0.120	1.00	0.026	4.550	0.57	1.26
		4ft	9,000	4,500	914	0.045	-0.120	0.75	0.020	2.400	0.60	1.23
		8ft	21,000	9,600	1,820	0.030	-0.095	0.85	0.028	2.220	0.60	1.28
	6/12	2ft	1,700	1,180	241	0.050	-0.100	0.75	0.022	4.635	0.54	1.30
		4ft	6,400	3,350	628	0.035	-0.090	0.80	0.026	2.200	0.60	1.26
		8ft	16,000	6,600	1,240	0.025	-0.080	0.80	0.023	2.160	0.65	1.28
8d common; 7/16	2/12	2ft	4,000	3,480	580	0.025	-0.065	0.60	0.050	3.600	0.75	1.22
		4ft	16,000	8,020	1,450	0.030	-0.080	0.60	0.060	1.978	0.73	1.20
		8ft	50,000	15,000	2,800	0.030	-0.055	0.60	0.040	1.838	0.75	1.28
	3/12	2ft	3,000	2,450	420	0.017	-0.080	0.65	0.045	3.500	0.70	1.26
		4ft	13,000	5,600	953	0.020	-0.065	0.60	0.050	1.838	0.70	1.24
		8ft	32,000	11,500	1,970	0.020	-0.060	0.75	0.042	1.400	0.73	1.28
	4/12	2ft	2,200	1,940	323	0.010	-0.080	1.00	0.040	3.200	0.75	1.28
		4ft	10,000	4,300	757	0.030	-0.065	1.00	0.050	1.600	0.70	1.28
		8ft	21,000	9,000	1,510	0.020	-0.070	1.00	0.048	1.450	0.70	1.28
	6/12	2ft	1,600	1,310	219	0.010	-0.080	1.00	0.042	2.800	0.75	1.30
		4ft	8,000	2,750	529	0.040	-0.060	0.75	0.045	1.600	0.65	1.28
		8ft	14,500	6,110	1,020	0.025	-0.065	1.00	0.046	1.480	0.75	1.28

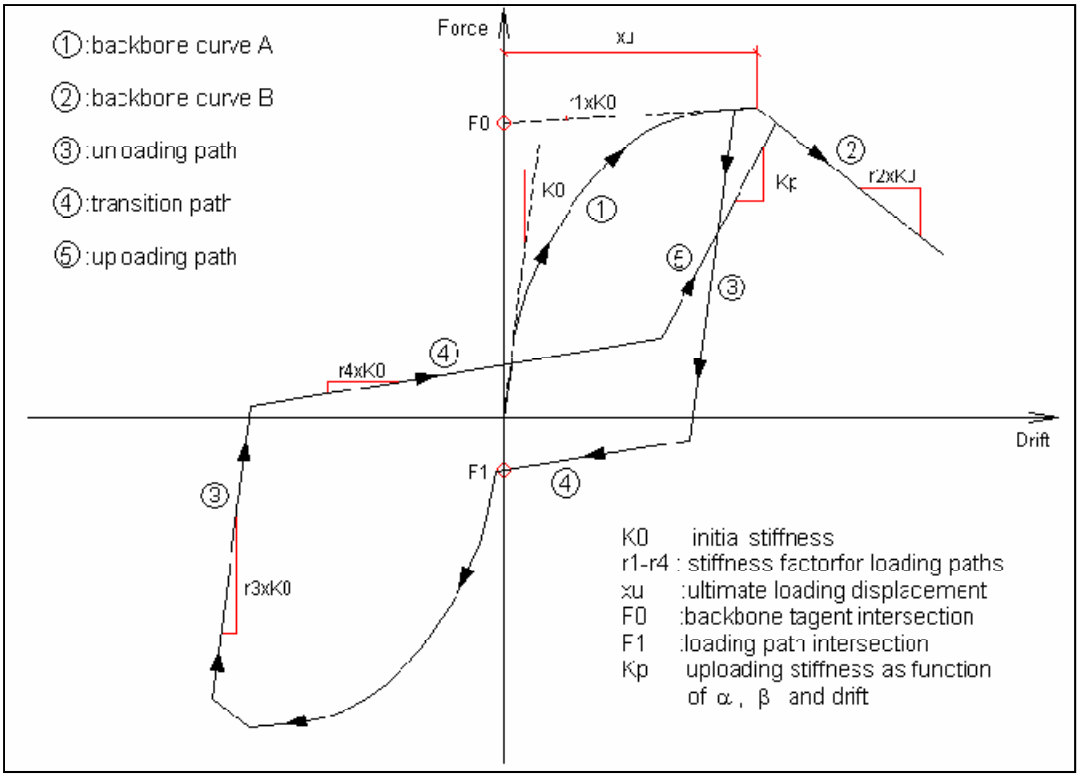

Figure A.1: Loading Paths and Parameters of SAWS Hysteretic Model (Source: Pei and van de Lindt, 2007)